FINITE ELEMENT ANALYSIS OF A TRANSPARENT COMPOSITE ARMOR WITH COMPUTATIONAL BALLISTIC TESTING

by

Burak Erdiş

Submitted to Graduate School of Natural and Applied Sciences
in Partial Fulfillment of the Requirements
for the Degree of Master of Science in
Mechanical Engineering

Yeditepe University

2019

FINITE ELEMENT ANALYSIS OF A TRANSPARENT COMPOSITE ARMOR WITH COMPUTATIONAL BALLISTIC TESTING

APPROVED BY:

Assist. Prof. Dr. Onur Cem Namlı .....
(Thesis Supervisor)
(Yeditepe University)

Assoc. Prof. Dr. Emre Alpman .....
(Marmara University)

Assist. Prof. Dr. Ali Fethi Okyar .....
(Yeditepe University)

DATE OF APPROVAL: ... /... /2019

ACKNOWLEDGEMENTS

I thank my Professor Onur Cem Namlı for his endless support and help in this study. Studying under his supervision has been a phenomenal experience and enlightenment. His assist has leaded us to this mind broadening journey. I am very grateful of him being my supervisor.

Finally, I also thank my family for their support and love. It makes this journey easier.

ABSTRACT

FINITE ELEMENT ANALYSIS OF A TRANSPARENT COMPOSITE ARMOR WITH COMPUTATIONAL BALLISTIC TESTING

Transparent armor systems are created for combining protection with vision. Vision is important for spotting the threat. With the usage of transparent armor, threat can be detected more effectively and do not have to sacrifice safety and protection of the target which is/are threatens. Transparent armors usage is more common when there is a delicate situation like protecting important people, military vehicles etc. This study aims to develop a transparent armor, analyze and test it, and compare it with the conventional armors to see the results. Material selection, projectile type and velocity, armor design, transparency, armor impact resistance and response are some of the points, which are investigated with researches and simulation in finite element analysis. Ballistic testing, tube test, composing materials are the techniques, which, are used for determining the results. Projectile is military type 7.62 millimeters bullet and its velocity is tested between 400-1200 m/s. Several materials and composite materials are tested, in order to find the proper selection for this study. For transparency and better resistance to projectile, materials are epoxy-resin composite and float glass. A new design is created for better resistance. Honeycomb transparent armor has minimum penetration, high performance and low cost according to results, when compare to other models. At final model only the first layer is failed and do not let the bullet through. According to this result, armor is successful at stopping the bullet.

ÖZET

BİLGİSAYAR YARDIMLI BALİSTİK TEST İLE SAYDAM ZIRH ANALİZİ

Saydam zırhlar, koruma ve görüş açısını aynı anda sağlamak için üretilmiştir. Görüş açısı tehlikeyi fark etmede çok önemli bir unsurdur. Saydam zırhlar sayesinde hem tehlikeyi fark etmede daha etkili olunabilirken, hem de korunmanızdan feragat etmemiş olursunuz. Önemli insanların korunmasında ve askeri araçlarda bu zırhların sıkça kullanıldığını görebiliriz. Bu çalışmada, bir saydam zırh geliştirilip, bilgisayar yardımıyla analizleri ve testleri yapılıp, geleneksel zırhlarla kıyaslayarak, sonuçlar ortaya konmuştur. Sonuç elde edilirken, balistik test, tüp testi, malzemeleri birleştirme gibi teknikler kullanılarak, sonuca varılmaya çalışılmıştır. Malzeme seçimi, mermi tipi ve hızı, zırh tasarımı, saydamlık, zırh direnci gibi noktalar araştırılmış ve gerekli simülasyonlarla incelenmiştir. Mermi 7,62 milimetre çapında askeri tip seçilmiş ve test edilirken 400'den 1200 m/s e kadar birçok hız denenmiştir. Malzeme seçiminde, birçok malzeme ve kompozit test edilmiş, en uygun malzeme seçilmeye çalışılmıştır. Saydamlık ve mermiye direnç, en önemli iki unsur olduğu için bunlara uygun olan epoksi-resin kompoziti ve cam, ana malzemeler olarak seçilmiştir. Bu araştırma için, yeni bir tasarım yaratılıp, arı peteklerinden oluşan küçük tüplerin birleştirilmesiyle oluşan arı peteği modeli geliştirilmiştir. Sonuçlara bakıldığından, geleneksel modellere göre arı peteği modeli daha dirençli, daha sağlam olup, aynı zamanda ağırlık ve fiyat konularında daha düşük olduğu gözlemlenmiştir. Son tasarımın sadece ilk katmanı zarar görmüş ve mermiyi geçirmemiştir.

TABLE OF CONTENTS

LIST OF FIGURES

LIST OF TABLES

LIST OF SYMBOLS/ABBREVIATIONS

C_{11}^{*}	Independent constant
C_{12}^{*}	Independent constant
C_{22}^{*}	Independent constant
C_{23}^{*}	Independent constant
C_{66}^{*}	Independent constant
E_{1}^{*}	Young's modulus on direction 1
E_f	Young's modulus of fiber
E_L	Young's modulus in longitudinal direction
E_m	Young's modulus of matrix
E_T	Young's modulus in transverse direction
G_{12}^{*}	Shear modulus in plane 12
G_{13}^{*}	Shear modulus in plane 13
G_{23}^{*}	Shear modulus in plane 23
G_f	Shear modulus of fiber
G_m	Shear modulus of matrix
G_{LT}	Shear modulus in longitudinal and transverse direction
K	Bulk modulus
K_{23}^{*}	Bulk modulus in plane 23
V	Volume fraction
V_f	Volume fraction of fiber
ν_m	Poisson's ratio of matrix
η_L	Constant that depends on geometry constant $(\frac{l_f}{d_f})$
ε_{11}	Strain in plane 1-1
ε_{12}	Strain in plane 1-2
ε_{13}	Strain in plane 1-3
ε_{22}	Strain in plane 2-2
ε_{23}	Strain in plane 2-3
ε_{33}	Strain in plane 3-3

v_{12}^{*}	Poisson's ratio in plane 12
v_{13}^{*}	Poisson's ratio in plane 13
v_{23}^{*}	Poisson's ratio in plane 23
ν_f	Poisson' ratio of fiber
ν_{LT}	Poisson' ratio in longitudinal and transverse direction
ρ	Density
σ_{11}	Stress in plane 1-1
σ_{12}	Stress in plane 1-2
σ_{13}	Stress in plane 1-3
σ_{22}	Stress in plane 2-2
σ_{23}	Stress in plane 2-3
σ_{33}	Stress in plane 3-3
τ_{11}	Shear stress in plane 1-1
τ_{12}	Shear stress in plane 1-2
τ_{13}	Shear stress in plane 1-3
τ_{22}	Shear stress in plane 2-2
τ_{23}	Shear stress in plane 2-3
τ_{33}	Shear stress in plane 3-3
Al	Aluminum
Al_2O_3	Alumina
AlON	Aluminum oxynitride
CCA	Concentric cylinder assemblage
CF	Carbon fiber
PC	Polycarbonate
PMMA	Polymethyl methacrylate
PU	Polyurethane
PVB	Polyvinyl butyral
SiC	Silicon carbide
SS	Stainless steel
VFD	Vanishing fiber diameter

1. INTRODUCTION

Protecting himself is a basic instinct for humans since they have born. For this purpose, humankind invented many things. Even being protected from each other is a problem. So, armors are created for themselves to wear, making their location safer or in gadgets they use to maintain safety. After improving armor systems in many ways, a new idea is revealed. Simply humankind wanted to see the thread behind the armor. So, transparent armors are created.

Transparent armor systems are varied so many fields like military, face shields, vehicle windshields and windows, aircrafts, blast shields [1]. These armors generally are consisted many layers [2], as shown at Figure 1.1.

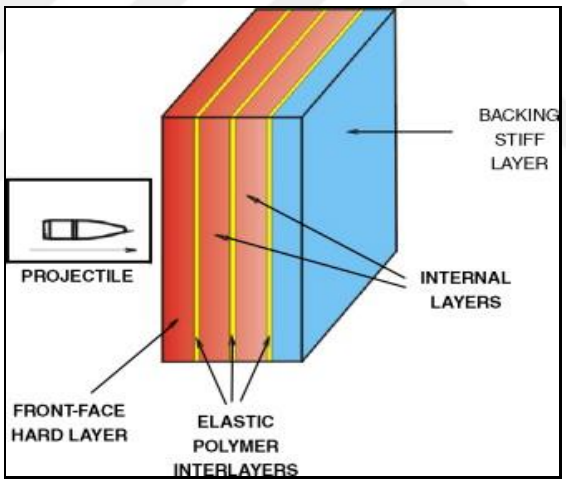

Figure 1.1. Conventional transparent armor [2]

Layers of armors have different specific materials for their own purposes. Mainly, Polymethyl methacrylate [3], float or soda lime glass [4], polycarbonate [5], polyurethane [6] or Polyvinyl Butyral [7] and AlON [8] or spinel [9] is used in armor layers. PMMA, float or soda glass is internal layers. PC, PU and PVB are interlayer. AlON and spinel are used for the first layer to make the first contact.

Individual armor is crucial for security. Increment of vital situations in military and force of law, has made the individual armor usage critical. Decreasing the effects of bullets, impacts and blows is essential at these areas of law. [10]

There are several research papers about using composite materials at armors to resist the bullets. Philip M. [11] studied the ballistic impact of M5 armor system which based on fibers and results show that M5 fiber-based armor can be lighter. Erol Ünaler [12] experimented on E-glass/unsaturated polyester composite laminates and multilayered sandwich utilizing aluminum (Al) plates and alumina (Al_2O_3) [13] tiles to advance the ballistic tolerance of the composites and with 1000 m/s shot speed of 7.62 millimeters bullet cannot be stopped without backing layer. K. Karthikeyan [14] investigated ballistic performance of plates made of stainless steel [15], carbon fiber/epoxy [16] and hybrid of those with spherical steel projectile and see that penetration velocity of SS plate is the highest and CF plate is the lowest. Yohannes Regassa [17] experimented on less cost and weighted models with simulations. Composite armor had Kevlar-29 fibers and polyester resin for 20 layers. Results show that armor is 1.5 kg and does not have penetration by projectile.

Also modeling and simulation of body armor with different materials and same weight is another subject of these types of researches. Materials are stainless steel 304, Kevlar-epoxy [18] composite with multi layers and experimented with different material layers and velocities. Results show that steel armor fail completely with no resistance and Kevlar-epoxy armor penetrated through the thickness of the armor. [19]

Computational and numerical analysis are enhancing, models can show the behavior and response of the material more accurately. With the software of nowadays, prediction of the failures and deformations are now easier and more accurate. Although the techniques are very accurate, investigation of different analysis techniques will be performed to determine the accuracy between experiments and analysis.

Polymeric transparent armor materials usage is very common in researches. These materials are PMMA, PU, PC, PVB etc. Combinations of these materials are also another crucial point of the experiments. Inappropriately combined materials can give very lousy result. On the other hand, accurately, combined layers can provide very efficient results.

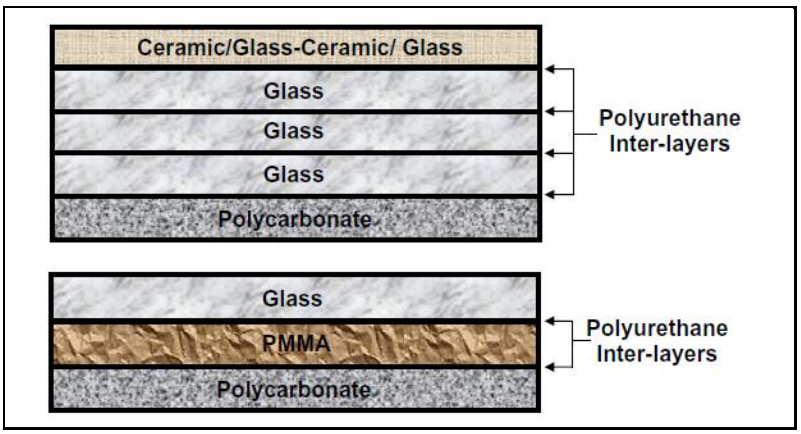

Figure 1.2. Examples of the combinations in transparent armor systems [20]

With the help of simulations, crack reproduction and predictions of a PC/PU/PMMA/PU/PC laminate [21] were invested and improving strength and failure models are analyzed according to researches.

Ballistic testing research on transparent armor is published by E. Straßburger [22]. By changing the geometry, material types and model, study achieve some results. According to results to reduce the weight, hard front ceramic layer is crucial. Strength and the efficiency increase if ceramic thickness is increased. But over some point increasing thickness, has no significant effect the efficiency.

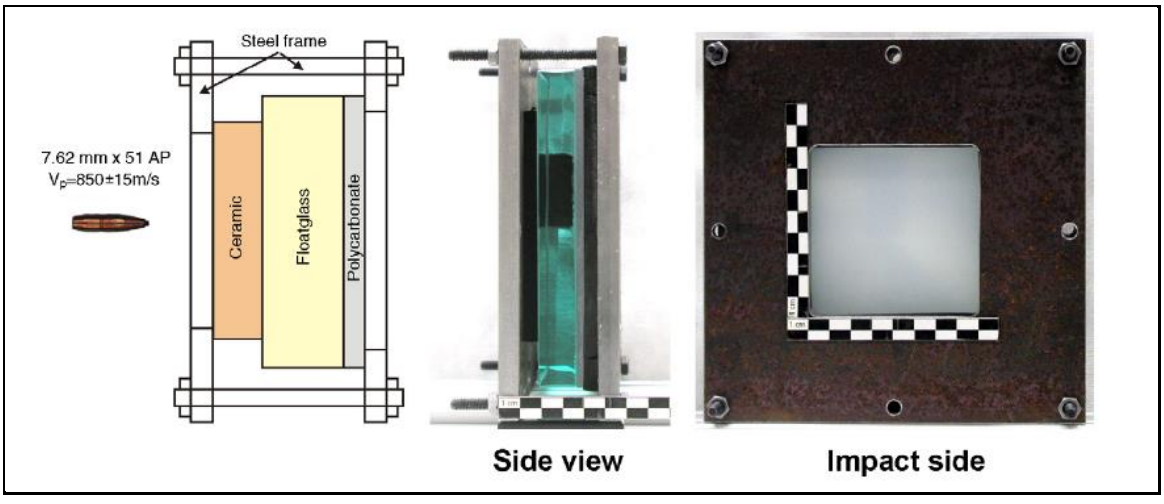

Figure 1.3. Schematic view of E. Straßburger's experiment [22]

Design and material selection have some difficulties to achieve the optimum results. For example, at armoring military vehicle windshields and side windows show that, it is not very

easy task to achieve. Single and multi-hit ballistic protection must provide with optical transparency. Also, low cost and light weight necessity is another side of the objective [23]. For those kinds of tasks to achieve, design, material selection, layer integration and fabrication of the armor must be precise and tested very well. Another research [24] shows that materials should be selected based on behaviors in a ballistic situation. PMMA was found to satisfy the requirements. Polymeric materials in laminate design, firstly tried to reduce the weight. Then it seems that hybrid glass-plastic armor is very effective for desired requirements

Ballistic performance of transparent armors has been investigated for years. Optimal solution has a sapphire/ceramic front/face layer. Internal layers are consisting float glass and backing layer is polycarbonate. High protection requires thicker armor, which can lead to high weight. These problems are solved by transparent ceramics of high hardness such as aluminum oxynitride, spinel and sapphire. And that is the reason for facing layer. The backing layer's purpose is to hold the armor together. Avoid from crack propagation is another purpose of the back layer. So, for these purposes stiff and tough material such as PC needs to be chosen. [25]

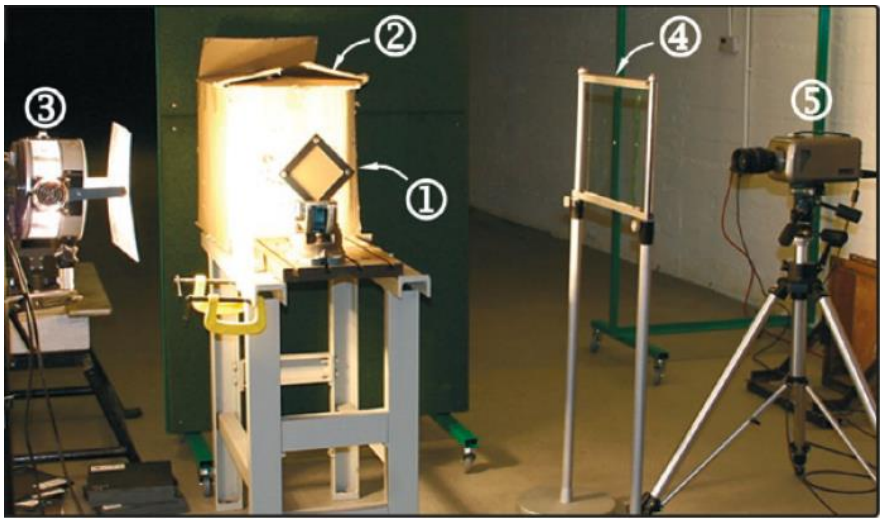

Figure 1.4. Experimental setup of ballistic test; 1-armor specimen 2-projectile recovery chamber 3-lightning system 4-protective screen 5-camera [25]

Purpose of this research is to improve the conventional armor and create a new, better design. In armor design, better means tougher, lighter, cheaper, better resistance to projectiles etc. First step of this study is to choose the proper materials for less penetration. Then these

materials are tested with computational software. In every step, geometry of the armor is improved, and modifications are added to make it better. After that, finite element analyses are done, and a prototype will be occurred.

On the other hand, beside the computational part, there is also modeling part of this research. Calculations need to be done to have accurate results. A proper model is chosen and implemented to armor. Results of this modeling part need to be similar with computational part. This similarity shows that design is accurate, and study is achievable. And after that, design will be proved to be better.

Simulating these situations has a lot of advantages. With finite element analysis method, objectives can be obtained easier, quicker and more effectively. For example, in ballistic testing, when correct parameters are given, computer analyze the situations and give the results in hours. It just will be needed to verify it for real life situations. However instead of using computer analysis, if real life experimenting is chosen to process the results, there will be a lot of work to complete in order to get results. Firstly, a proper laboratory will be needed. Tools need to be arranged to create the setup. In ballistic test, a high technology slow motion camera, material holding setup, necessary safety precaution, gun, setup for creating armor with different materials, sensors and measurement devices will be needed to start the experiment. After that, for shooting procedure, permits need to be taken from relevant authorities. Safety rules need to be accomplished. And a well-trained shooter will be needed to evaluate the test. These steps need time, resources and high budgets to complete. For these reasons, using a computer software and simulating the test will be convenient for getting easier, faster results.

2. BACKGROUND

At this part of the report, several suitable models for the research are explained. After discussing the available models that can be considered for the study, suitable and easier to be implanted one will be chosen to be used in modeling the transparent armor.

2.1. MORI-TANAKA METHOD

Mori-Tanaka model is an effective field approximation for inhomogeneity in infinite medium, based on Eshelby's elasticity solution. Average stress or average strain tensors and matrix to the average stress or average strain tensor relate the fourth-order concentration tensors [26]. Thermo elastic behavior of composites has more than a few percent reinforcement volume fractions and liable for interaction between inhomogeneities. Consistency of approximating the stresses acting on an inhomogeneity can be achieved by an appropriate average matrix stress. Concept of combining average matrix stress inclusion goes back to Mori and Tanaka (1973). This type of effective field theories called as Mori-Tanaka methods. [27]

2.2. MAXWELL SCHEMES

The scheme of Maxwell is the first micromechanical model that can be found in literature. The effective conductivities of inhomogeneous materials can be explained of a mean-field method in elasticity. [28] A single region of inhomogeneities (Figure 2.1) treated as dilute and the same region consists of a uniform effective material, average responses of those two configurations has to be equal. Analogous approaches were used by Giordano and independently of Maxwell's ideas, by Shen and Yi. [27]

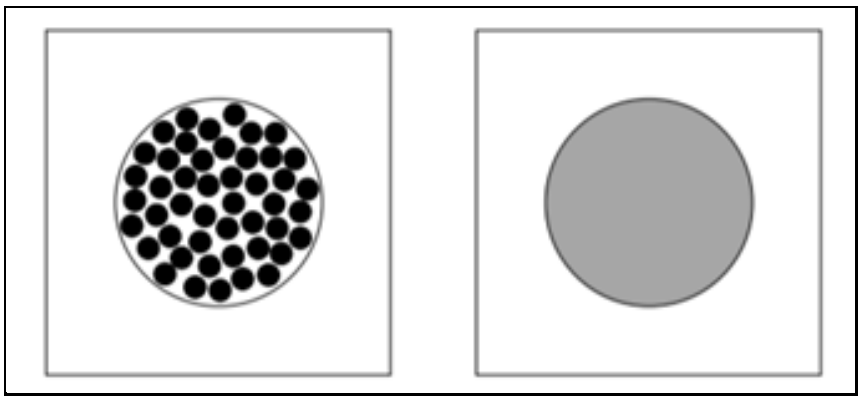

Figure 2.1. Sketch of the two configurations underlying Maxwell's scheme [28]

2.3. PONTE–WILLIS ESTIMATES

A mean field scheme for inhomogeneous materials that occurred from ellipsoidal arrangements of ellipsoidal inhomogeneities embedded in a matrix, explained by Ponte Castaneda and Willis [29]. In that kind of systems, correlations of inhomogeneity arrangement are described by Eshelby tensor Sd, where the shapes of inhomogeneities are explained by Eshelby tensor Si. This type of arrangements can be explained by extending Figure 2.2 to non-overlapping safety ellipsoids that contain aligned or non-aligned ellipsoidal inhomogeneities, aspect ratios of the safety ellipsoids and the inhomogeneities being different. [27]

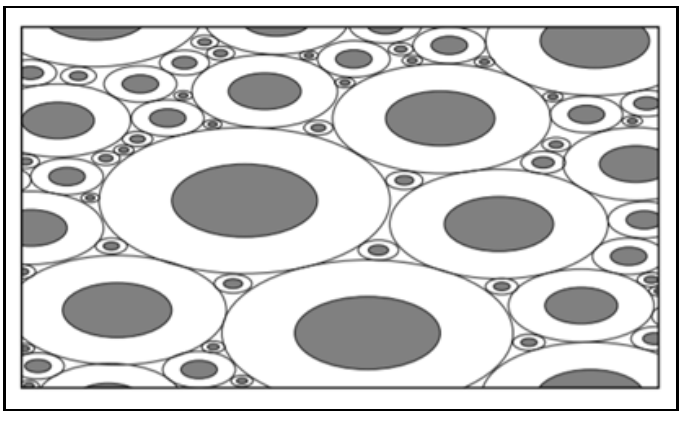

Figure 2.2. Sketch of ellipsoidal inhomogeneities in an aligned ellipsoidal distributed spatial arrangement as used implicitly used Mori Tanaka type models [27]

2.4. HASHIN–SHTRIKMAN ESTIMATES

Hashin-Shtrikman model can be described by bounds on the elastic module and tensors of transversally isotropic composites and isotropic composites. [30] Standard mean-field models can be solved by treating it as special cases of Hashin-Shtrikman methods by choices of the comparison material. For example, using the matrix as the comparison material conclusions in Mori-Tanaka methods, the selection of the effective material as comparison material leads to classical self-consistent schemes. [27]

2.5. THE VFD MODEL OF DVORAK AND BAHEI-EL-DIN

Combination of average stress and strain assumptions can be visualized as each fiber having a vanishing diameter yet finite volume. An approach that is closely related to the rules of mixture but gives consistent and unique overall material tensors for unidirectional continuously reinforced composites is known as the Vanishing Fiber Diameter (VFD) model. The physical interpretation of the VFD model is a composite containing aligned and continuous, but infinitely thin fibers (which strongly influence the axial effective behavior but affect the transverse behavior of the composite only via the macroscopic Poisson effect) in a matrix. [27]

2.6. DILUTE INHOMOGENEOUS INCLUSIONS

Mean field methods for dilute inhomogeneous matrix–inclusion composites typically aim at making use of Eshelby's expressions for the fields in a homogeneous inclusion subjected to an eigenstrain by using the concept of an equivalent homogeneous inclusion. This strategy involves replacing the actual inhomogeneous inclusion, which has different material properties than the matrix and which is subjected to a given unconstrained eigenstrain εt, with an "equivalent" homogeneous inclusion on which an equivalent eigenstrain $\varepsilon\tau$ is made to act. This equivalent eigenstrain must be chosen in such a way that the same stress and strain fields are obtained in the actual inhomogeneous inclusion and in the fictitious homogeneous inclusion. [27]

2.7. MISFIT STRAINS: ESHELBY'S SOLUTION

Most of the mean field definitions used in continuum micromechanics are based on Eshelby's work. He studied the stress and strain distributions in homogeneous media [31]. In that media there are sub-regions that have shape and size shifting so it no longer fits its previous space. Eshelby's work's results show that an elastic homogeneous ellipsoidal inclusion in an infinite matrix is subjected to a homogeneous strain εt, the stress and strain states in the constrained inclusion are uniform, i.e., σ (i) = hσi (i) and ε (i) = hεi (i). The uniform strain in the constrained inclusion, εc, is related to the stress-free strain εt by the expression. [27]

2.8. CONCENTRIC CYLINDER ASSEMBLAGE MODEL

For centuries mankind tend to improve the materials, which, they use in almost everything, in order to create better products. Composites are born to satisfy this need. As it's known, composites are consisting from two main parts, matrix and fiber. Matrix is the main material and fiber is the reinforcement that injected in matrix. This assembly technique has a lot of different types nowadays.

Generally, fibers have cylindrical shape in nature. Thus, Hashin and Rosen created a micromechanical model that the composite is assembled from concentric cylinders. The model is called concentric cylinder assemblage. As it is shown in Figure 2.3, inner cylinders are fibers and the outer part is matrix.

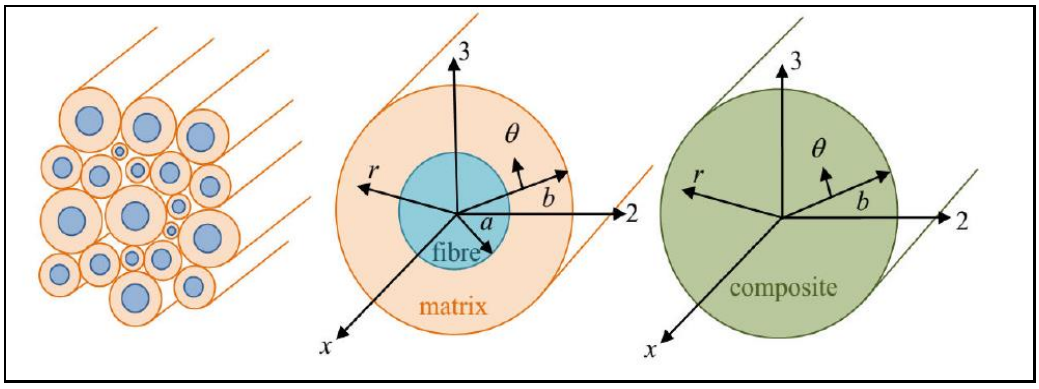

Figure 2.3. Different views of the model

In Figure 2.3 concentric cylinder assemblage model is consisted of concentric cylinders with different radius. Although the radius of cylinders is varying, the ratio of radius of fiber and matrix is same for all. So, the cylinders have same volume fraction. Volume fractions are calculated according to equation (2.1).

$$V_f = \frac{\pi a^2}{\pi b^2} = \frac{a^2}{b^2} \tag{2.1}$$

Constitutive relations between stress and strain are given below. From those relations one can derive relations between effective independent stiffness coefficients and effective engineering constants. Stress strain relations in 2-3 plane are written as;

$$\sigma_{11} = C_{11}^* \varepsilon_{11} + C_{12}^* \varepsilon_{22} + C_{12}^* \varepsilon_{33} \tag{2.2}$$

$$\sigma_{22} = C_{12}^* \varepsilon_{11} + C_{22}^* \varepsilon_{22} + C_{23}^* \varepsilon_{33} \tag{2.3}$$

$$\sigma_{33} = C_{12}^* \varepsilon_{11} + C_{23}^* \varepsilon_{22} + C_{22}^* \varepsilon_{33} \tag{2.4}$$

$$\tau_{33} = (C_{22}^* - C_{23}^*) \varepsilon_{23} \tag{2.5}$$

$$\tau_{13} = 2C_{66}^* \varepsilon_{13} \tag{2.6}$$

$$\tau_{12} = 2C_{66}^* \varepsilon_{12} \tag{2.7}$$

$C_{11}^*, C_{12}^*, C_{22}^*, C_{23}^*, C_{66}^*$ are independent constants. Effective properties of the composite are defined from these constants.

Assuming $\sigma_{11} = \sigma$ and $\sigma_{22} = \sigma_{33} = \sigma_{23} = \sigma_{13} = \sigma_{12} = 0$, putting these into equations (2.2), (2.3), (2.4), (2.5), (2.6), (2.7) give us normal strains as it is shown below.

$$\varepsilon_{11} = \frac{C_{22}^* + C_{23}^*}{C_{11}^* C_{22}^* - 2C_{12}^{*2} + C_{11}^* C_{23}^*} \sigma_{11} \tag{2.8}$$

$$\varepsilon_{22} = \frac{-C_{12}^*}{C_{11}^* C_{22}^* - 2C_{12}^{*2} + C_{11}^* C_{23}^*} \sigma_{11} \tag{2.9}$$

$$\varepsilon_{33} = \frac{-C_{12}^*}{C_{11}^* C_{22}^* - 2C_{12}^{*2} + C_{11}^* C_{23}^*} \sigma_{11} \tag{2.10}$$

From the equation (2.8), one can derive;

$$\sigma_{11} = (C_{11}^{*} - \frac{2C_{12}^{*2}}{C_{22}^{*} + C_{23}^{*}})\varepsilon_{11} \tag{2.11}$$

E_1^* is the effective axial modulus and define from the Hooke's law as;

$$\sigma_{11} = E_1^{*}\varepsilon_{11} \tag{2.12}$$

From the equations (2.11) and (2.12), one can write;

$$E_1^{*} = C_{11}^{*} - \frac{2C_{12}^{*2}}{C_{22}^{*} + C_{23}^{*}} \tag{2.13}$$

Poisson's ratios v_{12}^* and $v_{13}^*$are defined below.

$$v_{12}^{*} = -\frac{\varepsilon_{22}}{\varepsilon_{11}} \tag{2.14}$$

$$v_{13}^{*} = -\frac{\varepsilon_{33}}{\varepsilon_{11}} \tag{2.15}$$

By putting Poisson's ratios into equation (2.8), (2.9) and (2.10)

$$v_{12}^{*} = v_{13}^{*} = \frac{C_{12}^{*}}{C_{22}^{*} + C_{23}^{*}} \tag{2.16}$$

The other engineering constants are

$$G_{12}^{*} = G_{13}^{*} = C_{66}^{*} \tag{2.17}$$

$$G_{23}^{*} = \frac{C_{22}^{*} - C_{23}^{*}}{2} \tag{2.18}$$

Equations (2.13), (2.16), (2.17) and (2.18) are four equations with five effective stiffness constants. One more equation is needed in order to solve for $C_{11}^{*}, C_{12}^{*}, C_{22}^{*}, C_{23}^{*}$ and C_{66}^{*} in terms of effective engineering constants.

Last equation is bulk modulus equation and developed as follows.

$$\varepsilon_{11} = 0\,, \varepsilon_{22} = \varepsilon_{33} = \varepsilon \tag{2.19}$$

With these strains and the constitutive equations in equations (2.2), (2.3), (2.4), (2.5) and (2.6) the normal stresses are;

$$\sigma_{11} = 2C_{12}^{*}\varepsilon \tag{2.20}$$

$$\sigma_{22} = (C_{22}^{*} + C_{23}^{*})\varepsilon = \sigma \tag{2.21}$$

$$\sigma_{33} = (C_{22}^{*} + C_{23}^{*})\varepsilon = \sigma \tag{2.22}$$

From $\sigma = 2K_{23}^{*}\varepsilon$, effective plane strain bulk modulus given as

$$K_{23}^{*} = \frac{1}{2}(C_{22}^{*} + C_{23}^{*}) \tag{2.23}$$

Finally, equations (2.13), (2.16), (2.17), (2.18) and (2.23) are inverted to find,

$$C_{11}^{*} = E_{1}^{*} + 4\nu_{12}^{*2}K_{23}^{*} \tag{2.24}$$

$$C_{12}^{*} = 2K_{23}^{*}\nu_{12}^{*} \tag{2.25}$$

$$C_{22}^{*} = G_{23}^{*} + K_{23}^{*} \tag{2.26}$$

$$C_{23}^{*} = -G_{23}^{*} + K_{23}^{*} \tag{2.27}$$

$$C_{66}^{*} = G_{12}^{*} \tag{2.28}$$

CAA model is chosen for this study. The main reason of this choice is the similarity between the shapes of the constituents. Among all models that was examined, cylindrical shape is the closest shape to the honeycomb shaped armor. Honeycomb armor is a combination of a lot of honeycomb tubes. So, it is similar with different cylinders coming together are creating a composite.

On the other hand, this model is like a combination of several micromechanical composites models and developed from them. Thus, this model can be integrated to nowadays condition better than some other models.

The other advantage of this model that, assumptions can be made from one concentric cylinder and those assumptions are valid for the others and whole composite. This condition makes easy to get correct, simple and efficient results. [24]

3. FINITE ELEMENT ANALYSIS (FEA) OF TRANSPARENT ARMOR (BALLISTIC TEST)

In Figure 3.1, steps of the analysis are presented. First, the FEA is performed and the results are obtained. Then the modeling is executed with the help of the FEA results. Mechanical properties are calculated, and the results of the modeling are introduced as the input to the finite element analysis. This process helps to find the accurate results with comparing simulations and calculation each other.

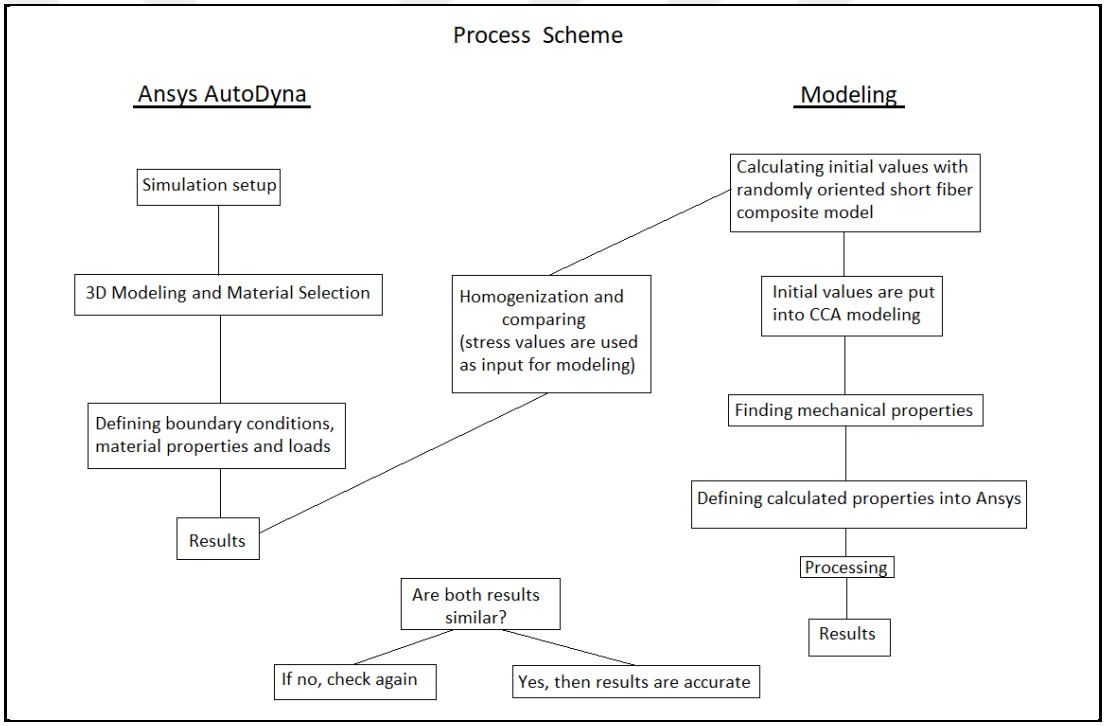

Figure 3.1. Process scheme

3.1. SIMULATIONS

3.1.1. Case 1 – 3 Layers, 500 m/s, 18 mm Diameter

Armor has three layers. Each layer has two sub-layers which are epoxy and glass. Glass sub-layer has two millimeters thickness and epoxy e-glass has 0.7 mm thickness. In other words, internal layers are glass and interlayer are epoxy e-glass. Epoxy e-glass's density is 2000

kg/m^3, Young's modulus is 45 GPa and Poisson's ratio is 0.3. Glass's density is 2530 kg/m^3, Young's modulus is 74.5 GPa and Poisson's ratio is 0.226. Geometry of layers is 100x100 mm square plate.

Projectile is in bullet shape. Its material is structural steel. Its velocity is 500 m/s. It has 18 mm diameter.

Purpose of this case is to see the response of the armor and according to that response, create a starting point to evaluate the armor.

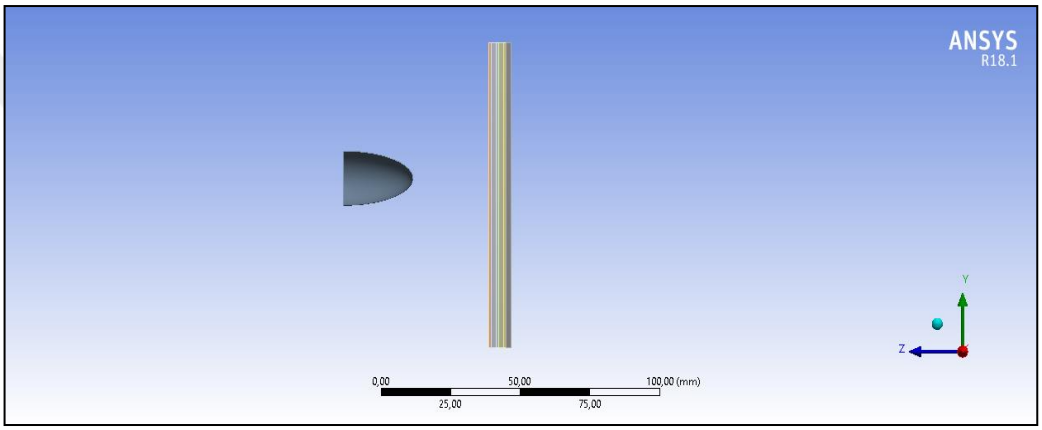

Figure 3.2. Beginning of the case 1

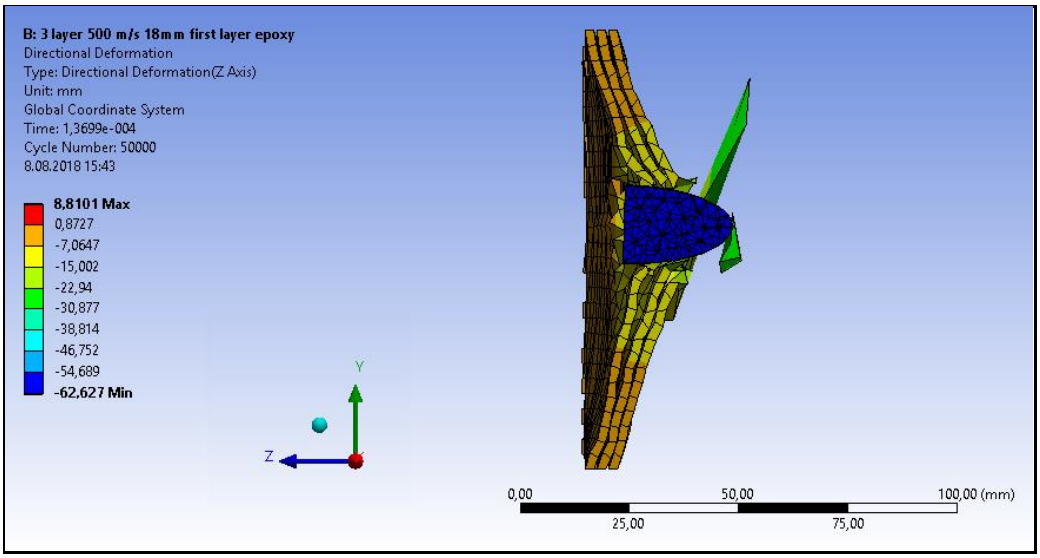

Figure 3.3. Ending of the case 1

As it is shown in Figure 3.3 projectile goes through the all three layers and creates a hole in armor. So, it can be said that the armor failed. From the results, one can assume that three layers aren't enough for this projectile or projectile is too big for this armor.

3.1.2. Case 2 - 3 Layers, 500 m/s, 4.5 mm Diameter

Armor has three layers. Each layer has two sub-layers which are epoxy and glass. Glass sub-layer has two millimeters thickness and epoxy e-glass has 0.7 mm thickness. In other words, internal layers are glass and interlayer are epoxy e-glass. Epoxy e-glass's density is 2000 kg/m^3, Young's modulus is 45 GPa and Poisson's ratio is 0.3. Glass's density is 2530 kg/m^3, Young's modulus is 74.5 GPa and Poisson's ratio is 0.226. Geometry of layers is 100x100 mm square plate.

Projectile is in bullet shape. Its material is structural steel. Its velocity is 500 m/s. It has 4.5 mm diameter.

After observing the results of case 1, reduction of the projectile diameter is decided. To see the effect of the projectile diameter, smaller projectile must be used this time.

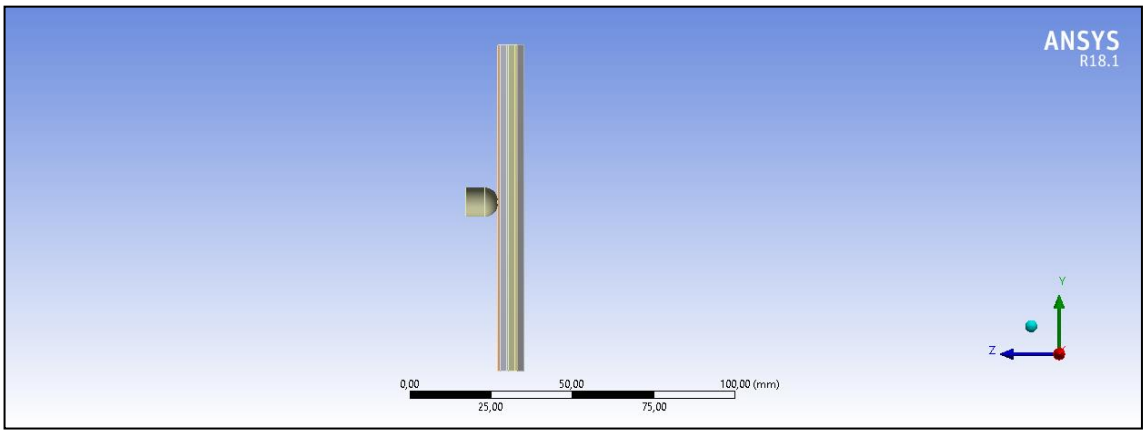

Figure 3.4. Beginning of the case 2

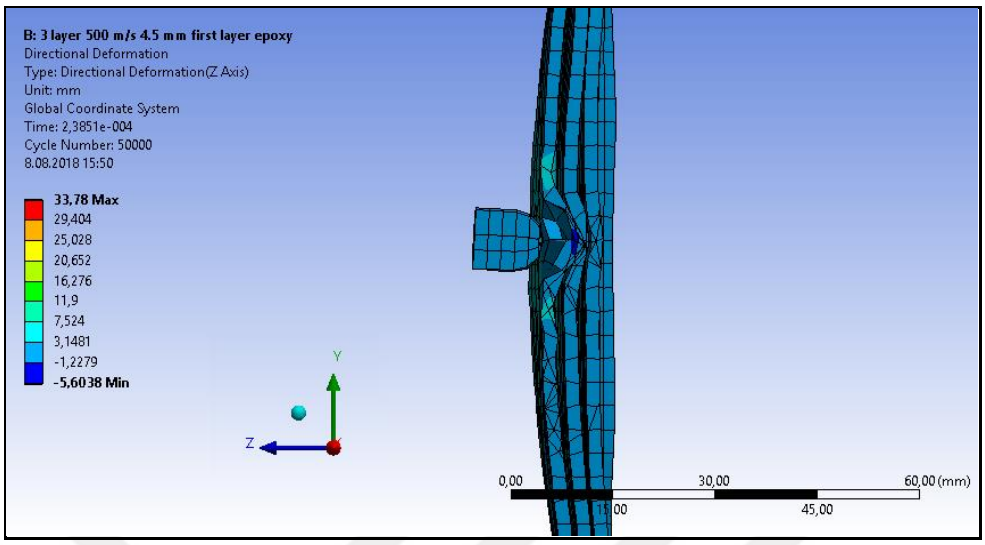

Figure 3.5. Ending of the case 2

At this case size of the projectile is not enough to destroy the armor. Relatively little bullet can only create failure at the first layer and the other two layers are perfectly conserve their shapes. Three layers armor has succeeded its objective against 4.5 mm projectile with only first layer deformation.

3.1.3. Case 3 - 3 Layers, 1250 m/s, 4.5 mm Diameter

Armor has three layers. Each layer has two sub-layers which are epoxy e-glass and glass. Glass sub-layer has two mm thickness and epoxy e-glass has 0.7 millimeters thickness. In other words, internal layers are glass and interlayer are epoxy e-glass. Epoxy e-glass's density is 2000 kg/m^3, Young's modulus is 45GPa and Poisson's ratio is 0.3. Glass's density is 2530 kg/m^3, Young's modulus is 74.5 GPa and Poisson's ratio is 0.226. Geometry of layers is 100x100 mm square plate.

Projectile is in bullet shape. Its material is structural steel. Its velocity is 1250 m/s. It has 4.5 mm diameter. Purpose of this case is to see the effect of velocity. So that, compare to case 2, this time, higher velocity value is defined to projectile.

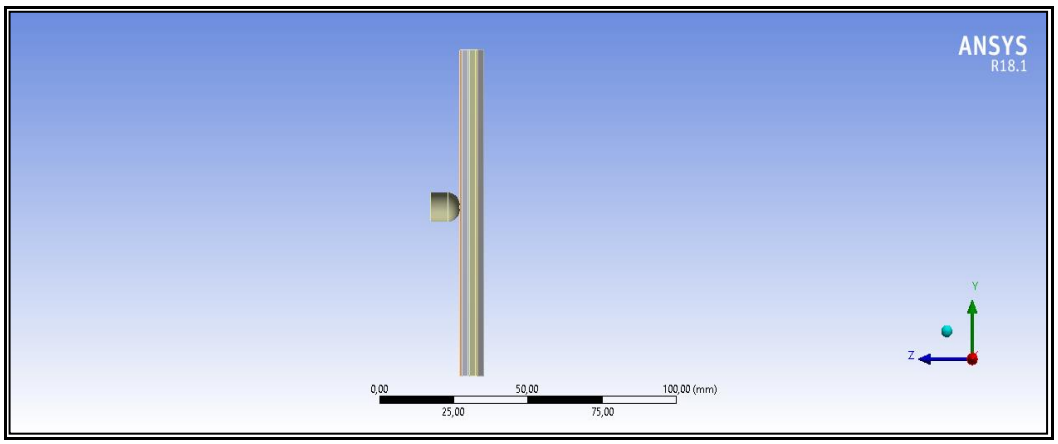

Figure 3.6. Beginning of the case 3

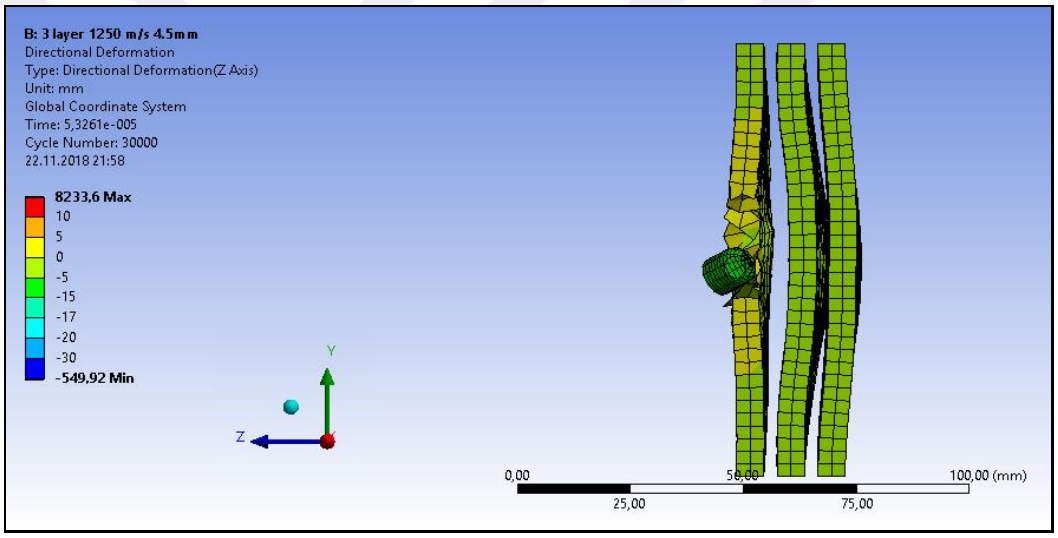

Figure 3.7. Side view of ending of the case 3

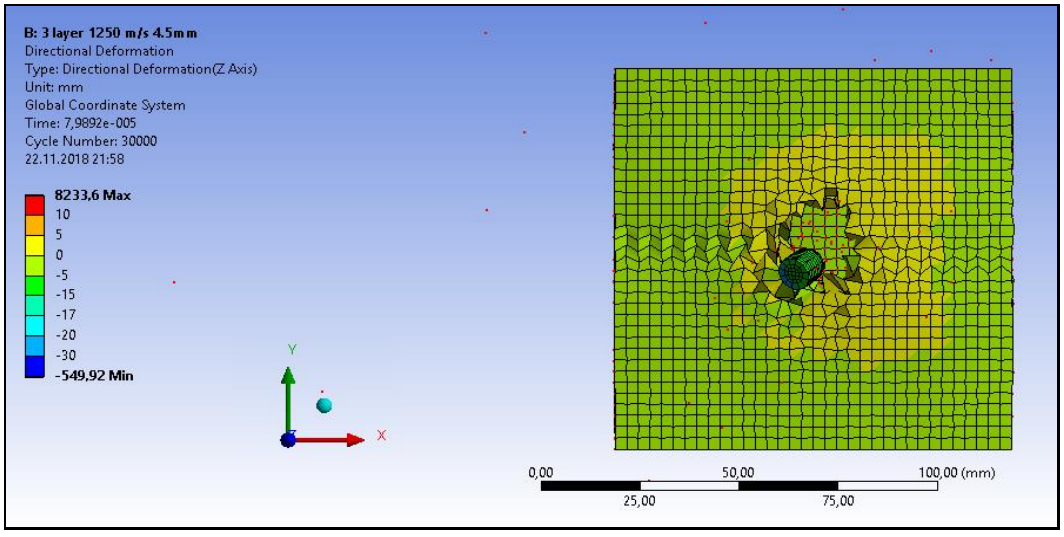

Figure 3.8. Front view of ending of the case

Compared to case 2, this time same projectile is shot with greater velocity. Figure 3.7 and Figure 3.8 you can see that the first layer is completely failed and destroyed. According to case 2, amount of deformation is greater.

3.1.4. Case 4 - 4 Layers, 500 m/s, 18 mm Diameter

Armor has four layers. Each layer has two sub-layers which are epoxy and glass. Glass sub-layer has two millimeters thickness and epoxy has 0.7 mm thickness. In other words, internal layers are glass and interlayer are epoxy. Epoxy's density is 1540 kg/m^3, Young's modulus is 3.5 GPa and Poisson's ratio is 0.33. Glass's density is 2530 kg/m^3, Young's modulus is 74.5 GPa and Poisson's ratio is 0.226. Geometry of layers is 100x100 mm square plate.

Projectile is in bullet shape. Its material is structural steel. Its velocity is 500 m/s. It has 18 mm diameter.

Purpose of this case is to see the extra resistance which comes from an extra layer. Difference of this case is adding a fourth layer to armor. Expectation is to observe a better response and resistance from armor.

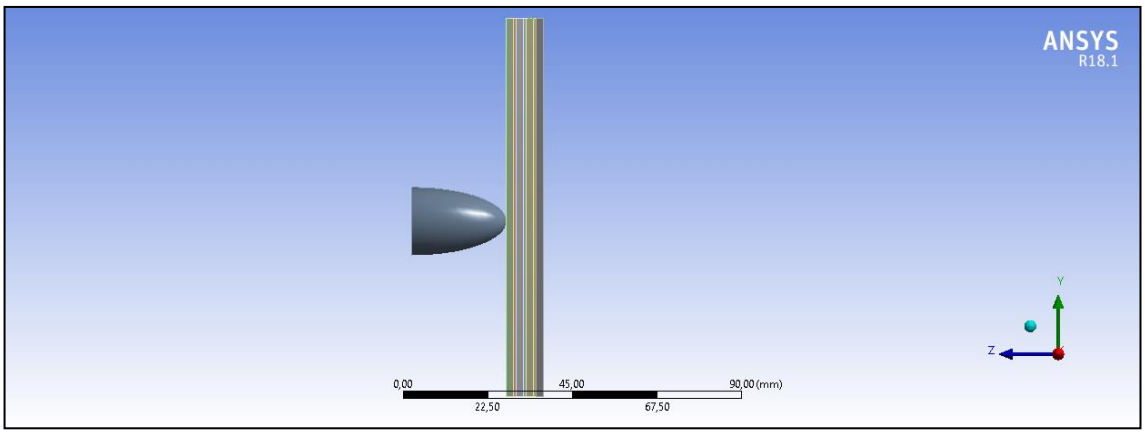

Figure 3.9. Beginning of the case 4

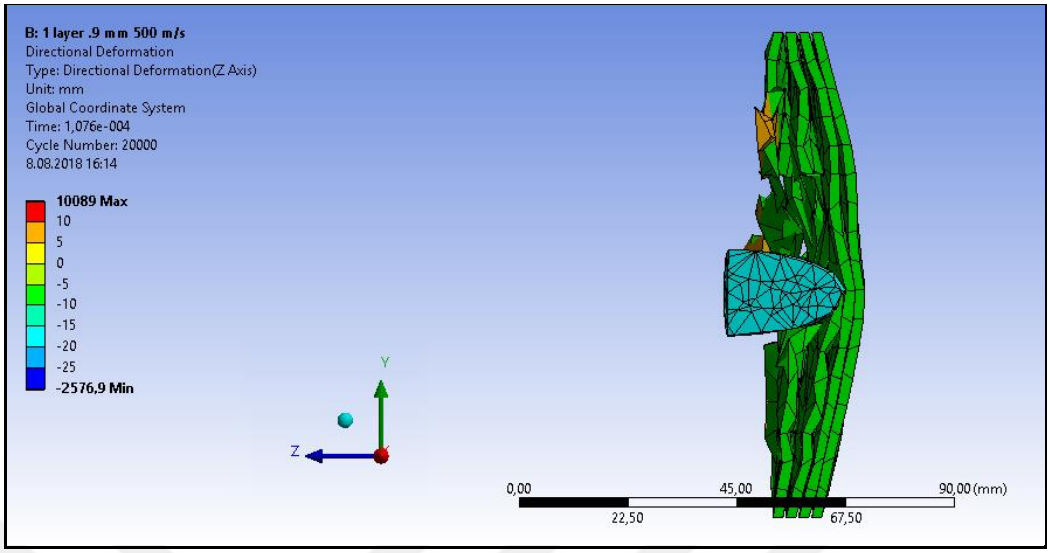

Figure 3.10. Ending of the case 4

This time an extra layer is added to armor and the bullet diameter is extended. The extra layer has created endurance to this larger projectile and even though the first two layers are failed, armor has done its job and stopped the projectile. When compare to case 1 which has same properties with this case (except the layer quantity), projectile has stopped at a certain layer. This shows as that the extra layer can give positive feedback at the result.

3.1.5. Case 5 - 4 Layers, 650 m/s, 18 mm Diameter

Armor has four layers. Each layer has two sub-layers which are all glass. Glass sub-layer has two millimeters thickness. In other words, internal layers and interlayer are all glass. Glass's density is 2530 kg/m^3, Young's modulus is 74.5 GPa and Poisson's ratio is 0.226. Geometry of layers is 100x100 mm square plate.

Projectile is in bullet shape. Its material is structural steel. Its velocity is 650 m/s. It has 18 mm diameter.

At this case, main objective is to find the glass's resistance limit in four layers armor. At which velocity, bullet will not go through the armor, is the question that, one is looking for the answer.

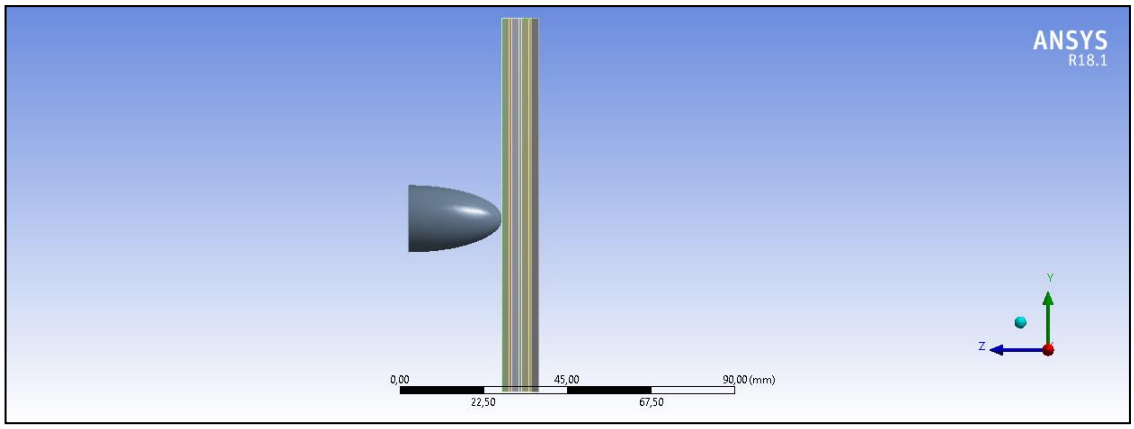

Figure 3.11. Beginning of the case 5

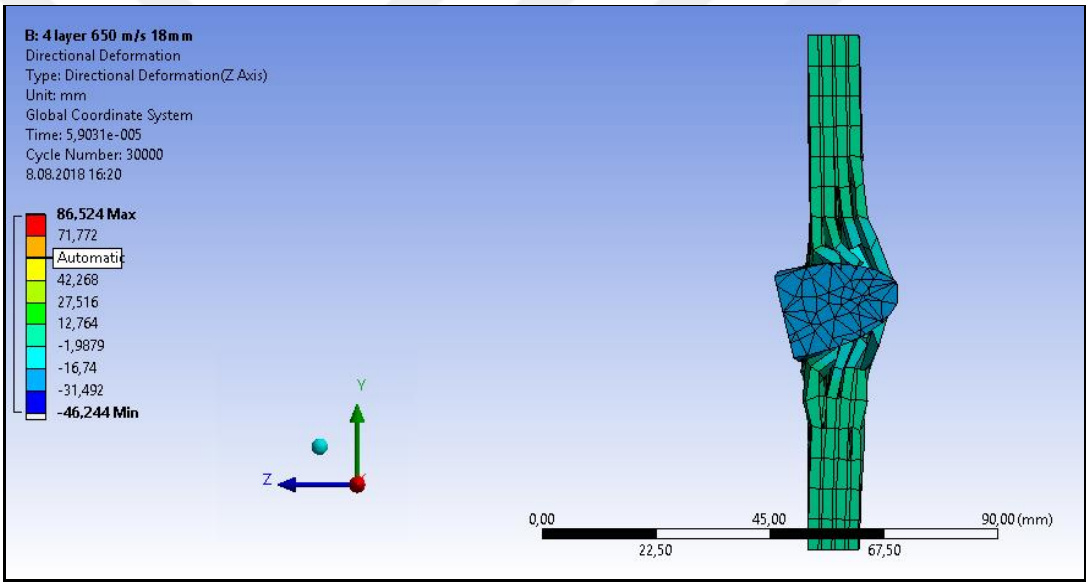

Figure 3.12. Ending of the case 5

In order to see the velocity limit of the failure, case 5 is done. Projectile's diameter is 18 millimeters, but the velocity is 650 m/s. A lot of different velocities from 400 to 1200 m/s are tried in this case. At this velocity all the layers are failed but projectile stuck in the armor. So, one can say that the limit is 650 m/s. Under that velocity, armor has a successful response.

3.1.6. Case 6 - 10 Layers, 500 m/s, 7.62 mm Diameter (Composite Matrix)

Armor has 10 layers. Each layer has two sub-layers which are epoxy-carbon and glass. Glass sub-layer has two millimeters thickness and epoxy has 0.7 mm thickness. Epoxy's density

is 1540 kg/m^3, Young's modulus is 95 GPa and Poisson's ratio is 0.27. Glass's density is 2530 kg/m^3, Young's modulus is 74.5 GPa and Poisson's ratio is 0.226. In other words, internal layers are glass and interlayer are epoxy. Geometry of layers is 100x100 millimeters square plate.

Projectile is in bullet shape. Its material is structural steel. Its velocity is 500 m/s. It has 7.62 mm diameter. Projectile is adjusted to conventional shape that used nowadays. Tip of the projectile is chosen pointy head, in order to make a greater impact at the armor.

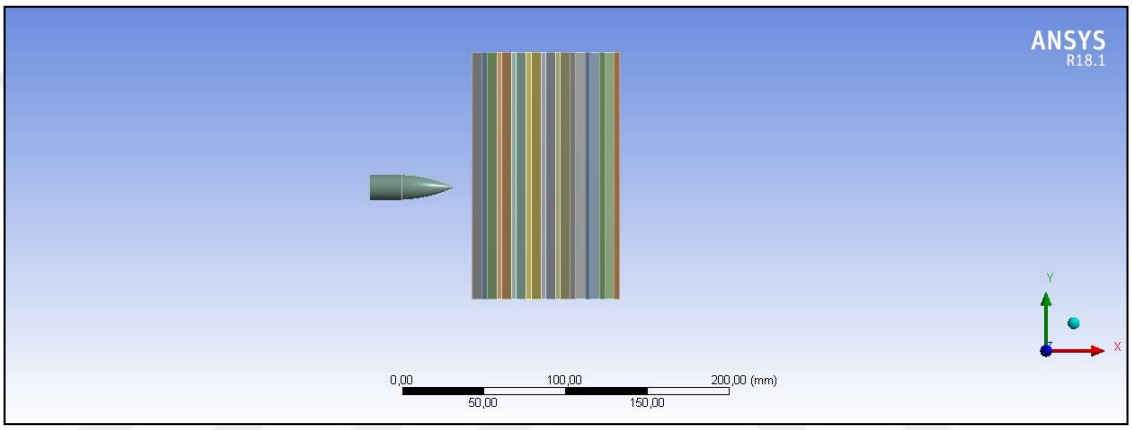

Figure 3.13. Beginning of the case 6

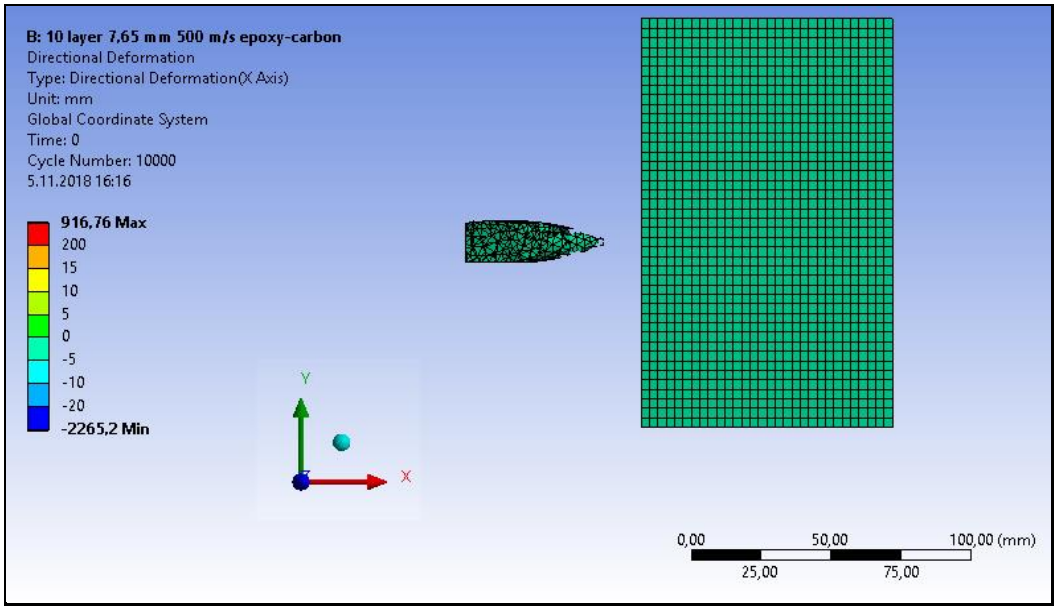

Figure 3.14. Case 6, step 1

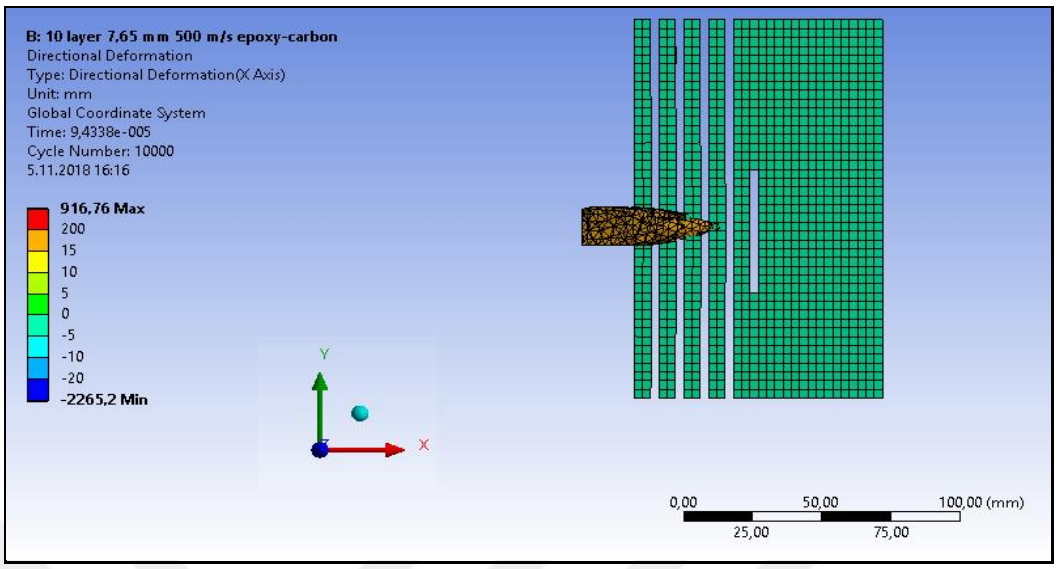

Figure 3.15. Case 6, step 2

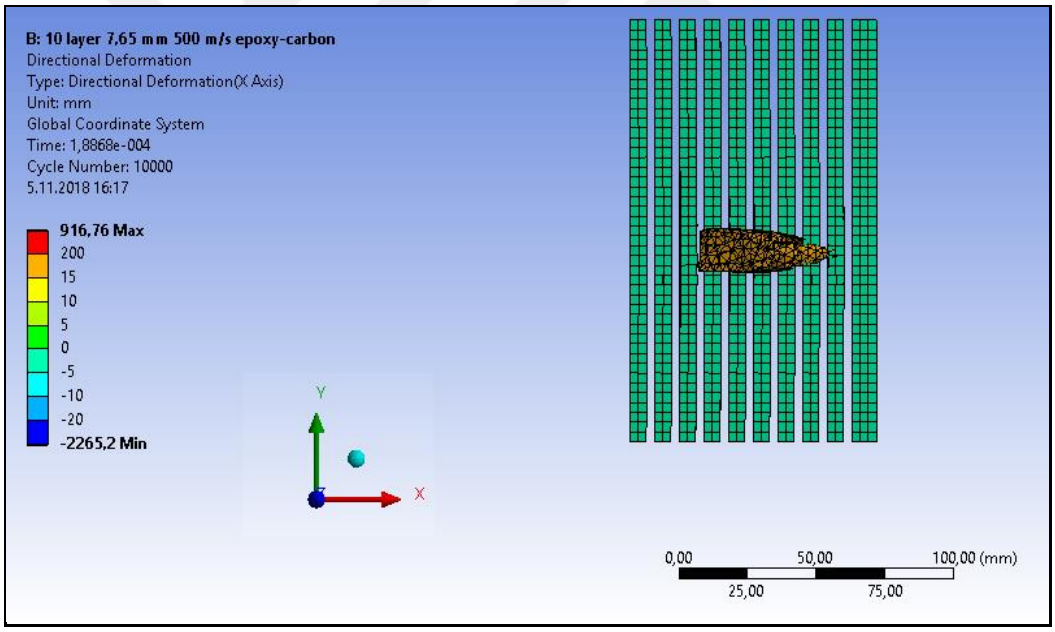

Figure 3.16. Case 6, step 3

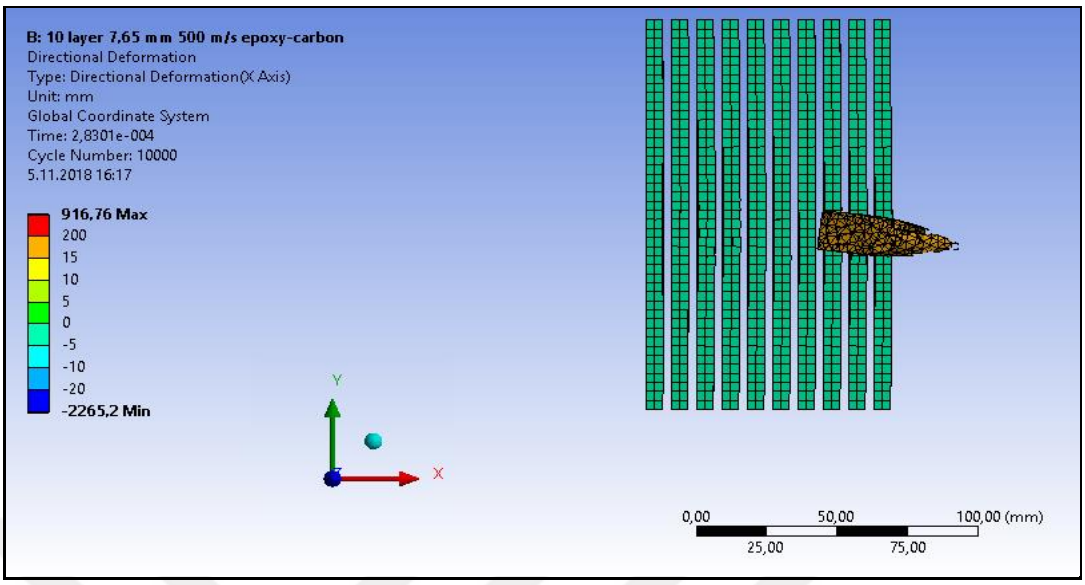

Figure 3.17. Case 6, step 4

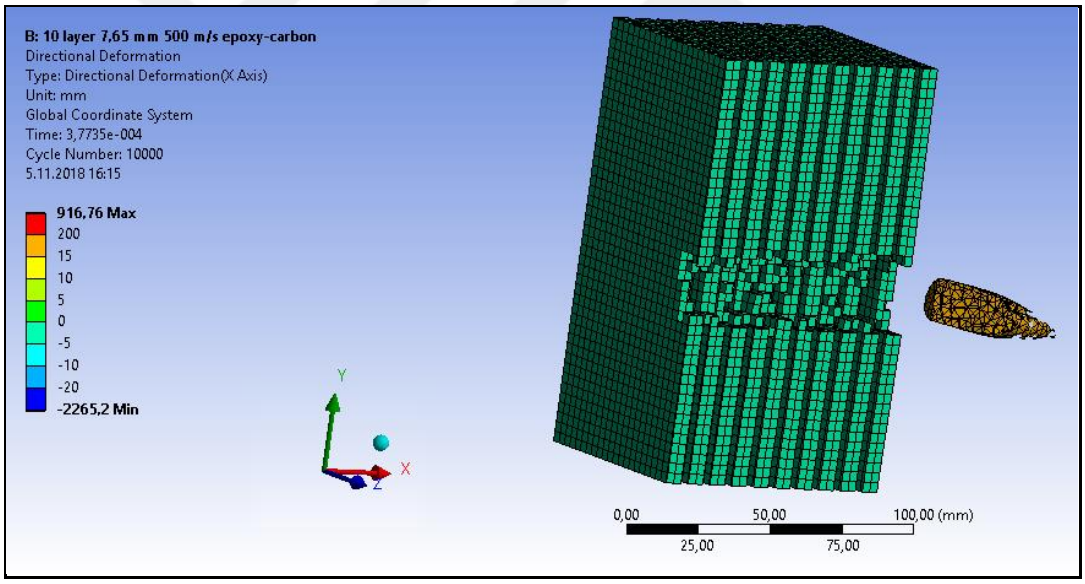

Figure 3.18. Ending of case 6

At case 6, shape of the projectile is investigated. The tip of the projectile is pointy.10 layers of material are put in front of the projectile to observe the effect of the tip of the projectile. Results show that pointy tip can make much bigger damage compared to other types. The shape of the projectile is inspired from military bullets.

3.1.7. Case 7 - 10 Layers, 500 m/s, 7.62 mm Diameter (Composite Matrix)

Armor has 10 layers. Each layer has two sub-layers which are copper alloy and glass. Glass sub-layer has two millimeters thickness and copper alloy has 0.7 mm thickness. In other words, internal layers are glass and interlayer are epoxy. Copper alloy's density is 8300 kg/m^3, Young's modulus is 110 GPa and Poisson's ratio is 0.34. Glass's density is 2530 kg/m^3, Young's modulus is 74.5 GPa and Poisson's ratio is 0.226. Geometry of layers is 100x100 mm square plate.

Projectile is in bullet shape. Its material is structural steel. Its velocity is 500 m/s. It has 7.62 mm diameter. Projectile is adjusted to conventional shape that used nowadays. Tip of the projectile is chosen pointy head, in order to make a greater impact at the armor. Purpose of this case is to investigate other materials for interlayer.

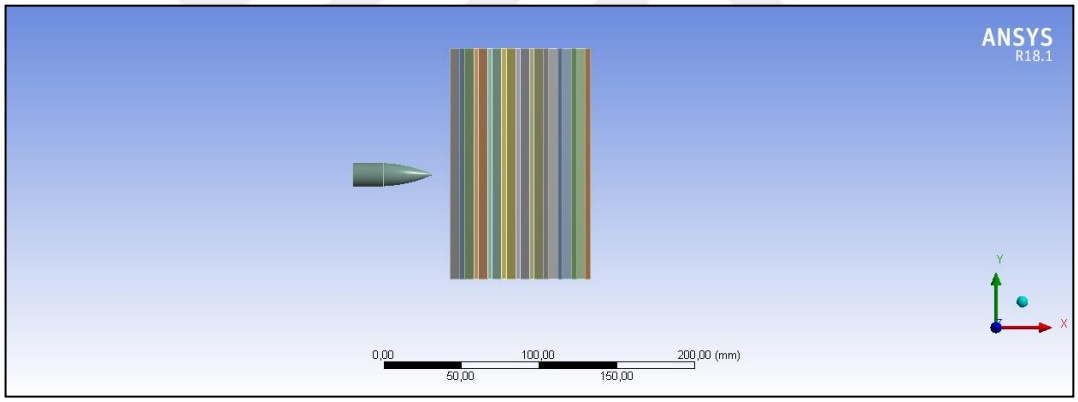

Figure 3.19.Beginning of the case 7

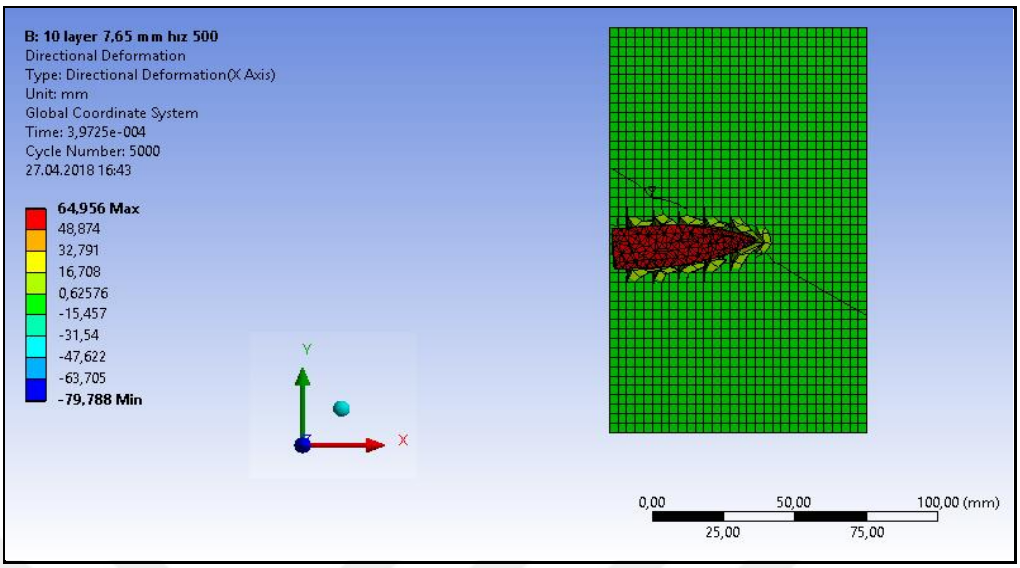

Figure 3.20. Ending of the case 6

After the projectile shape is investigated, another important issue is to choose the material. At this case different type of fibers are used to see the difference. With copper alloy, the projectile is stopped at the sixth layer. Although copper alloy has successful result, weight and cost of this armor is another important criterion. So, this case is mostly done for observation purposes.

3.1.8. Case 8 - 10 Layers, 500 m/s, 7.62 mm Diameter (Composite Matrix)

Armor has 10 layers. Each layer has two sub-layers which are SiC, epoxy and glass. Glass sub-layer has two millimeters thickness and SiC-epoxy has 0.7 mm thickness. In other words, internal layers are glass and interlayer are SiC-epoxy. SiC-epoxy composite is calculated. 10 percent SiC, 90 percent epoxy is decided for this composite. SiC-Epoxy's density is 3100 kg/m^3, Young's modulus is 56 GPa and Poisson's ratio is 0.36. Glass's density is 2530 kg/m^3, Young's modulus is 74.5 GPa and Poisson's ratio is 0.226. Geometry of layers is 100x100 mm square plate.

Projectile is in bullet shape. Its material is structural steel. Its velocity is 500 m/s. It has 7.62 mm diameter. Projectile is adjusted to conventional shape that used nowadays. Tip of the projectile is chosen pointy head, in order to make a greater impact at the armor. Purpose of this case is to investigate other materials for interlayer.

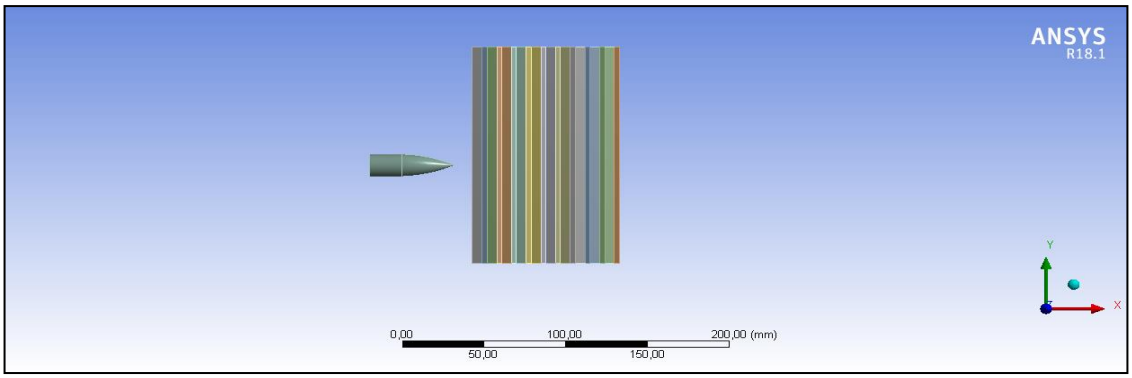

Figure 3.21. Beginning of the case 8

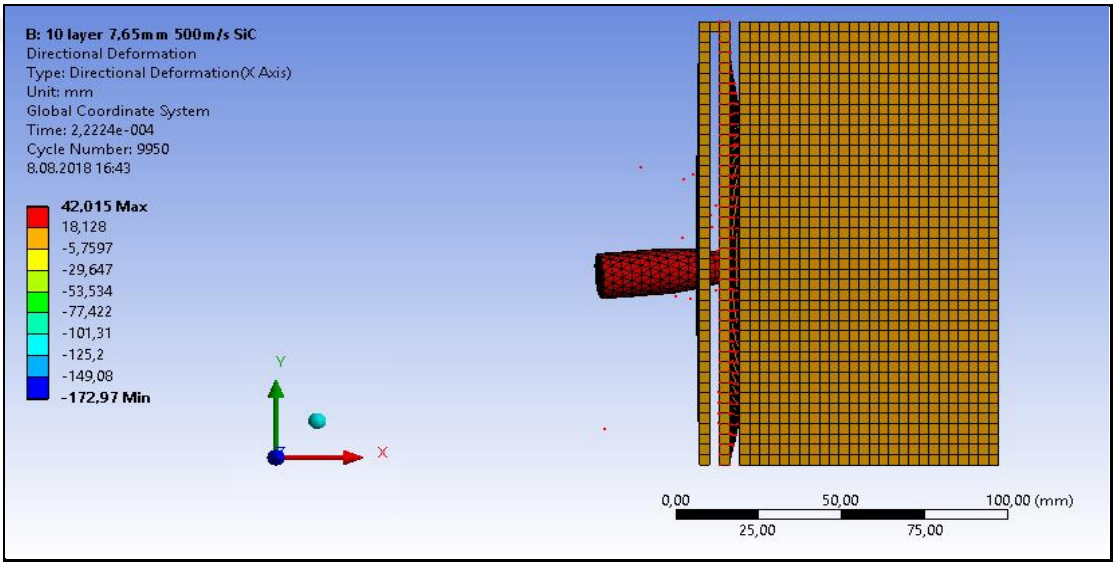

Figure 3.22. Case 8, step 1

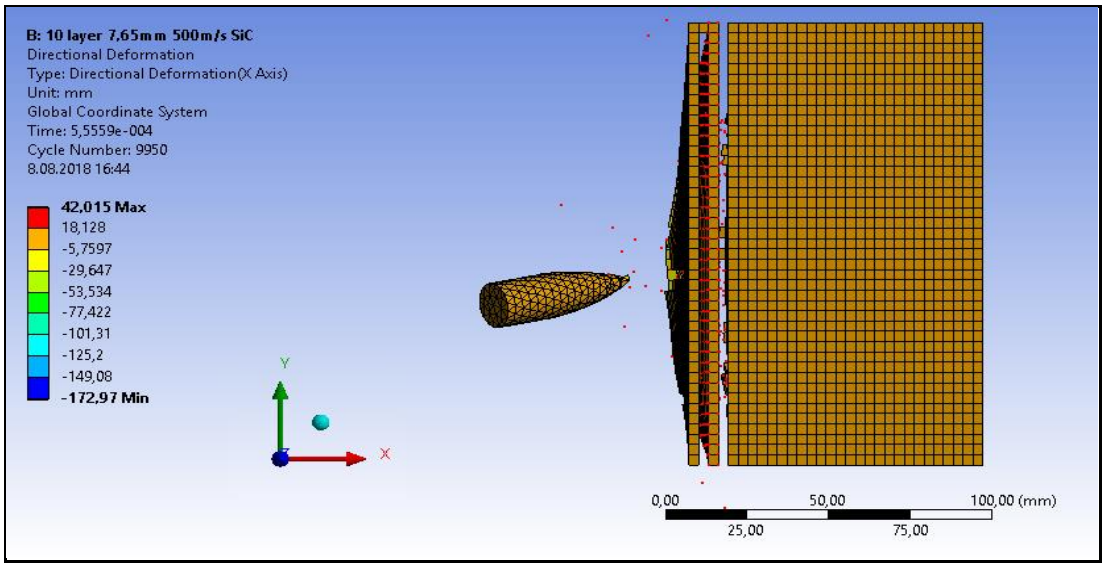

Figure 3.23. Case 8, step 2

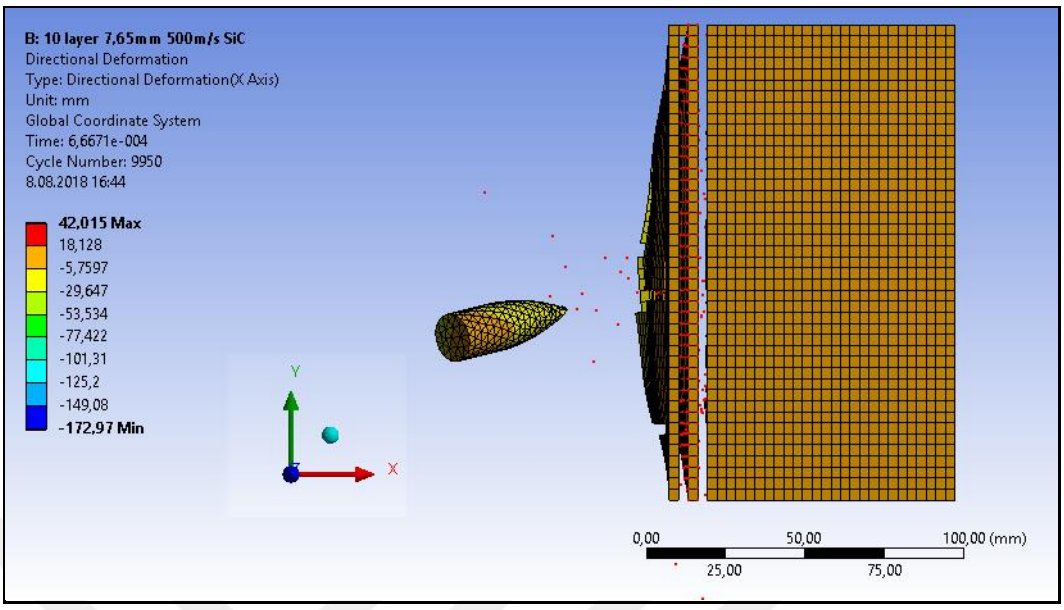

Figure 3.24. Side view of ending of the case 8

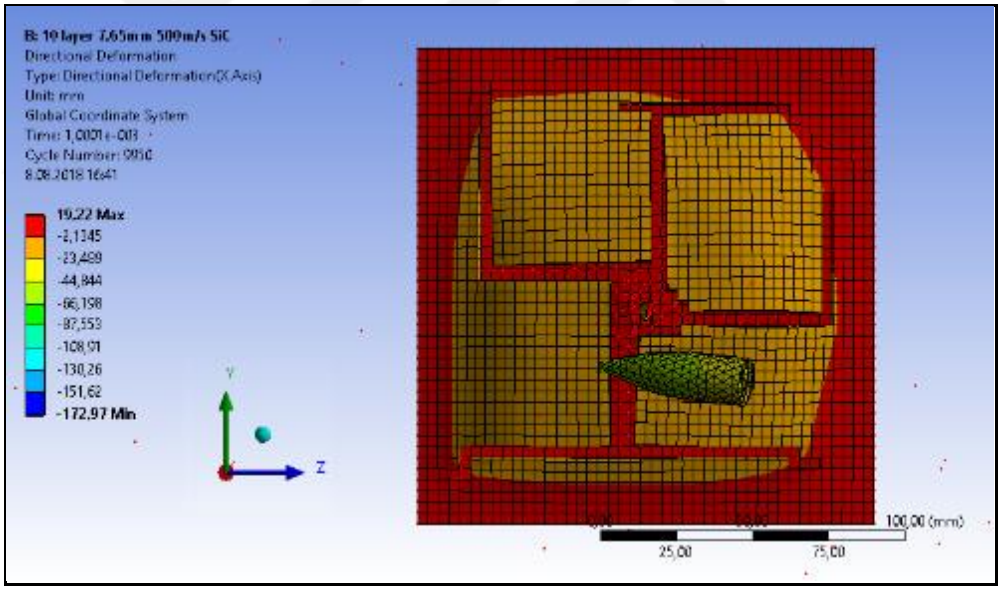

Figure 3.25. Front view of ending of the case 8

Compared to case 7, this time, a tougher material which is Sic, is chosen. The results show that the projectile bounces back from the second layer. And SiC is tougher than copper-alloy.

3.1.9. Case 9 – Tube Test

Projectile is shot at the middle of a circular tube to see the penetration. Several materials are tested and observed. Tube is one meter long and its diameter is 15 mm. Bullet is 7.62 mm

pointy tip. The experiment has helped in material selection. As it is known, main purpose of the armor is resistance to projectile, avoid the penetration if possible. The penetration distance can give information about resistance of that material.

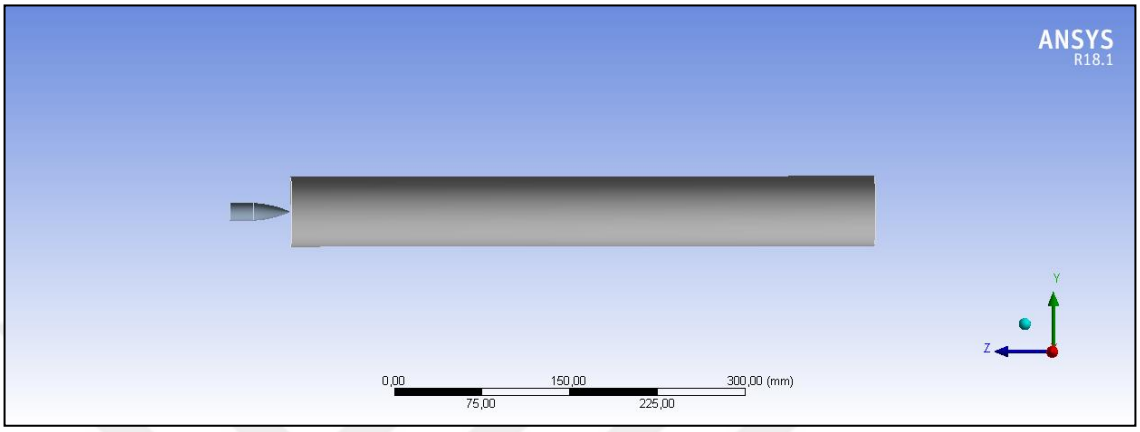

Figure 3.26. Beginning of tube test

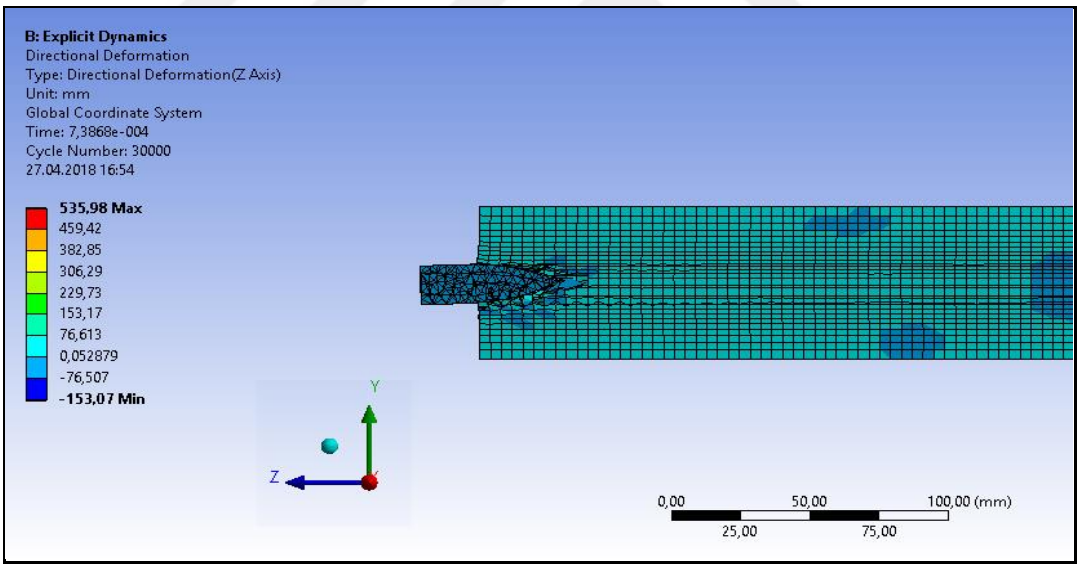

Figure 3.27. Ending of tube test

Penetration distances are shown at the Table 3.1. Minimum penetration is the desired result, but weight, transparency and cost are other important properties that need to be considered. So, after this test epoxy-resin is the most suitable material for our experiment although there are tougher materials exist.

Table 3.1. Results of tube test

Material of the tube	Penetrated distance (mm)
Al_2O_3	3.4
AlON	0
Epoxy-resin	11.5
Glass	29
PC	42
PMMA	168
Polypropylene	33
Spinel	0
Quartz glass	8.3

3.1.10. Case 10 – Honeycomb Test

Design of the armor is change. Honeycomb shaped glass tubes are put into epoxy plates which are also honeycomb shaped. The purpose of this geometry is to have additional fibers at direction-z. Hexagons have 15 mm sidelines. Glass tubes have six millimeters of thickness and epoxy-resin plates have four millimeters thickness. So 6mm of glass and four millimeter of epoxy-resin behind it, make one layer of armor. In this test five layers are combined. It has a similar structure to plate to plate armors. Bullet is shot to two different points which you can see at the Figure 3.28. Velocity of the bullet is 500 m/s.

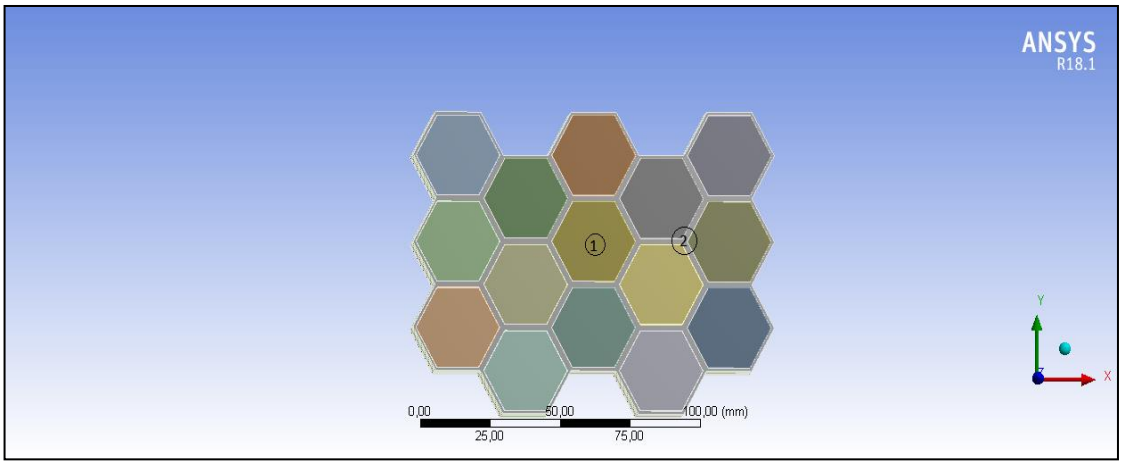

Figure 3.28. Front view of the honeycomb armor

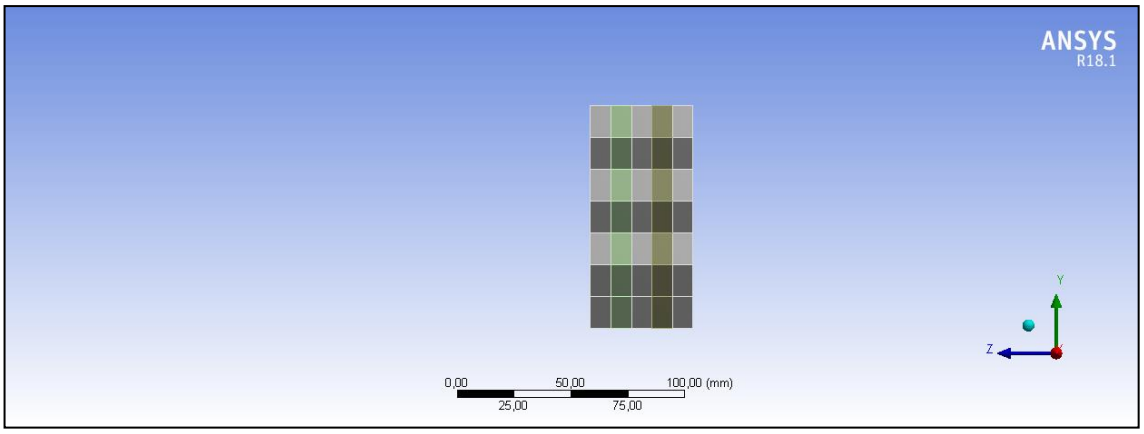

Figure 3.29. Side view of the honeycomb armor

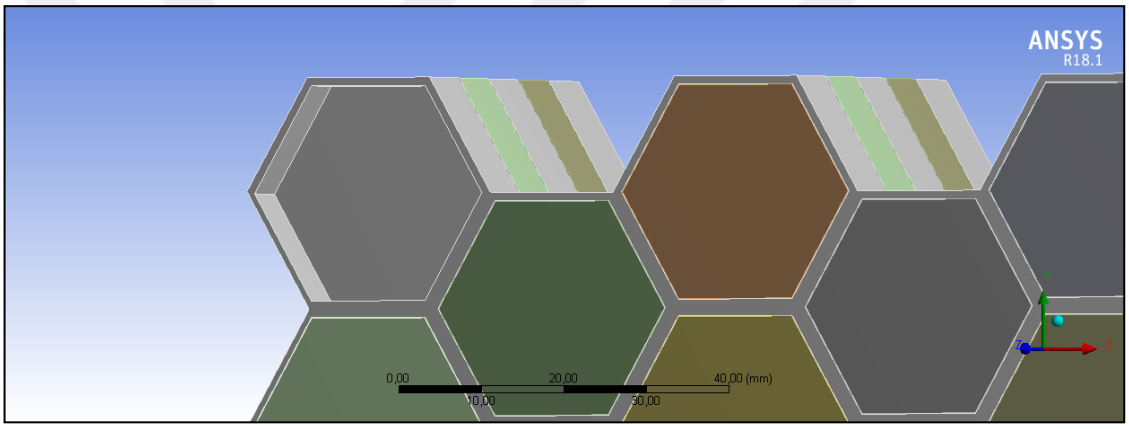

Figure 3.30. Detailed view of the glass tubes of honeycomb armor

7.62 mm projectile is shot at point 1. Purpose of this case is to see the effect of extra fiber resistance at z direction. Expectation is to create a tougher armor that can stop the projectile.

In Figure 3.33 and Figure 3.34, one sees that the armor is completely failed and destroyed. Then it can be observed that at point 1, there are no z direction resistance and the design need to be updated.

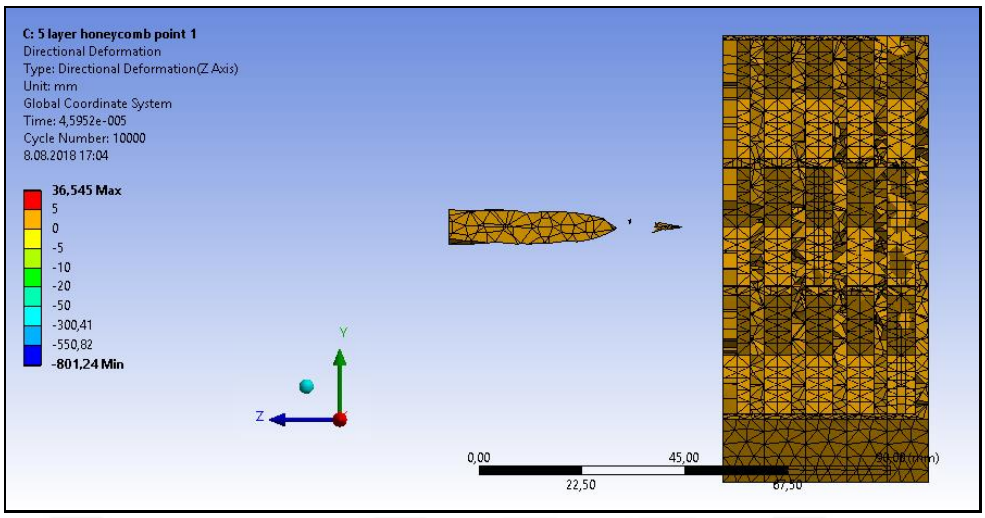

Figure 3.31. Beginning of the point 1 shot

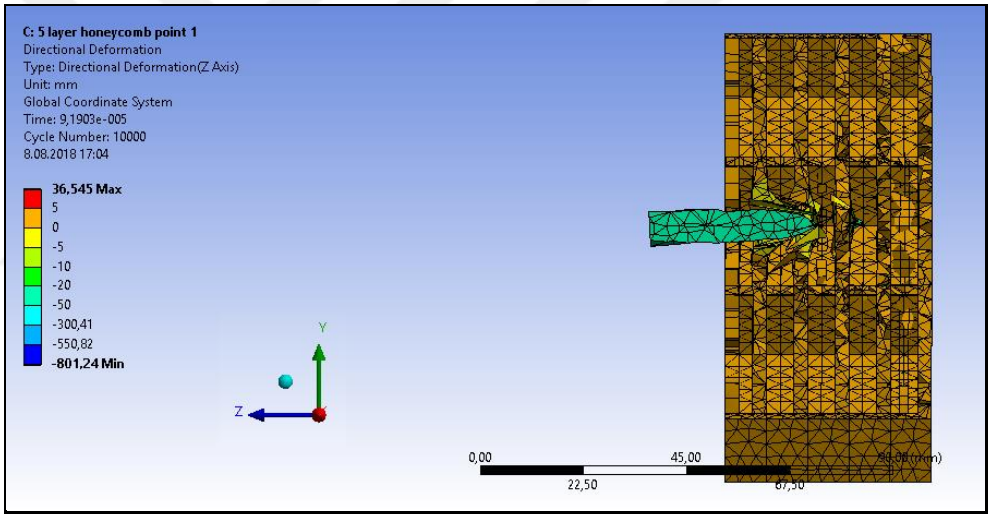

Figure 3.32. Progression of the point 1 shot

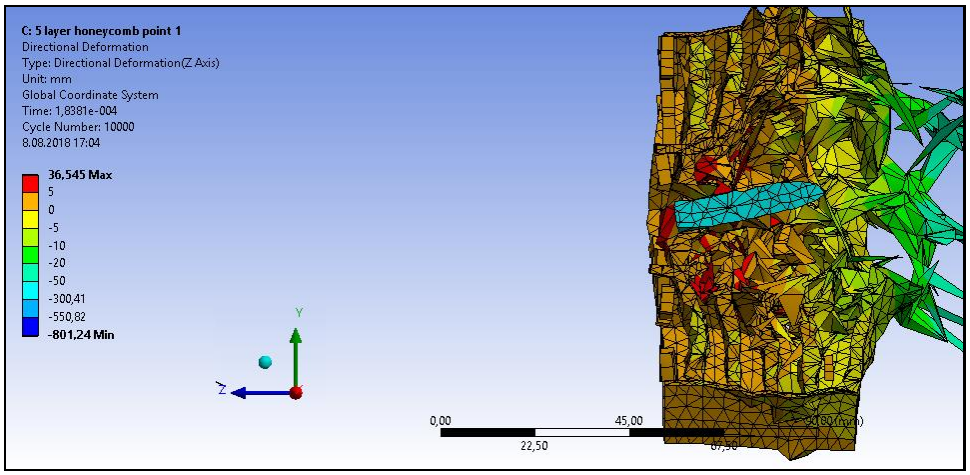

Figure 3.33. Ending of the point 1 shot

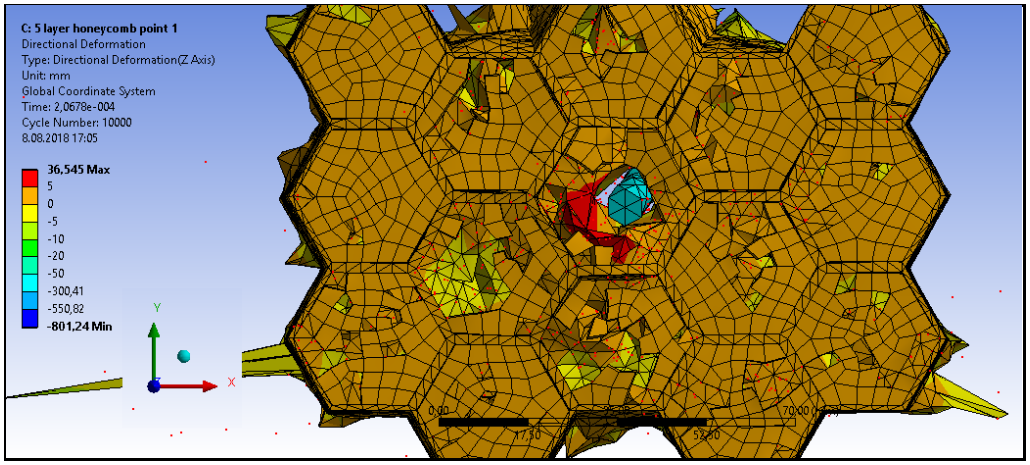

Figure 3.34. Front view of ending of the point 1 shot

7.62 mm bullet is shot at point 2. Purpose of this case is to see the effect of extra fiber resistance at z direction. Expectation is to create a tougher armor that can stop the projectile. But this time at point 2, one expects to see more resistance than point 1.

In Figure 3.38, one sees that, this time there is more resistance and one assume that it is come from z direction fibers. This extra resistance is important for our objective. Projectile stuck in second layer. Results show us, z direction fiber resistance can be occurred at some points of the armor, it is not homogeneous.

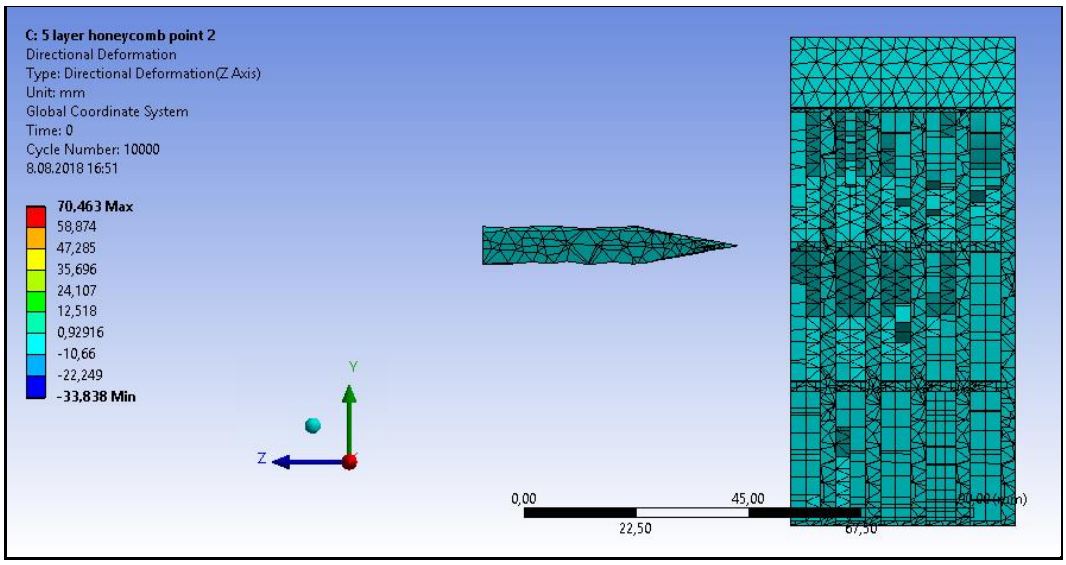

Figure 3.35. Beginning of the point 2 shot

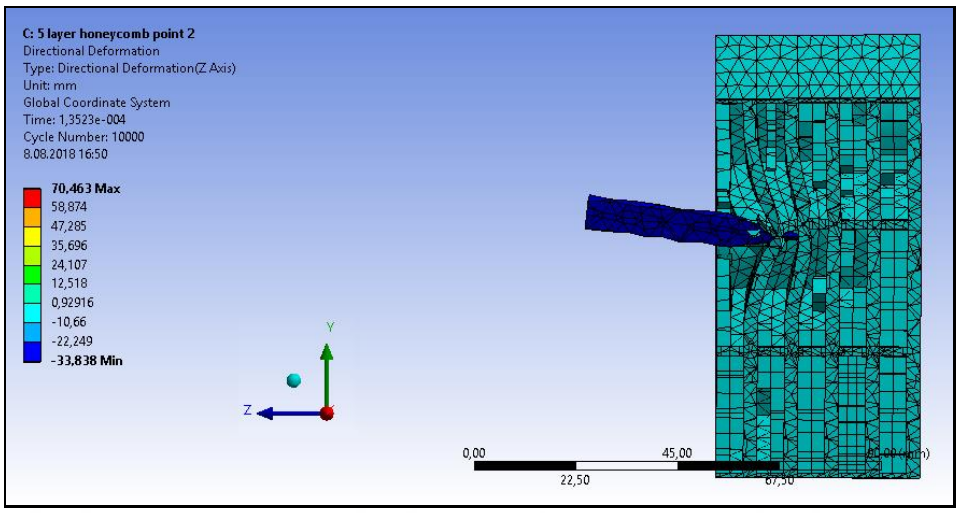

Figure 3.36. Step 1 of the point 2 shot

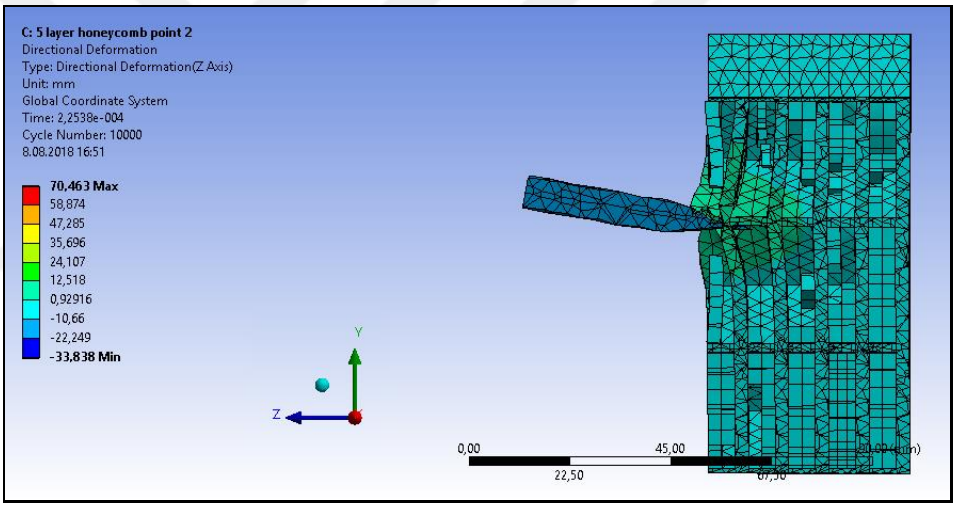

Figure 3.37. Step two of the point 2 shot

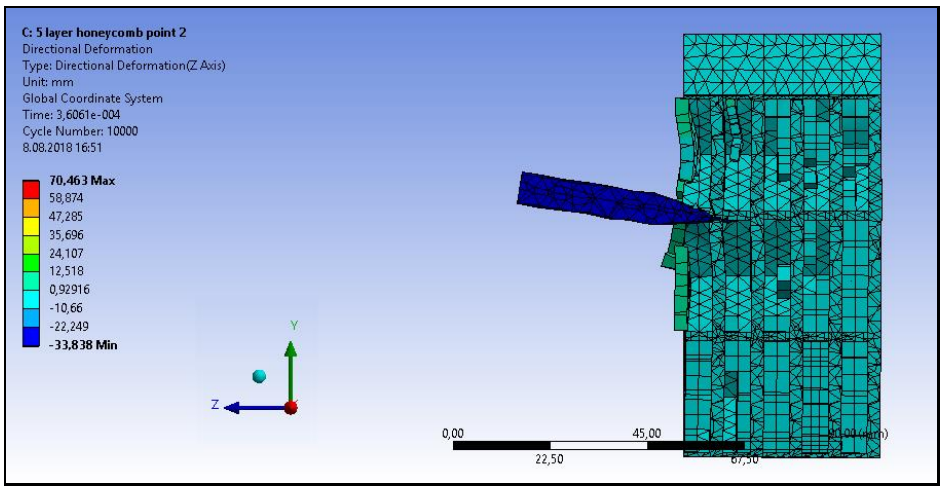

Figure 3.38. Ending of the point 2 shot

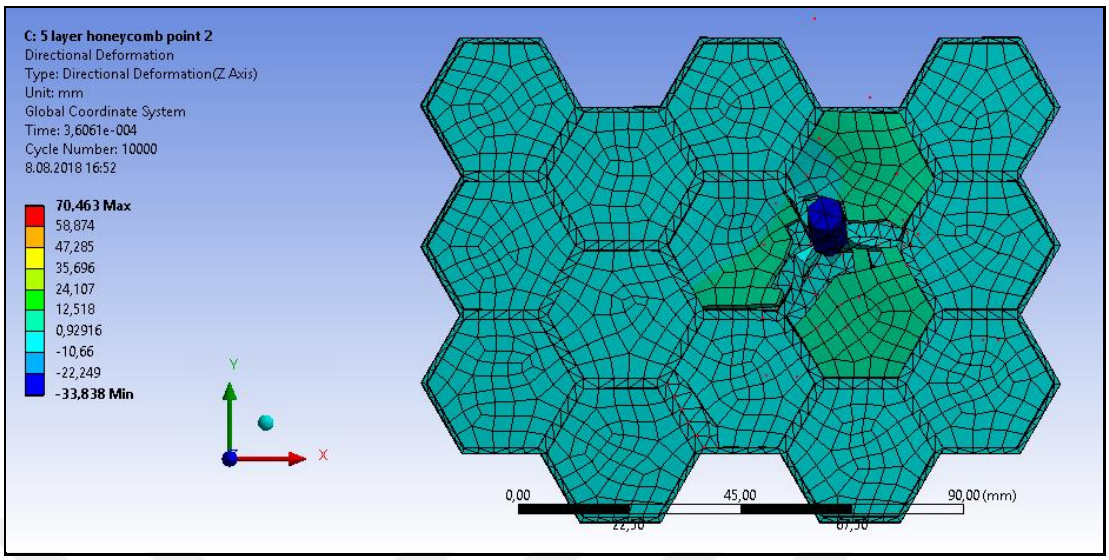

Figure 3.39. Front view of ending of the point 2 shot

In conclusion, fibers at direction-z influence stopping to projectile and this effect is not small to avoid. But at the above design it is not distributed properly. As you can see in the results, at the point 2 which has fibers at direction-z, projectile cannot go through the armor. But at the zones like point 1 which does not have any fibers at direction-z, projectile can go through the armor. These zones have created vulnerability at this design.

3.1.11. Case 11 – Honeycomb Model with Different Layer Formation

Case 11 is the repetition of case 10 except the positions of the layers are changed. It can be seen at the Figure 3.40. Geometry is simulated after the result of the first honeycomb model is observed. The main reason of the honeycomb model is to have extra fibers at z-direction. But at the previous model, these fibers can only exist at sides of the glass tubes so that create an inhomogeneity. The resistance, which fibers need to create, cannot be seen at the center of the individual tubes. With the new design, fibers at z-direction are distributed as homogeneously as possible. So, resistance will be approximately same at all points of the armor. It will have same resistance wherever the projectile hit.

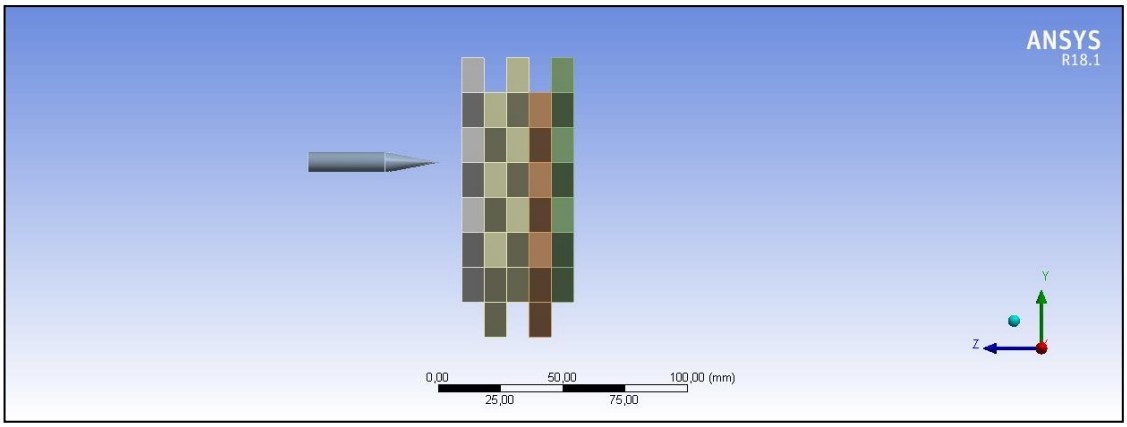

Figure 3.40. Side view of the new honeycomb model

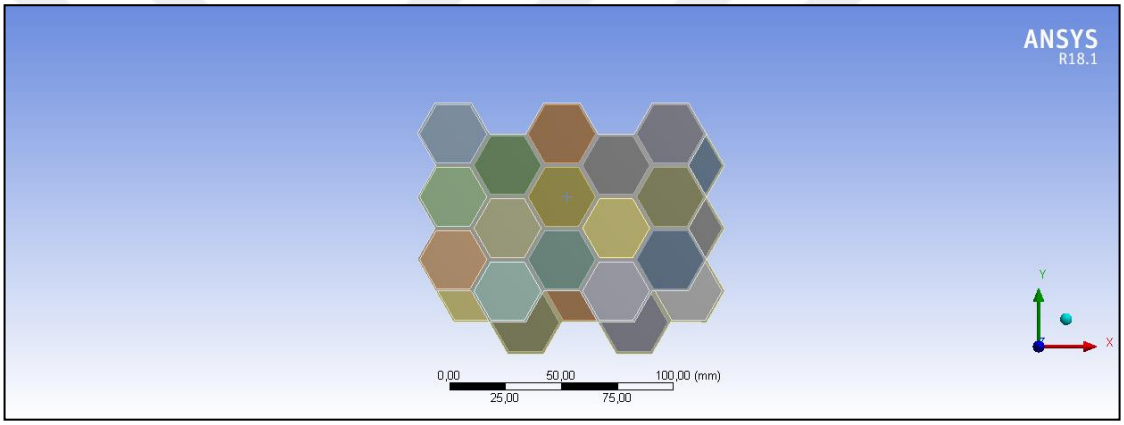

Figure 3.41. Front view of the new honeycomb model

7.62 mm bullet is shot at point 1. The purpose of this case is to distribute the z direction fibers homogeneously and get same reactions at any point. And projectile finally goes through two layers. It is same with the case 11, point 2 shot.

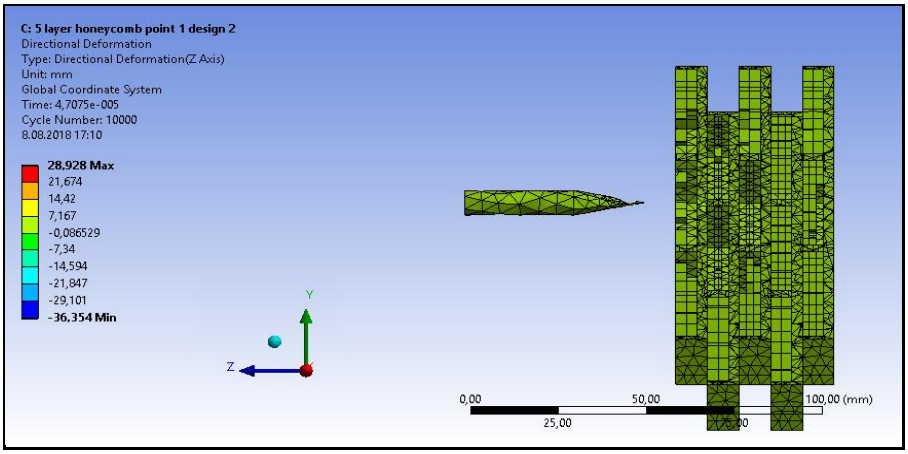

Figure 3.42. Beginning of the point 1 shot

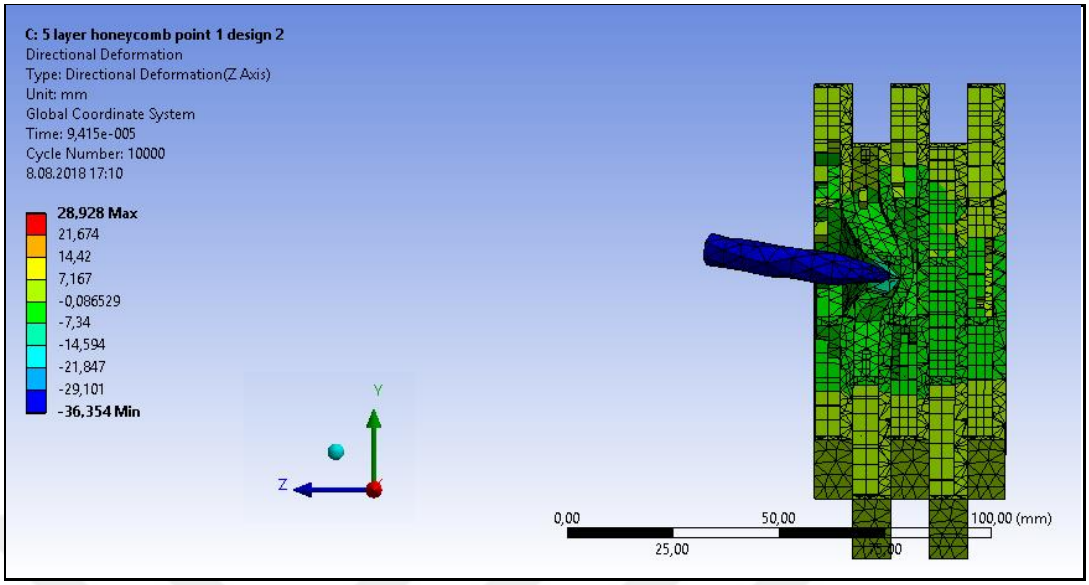

Figure 3.43. Progression of the point 1 shot

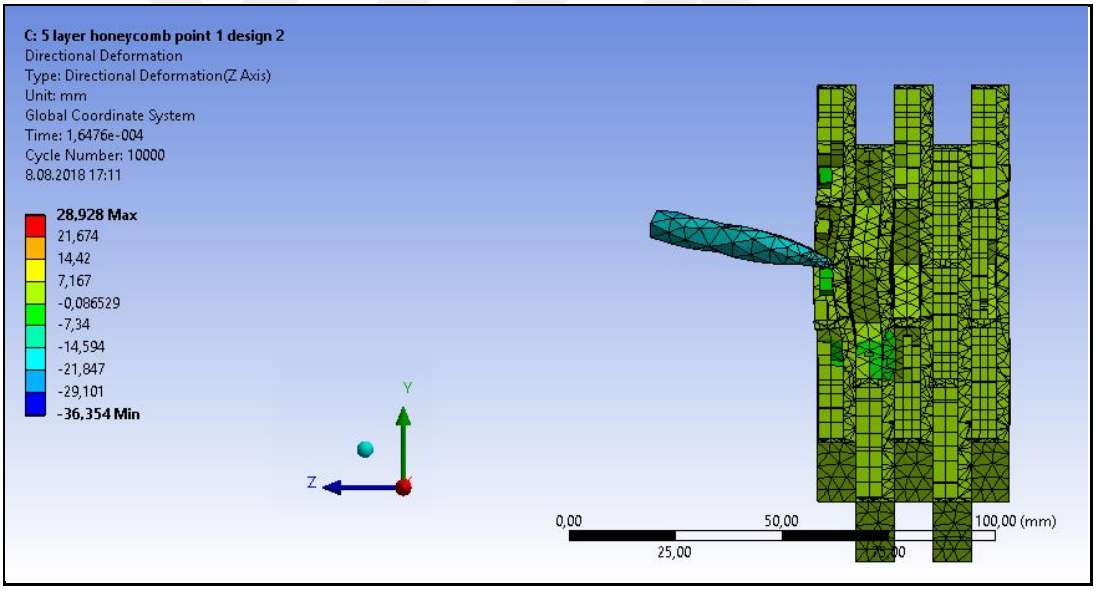

Figure 3.44. Ending of the point 1 shot

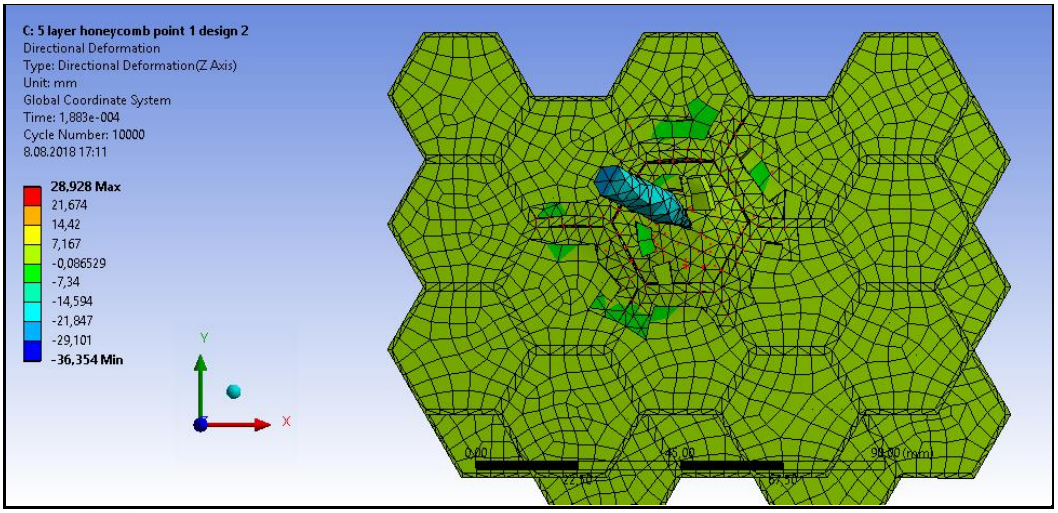

Figure 3.45. Front view of ending of the point 1 shot

7.62 mm bullet is shot at point 2. Projectile goes through two layers. Now, one can make general assumptions. At this design, resistance is distributed properly. Expected results are observed at this case.

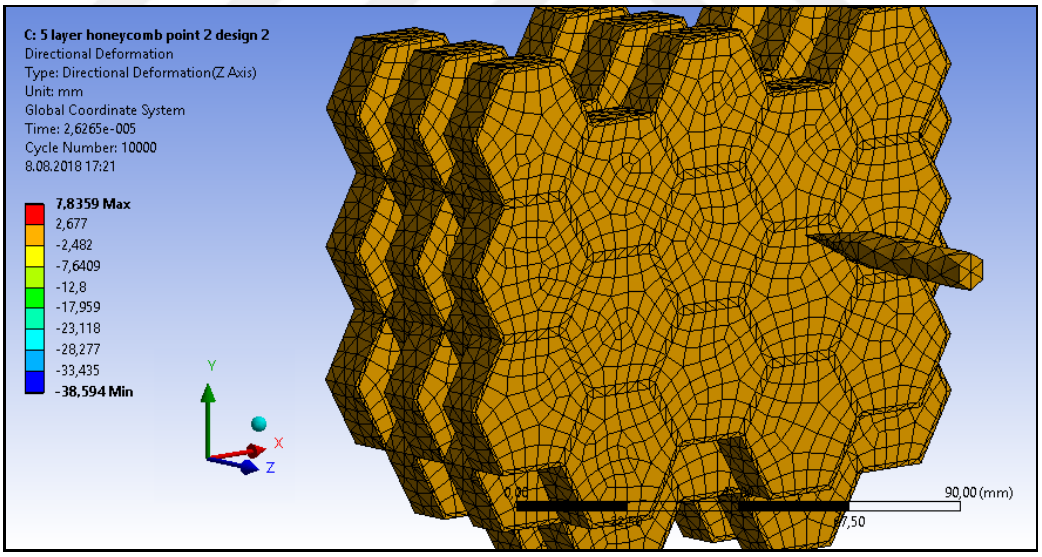

Figure 3.46. Beginning of the point 2 shot

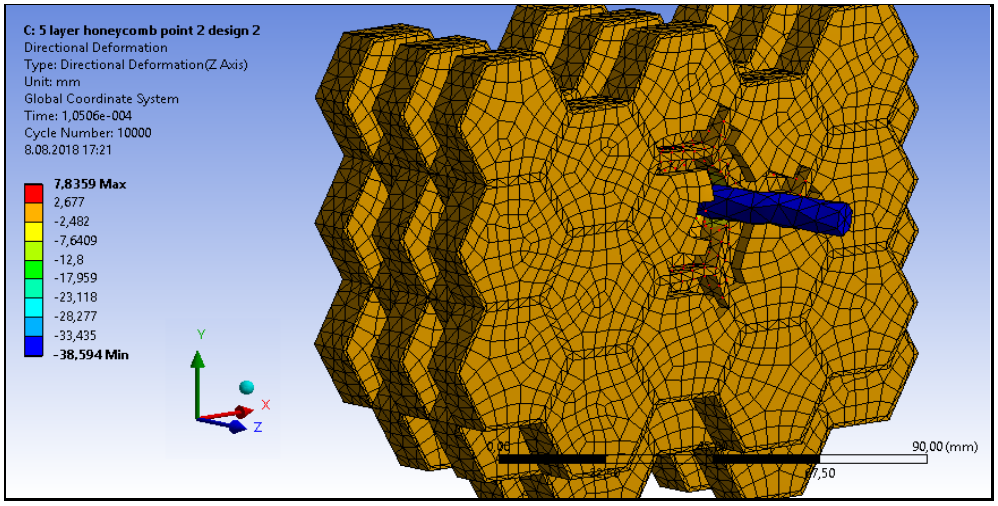

Figure 3.47. Step 1 of the point 2 shot

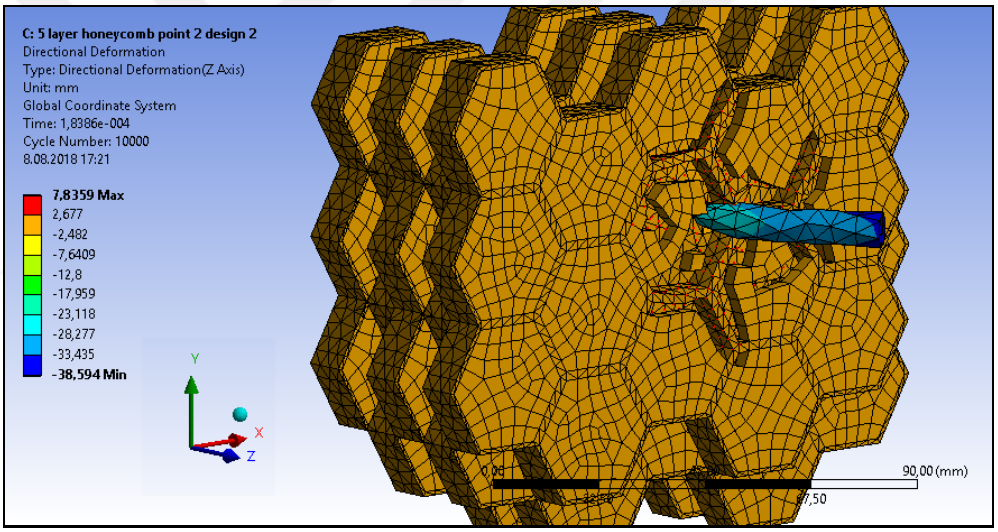

Figure 3.48. Step 2 of the point 2 shot

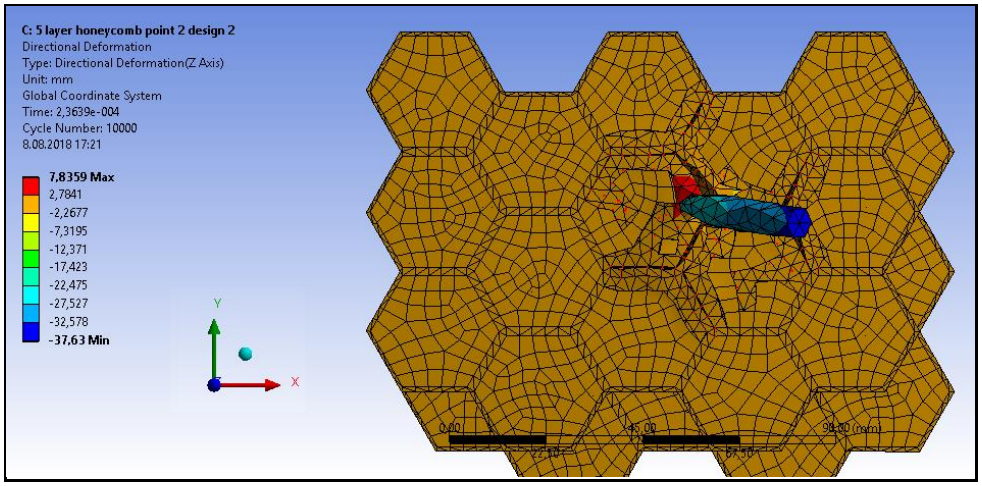

Figure 3.49. Front view of ending of the point 2 shot

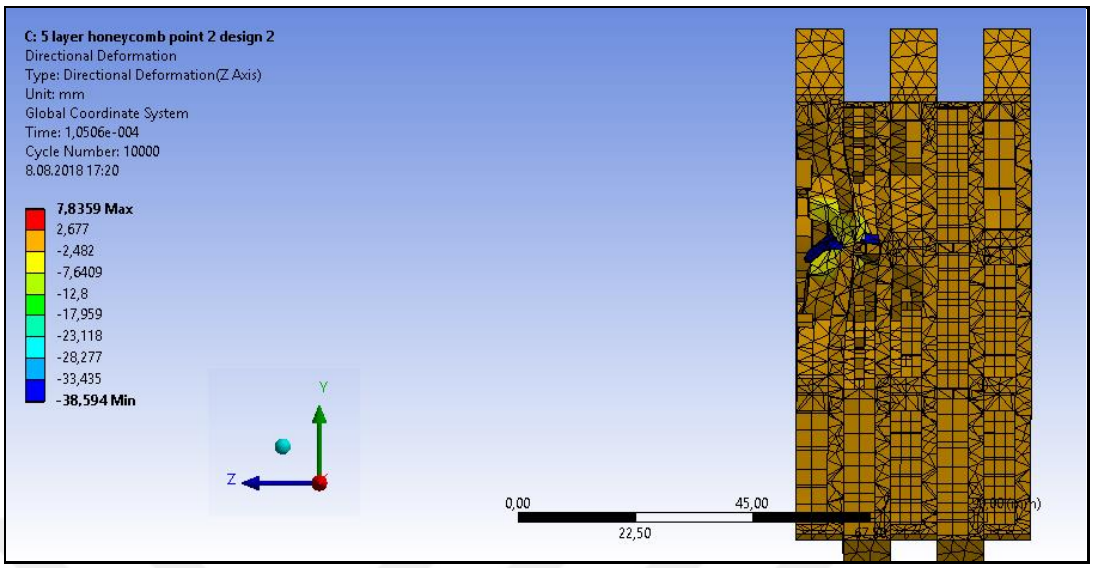

Figure 3.50. Ending of the point 2 shot

When the fibers at z-direction, distributed homogenously, armor has same reaction to projectile, independent from area where the projectile impacts. Difference between the designs of case 10 and 11, at case11, there are no vulnerabilities such as the point 1 at case 10.

To have a general idea of the other points of the armor, projectile is shot to side of the armor. By doing this, it will be seen that if the side points are vulnerable or not.

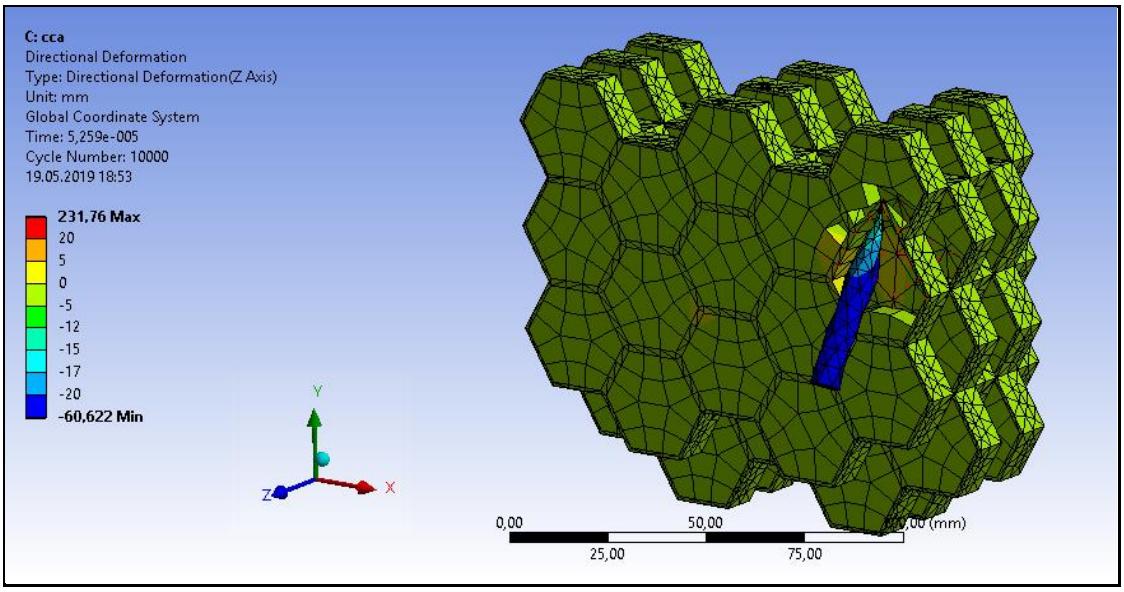

Figure 3.51. Side shot of the armor #1

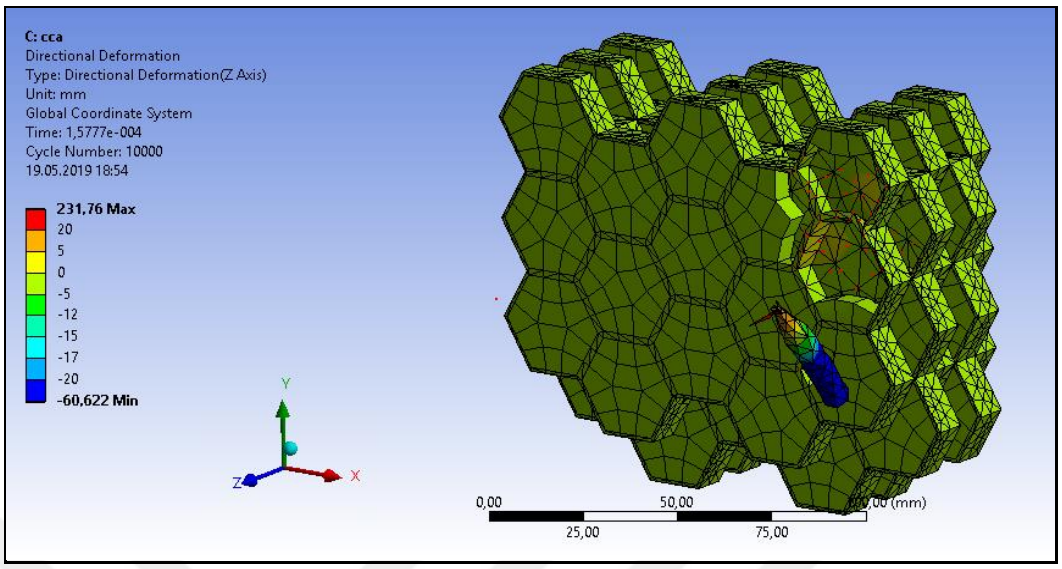

Figure 3.52. Side shot of the armor #2

As it is shown in Figure 3.51 and Figure 3.52 projectile penetrate the first layer and bounce back from second layer. It can be said that, beside the critical points, armor is achieved its objective at all points of the armor.

3.1.12. Case 12 – 21 mm Bullet

At this case, everything is similar with trial 11 but the bullets are bigger. And the velocity (288 m/s) of the bullet is adjusted in order to preserve the kinetic energy. Main purpose of this case is to see what is happening when bullet diameter / honeycomb diameter ratio increase. In order to observe the difference, all the other inputs are conserved exactly same.

21 mm bullet is shot at point 1. Bullet can only go through the first three layers. (Figure 3.53)

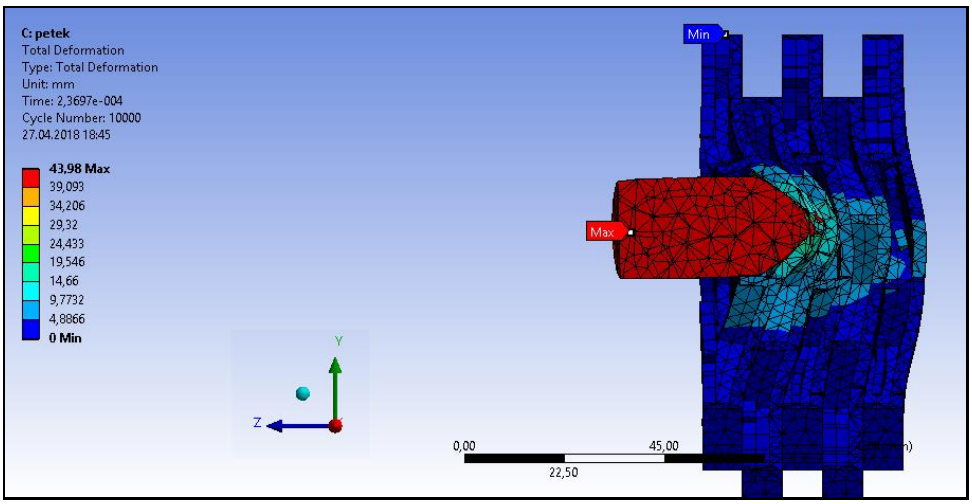

Figure 3.53. Ending of the point 1 shot

21 mm bullet is shot at point 2. Projectile can only go through the first four layers. (Figure 3.54)

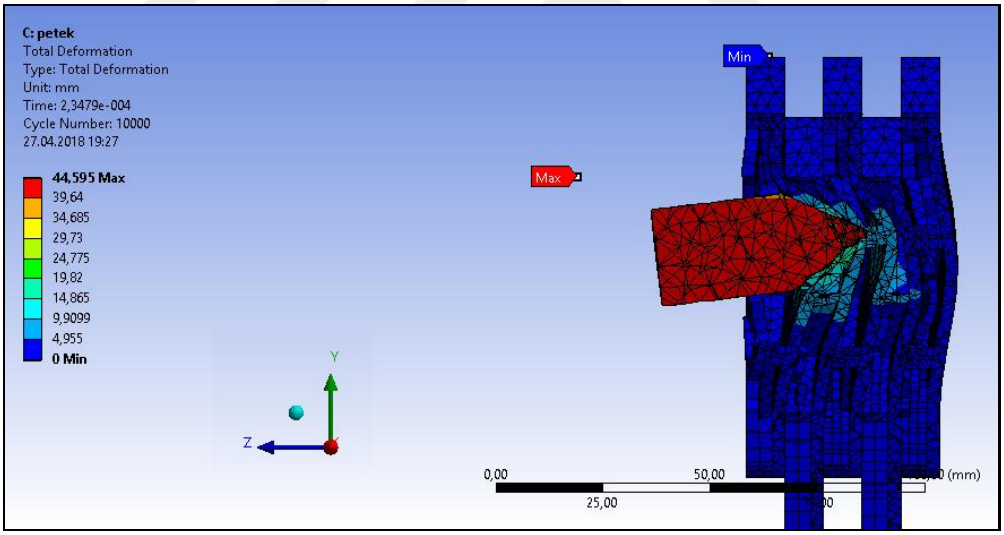

Figure 3.54. Ending of the point 2 shot

At this case, after the design and material selection is completed of our armor, extreme conditions are tested. Projectile is much bigger than it should be. Even so, armor keeps its functionality and stops the projectile with a success.

3.1.13. Case 13 – Larger armor

Case 13 is the repetition of case 11 but this time armor is triple times larger. Aim of this trial is to see the reaction of the armor when it is larger. Projectile velocity is 500 m/approximate surface area is 300x300 mm. Geometry type and materials are exactly same with case 11.

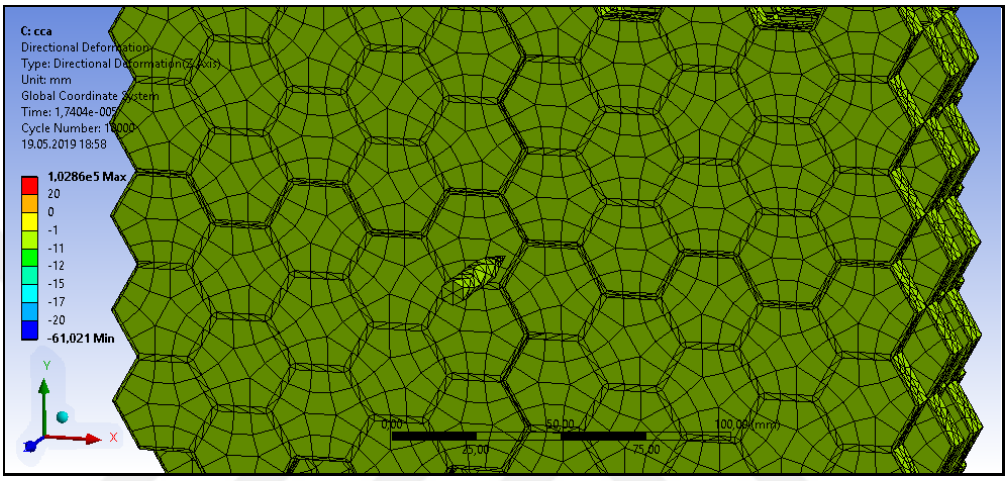

Figure 3.55. Shot on larger armor step 1

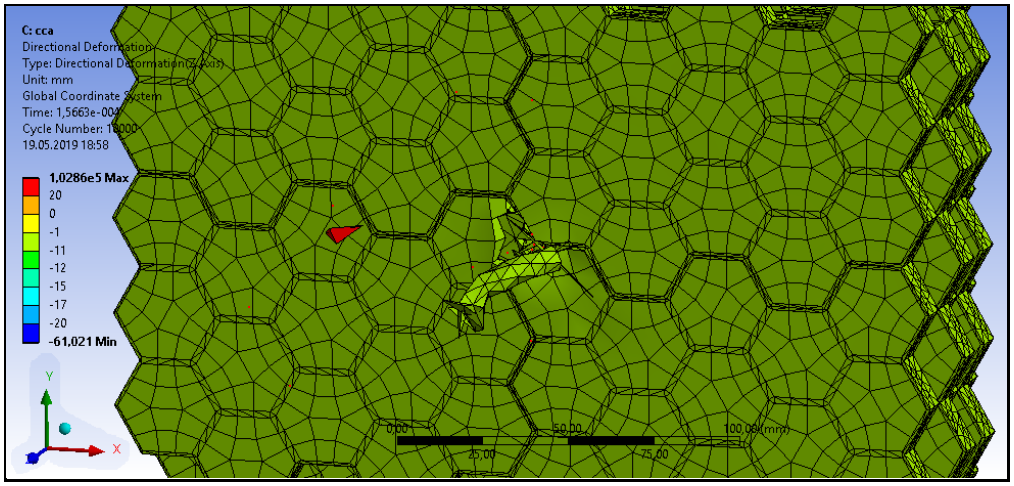

Figure 3.56. Shot on larger armor step 2

This trial shows that enlargement of the armor has similar but better results. Projectile can penetrate only to second layer. When supported from the side surfaces of the armor, larger armor reacts better than smaller one.

4. MODELING

At this part, prediction of armor's behavior is determined. By the help of several rules, equations and initial material properties, mechanical properties of the final material are occurred. The first step is to use randomly oriented short fiber composite model. With this model, necessary inputs for CCA model are found. After that with CCA model, mechanical properties of armor which is final material and assemblage of resin-epoxy and float glass, are found and can be discussed on. At Table 4.1, properties of resin-epoxy and float glass are presented.

Table 4.1. Properties of materials

	Resin-epoxy (matrix)	**Float Glass (fiber)**
Density (ρ)	$1160\,\frac{\mathrm{kg}}{\mathrm{m}^3}$	$2530\,\frac{\mathrm{kg}}{\mathrm{m}^3}$
Young's Modulus (E)	$3.78\text{x}10^9\text{Pa}$	$7.45\text{x}10^{10}\text{Pa}$
Poisson's Ratio (ν)	0,35	0.22629
Bulk Modulus (K)	$4.25\text{x}10^9\text{Pa}$	$4.54\text{x}10^{10}\text{Pa}$
Shear Modulus (G)	$1.4\text{x}10^9\text{Pa}$	$3.04\text{x}10^{10}\text{Pa}$
Volume fraction (V)	0.424	0.576

(4.1), (4.2), (4.3), (4.4), (4.5), (4.6),

(4.7) are the equations of randomly oriented short fiber composite. CCA analysis needs some starting values in order to proceed. These values are experimental values. But this research does not have experimental setup, so to find those starting values, randomly oriented short fiber composite equations are used. Before applying CCA model and starting the calculations, it is necessary to find some initial values to proceed. These values are $E_1, G_{12}, G_{23}, \nu_{12}, K$. In order to find these values, properties of matrix and fiber, which are presented in Table 4.1, put in equation (4.1), (4.2), (4.3), (4.4), (4.5), (4.6),

(4.7);

$$\eta_L = \frac{\frac{E_f}{E_m} - 1}{\frac{E_f}{E_m} + 2\left(\frac{l_f}{d_f}\right)} \tag{4.1}$$

$$\eta_T = \frac{\frac{E_f}{E_m} - 1}{\frac{E_f}{E_m} + 2} \tag{4.2}$$

$$\eta_G = \frac{\frac{G_f}{G_m} - 1}{\frac{G_f}{E_m} + 1} \tag{4.3}$$

$$E_L = \frac{1 + 2(\frac{l_f}{d_f})\eta_L V_f}{1 - \eta_L V_f} \tag{4.4}$$

$$E_T = \frac{1 + 2\eta_T V_f}{1 - \eta_T V_f} \tag{4.5}$$

$$G_{LT} = \frac{1 + \eta_G V_f}{1 - \eta_G V_f} \tag{4.6}$$

$$\nu_{LT} = V_f \nu_f + V_m \nu_m \tag{4.7}$$

At the above equations, longitudinal direction which is denoted with L is direction 1. Direction 1 is axis-z in finite element analysis. Transverse direction, which is denoted with T, is direction 2. Direction 2 is axis-x in finite element analysis.

E_L,ν_{LT},G_{LT} which are E_1,G_{12} ,ν_{12} are found with randomly oriented short fiber composite equations. 2-3 directions are isotropic directions so K and G_{23} are equal to K_m and G_m. They are taken from Table 4.1.

Table 4.2. Results of randomly oriented short fiber composite calculations

E_1	$4.4515x10^{10}$Pa
G_{12}	$1.4x10^{9}$Pa
G_{23}	$6.7898x10^{8}$Pa
K	$4.4x10^{9}$Pa
ν_{12}	0.2787

E_1,G_{12},G_{23},ν_{12}, K are found and presented in Table 4.2.After finding the necessary initial values, put these values into equations (2.24), (2.25), (2.26), (2.27) and (2.28) of concentric

cylinder assemblage model (explained in background) to find the constants of CCA model. Matlab code is used to solve these equations and presented in appendix a.

Defined stress result array is taken from finite element analysis to check the accuracy of the simulation. Now with the help of the constants that is founded and Matlab, effective properties are calculated. Effective properties are shown in Table 4.3.

Table 4.3. Material properties calculated with CCA method.

E_1	$1.4958x10^{10}Pa$
E_2	$9.8907x10^{9}Pa$
G_{12}	$4.4983x10^{9}Pa$
G_{23}	$1.4x10^{8}Pa$
K	$4.25x10^{9}Pa$
ν_{12}	0.2787
ν_{23}	0.4722
C_{11}^{*}	$1.6279x10^{10}Pa$
C_{12}^{*}	$2.3693x10^{9}Pa$
C_{22}^{*}	$5.65x10^{9}Pa$
C_{23}^{*}	$2.85x10^{9}Pa$
C_{66}^{*}	$4.4983x10^{9}Pa$

So, from one of the finite element analyses, array of stress values is observed and taken to find strain values with CCA constants. After stress and strain values are calculated, stress-strain curves can be plotted. Stress values are taken from FEA analysis and it goes from 0 to 45 GPa.

4.1. STRESS-STRAIN GRAPHS OF CCA MODEL

In order to analyze stress-strain graphs, the data are observed, and shear locking is spotted. This error has a huge effect to the results.

Shear locking is a type of error that occurs in FEA. When the model is under bending, curvatures occur in the actual material. These curvatures are difficult to model by linear

elements, so an additional shear stress is introduced. This shear stress makes the element stiffer than reality and the element reach equilibrium with displacements smaller than it should be. In other words, displacements are defined by linear functions. The derivatives of these functions are constant. So, the strains are also constant. But on the other hand, this is not the case. By an inaccurate estimation, stiffness can be calculated much larger. This can lead to smaller displacements, which is not even close to reality. So, at some node's values are higher than it should be. And some unrelated peaks are occurred because of the shear locking. To prevent this problem, mesh refinement is applied. The graphs with shear locking are presented in Figure 4.1, so that it can be compared with the correct results which are in Figure 4.3.

In Figure 4.1, $\varepsilon_{11} - \sigma_{11}$ (a in Figure 4.1), $\varepsilon_{22} - \sigma_{11}$ (b in Figure 4.1), $\varepsilon_{33} - \sigma_{11}$ (c in Figure 4.1), $\varepsilon_{eq} - \sigma_{11}$ (d in Figure 4.1) are presented. These graphs have shear locking problem. Strain values can go up to 0.03 which is extremely high. Stress values are taken from finite element analysis in order to compare the results. Because of the several nodes' behavior, these inaccurate results are obtained and used for calculation. And they are presented in order to see the difference.

To prevent shear locking problem, mesh refinement is done in same finite element analysis. After that a correction is stress values, is observed. With accurate results, stress values are taken from FEA and it goes from 0 to 120 MPa and stress-strain curves are plotted.

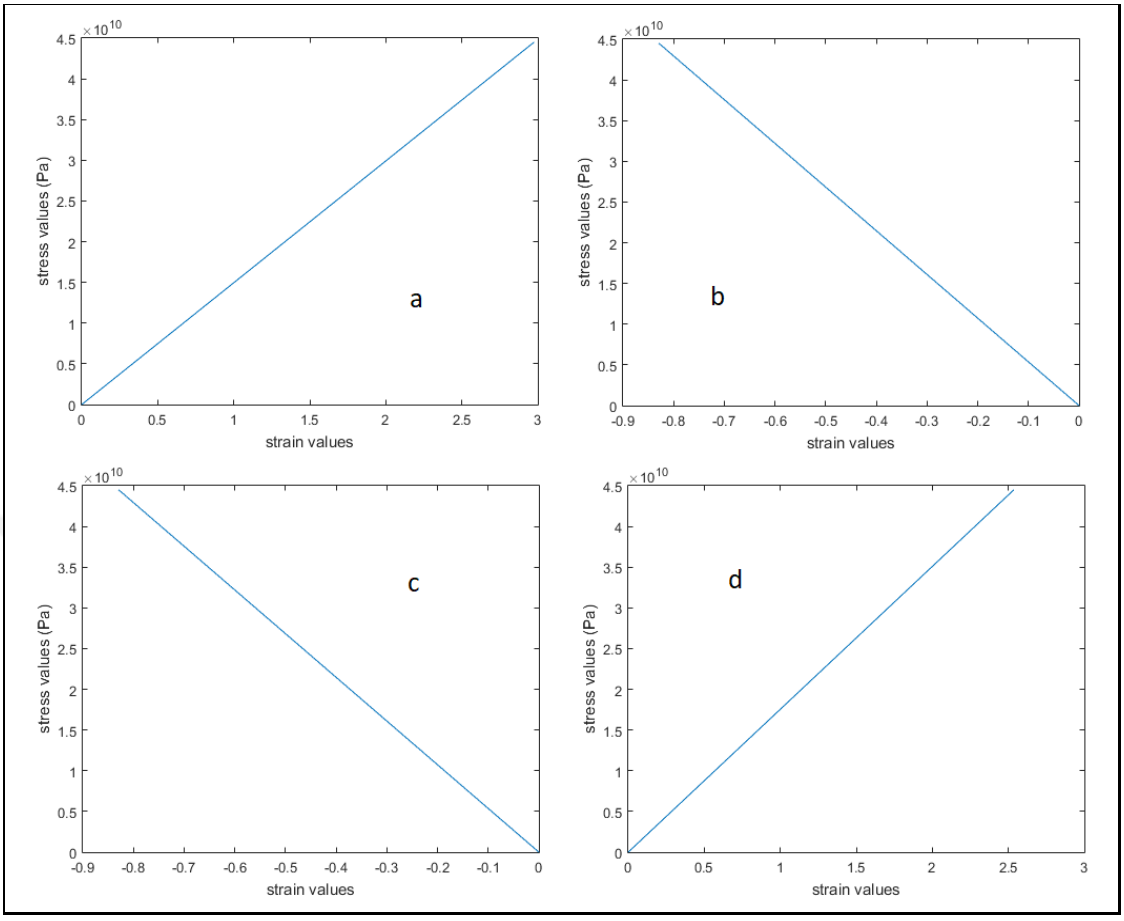

Figure 4.1. Graphs with shear locking, (a) $\varepsilon_{11} - \sigma_{11}$, (b) $\varepsilon_{22} - \sigma_{11}$, (c) $\varepsilon_{33} - \sigma_{11}$, (d) $\varepsilon_{eq} - \sigma_{11}$

Free mesh is used. This mesh has no specified pattern and no restrictions in element shapes according to mapped mesh. Element size is defined 3.5 mm for more accurate and detailed results. First element shape is triangle at all parts of the geometry. But results of this analysis are problematic. Impossible values are obtained so mesh is needed to be refined. Quadrilateral element shape is chosen to create more elements to affect the results. But this time analysis takes too much time to execute. So, idea of mixing different element shape is occurred. For critical places quadrilateral shape is used and for the rest of the geometry, triangle shape is used. Glass tubes are the critical part of the geometry. They are taking most of the impact and creating the strength of the armor. Rest of the geometry is taken triangle shape. This operation reduces analysis time dramatically. After this operation, analysis creates a new error to solve. This error is contact problem. Layers of the armor have contacts between each other. Because of this contact, between these layers, several nodes have more than one element, so this creates an error. In order to eliminate this error, contact matching

is done. For example, first layer's back side and second layer's front side is defined as contact to not create more than one element for one node.

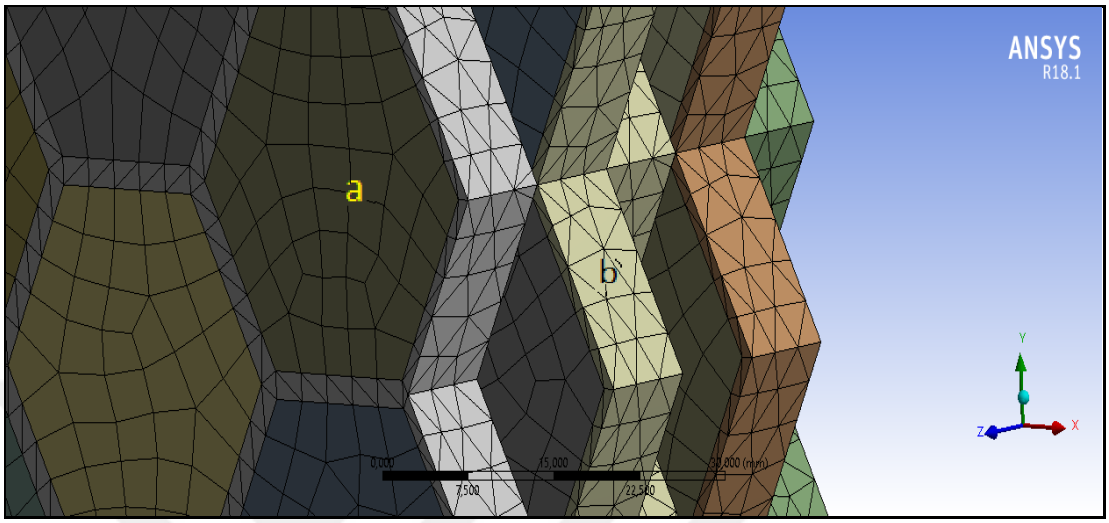

Figure 4.2. Refined mesh of armor (a) quadrilateral shape, (b) triangle shape

After the mesh refinement is done, results become more accurate and reasonable. Figure 4.3 shows graphs of the correct results. When compared with Figure 4.1 which is graphs of inaccurate results, effect of mesh refinement is seen obviously. Values are affected by mesh and in order to have proper results mesh is crucial.

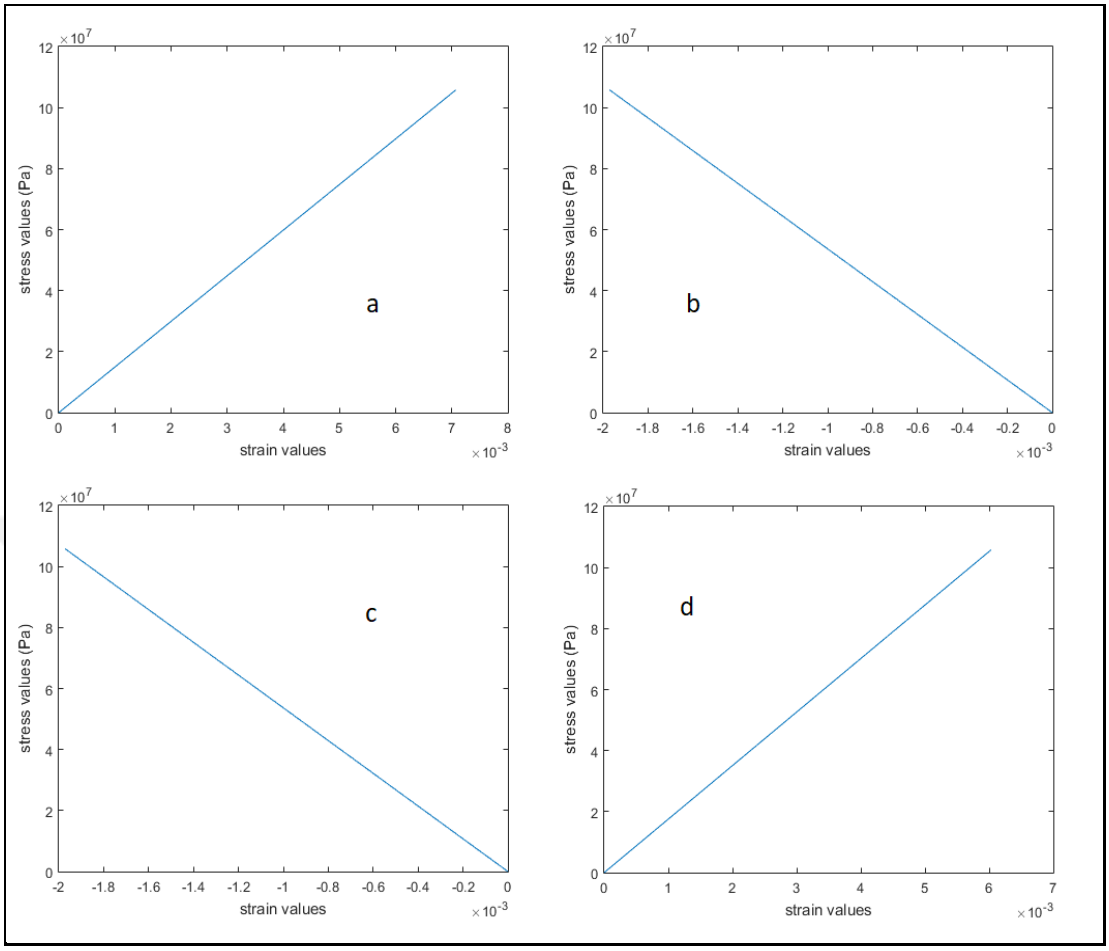

Figure 4.3. Correct graphs, (a) $\varepsilon_{11} - \sigma_{11}$, (b) $\varepsilon_{22} - \sigma_{11}$, (c) $\varepsilon_{33} - \sigma_{11}$, (d) $\varepsilon_{eq} - \sigma_{11}$

In Figure 4.3, $\varepsilon_{11} - \sigma_{11}$ (a in Figure 4.3), $\varepsilon_{22} - \sigma_{11}$ (b in Figure 4.3), $\varepsilon_{33} - \sigma_{11}$ (c in Figure 4.3), $\varepsilon_{eq} - \sigma_{11}$ (d in Figure 4.3) are presented. After the shear locking problem is solved, it is shown that the stress values can go up to only 120 MPa and that is acceptable for our situation. High strain values are also corrected.

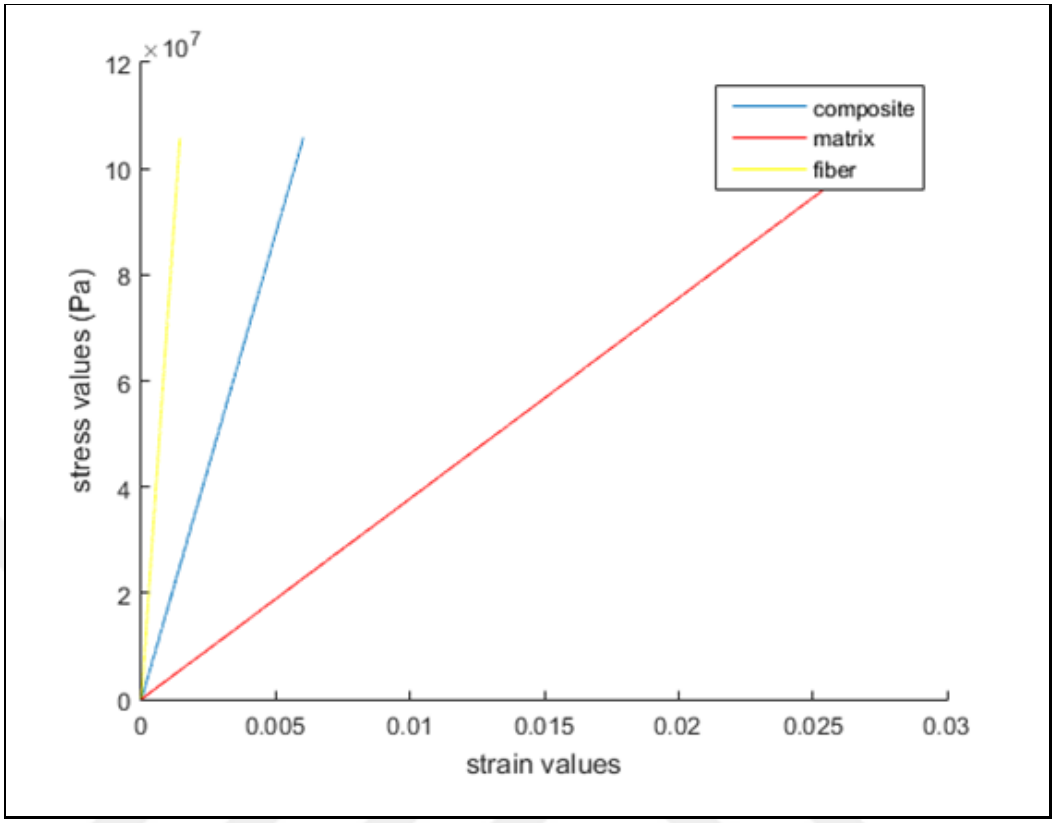

Figure 4.4. Combined graph

In Figure 4.4, stress-strain graphs of fiber (float glass), matrix (epoxy-resin) and created composite material are shown together. Strain values are equivalent strain values of materials. With the slope of this graph, approximate Young's modulus values can be calculated. And it can be said that our fiber is the toughest material, according to slope. Curve of the composite material is between the curve of fiber and curve of matrix, as it should. Composite material is also a tough material and it close to fiber's toughness. But with composing fiber and matrix, energy absorption and elasticity are reinforced. So, obtained material is tough but, it is not as brittle as the fiber.

5. RESULTS

At this section, final model is compared with conventional model and CCA model. Purpose of this is to see the achievements and accuracy of the model. Before final model is created, trials are made to progress. Results of these trials are shown in Table 5.1.

Table 5.1. Results of FEA analysis

Case	# of Layers	Armor materials	Armor thickness (mm)	Projectile type	Projectile diameter (mm)	Projectile velocity (m/s)	Result
1	3	Glass-epoxy	8.1	Circular tip bullet	18	500	Failed
2	3	Glass-epoxy	8.1	Circular tip bullet	4.5	500	Stuck in second layer
3	3	Glass-epoxy	8.1	Circular tip bullet	4.5	1250	Failed
4	4	Glass-epoxy	10.8	Circular tip bullet	18	500	Stuck in third layer
5	4	Glass-epoxy	10.8	Circular tip bullet	18	650	Failed
6	10	Glass-epoxy-resin	27	Pointy tip bullet	7.62	500	Failed
7	10	Glass-epoxy-carbon	27	Pointy tip bullet	7.62	500	Stuck in sixth layer
8	10	Glass-epoxy-SiC	27	Pointy tip bullet	7.62	500	Bounces from second layer

After the simulations are done and the armor is created, it needs to be compared with other conventional models to see the objectives are succeeded or not. Conventional model is arranged at same sizes and same materials with the honeycomb model. It has five layers of glass and behind those glass layers; there are epoxy-resin layers. Images of the both conditions which are very similar with each other, except the shape of the armor.

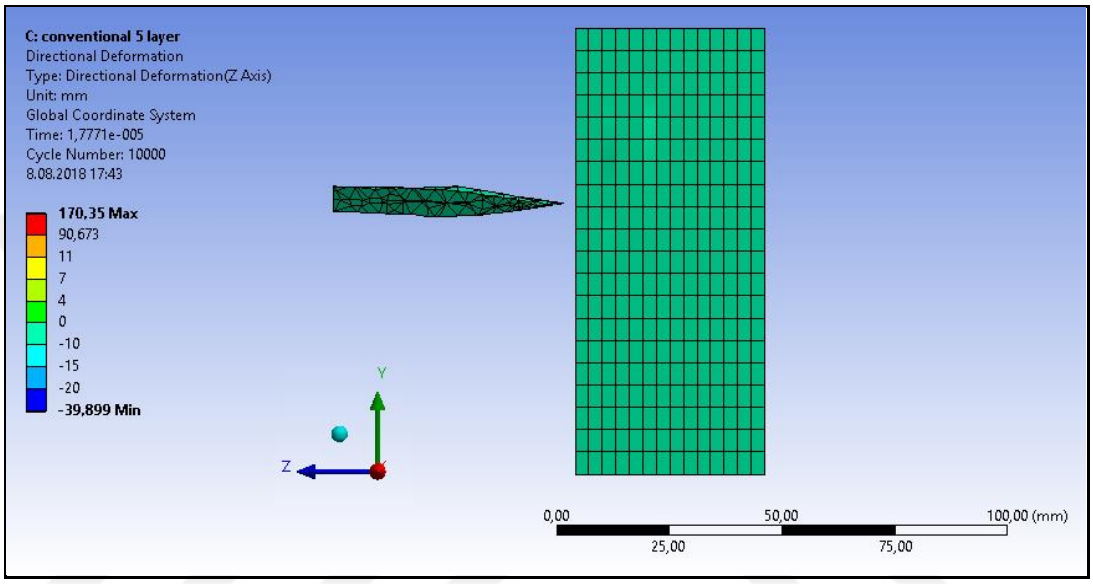

Figure 5.1. Beginning of the test of the conventional model

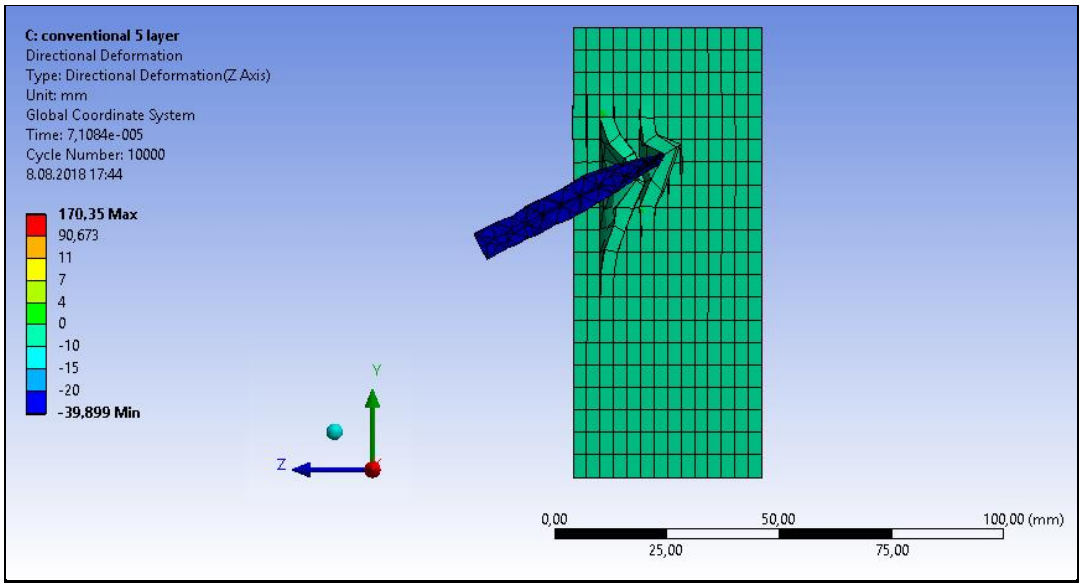

Figure 5.2. Progression of the test of the conventional model

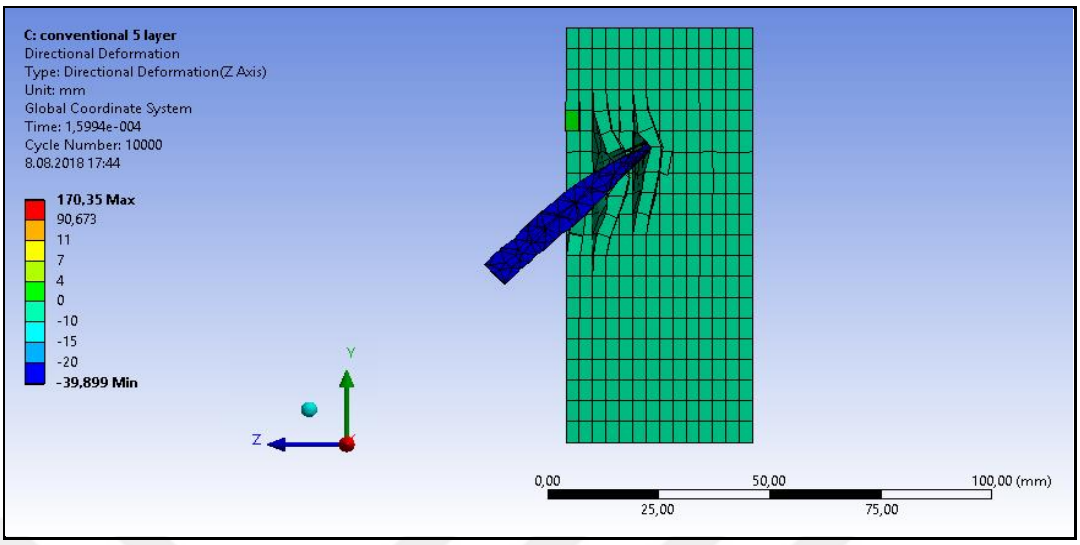

Figure 5.3. Ending of the test of the conventional model

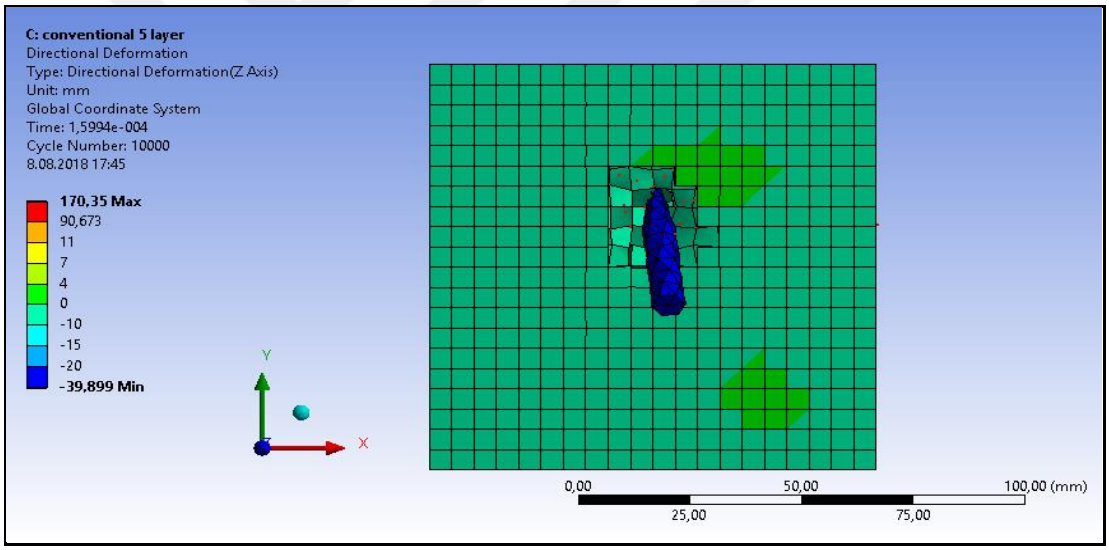

Figure 5.4. Front view of ending of the test of the conventional model

In Figure 5.1, Figure 5.2, Figure 5.3 and Figure 5.4 test of the conventional model is shown step by step. Same projectile as it used in honeycomb model is used and velocity of it is 500 m/s. Layers are consisted of six millimeters glass and four-millimeter epoxy resin

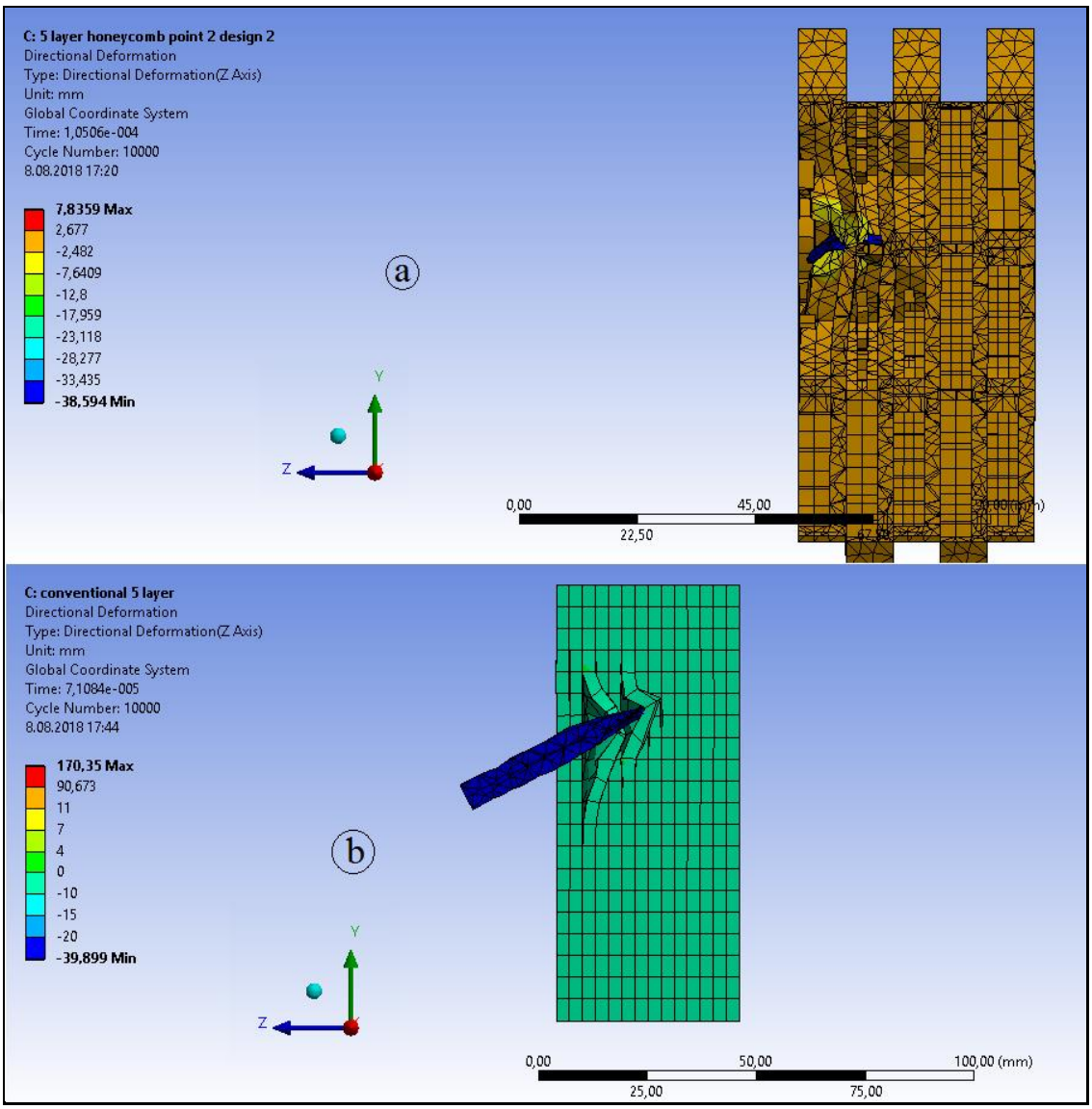

Figure 5.5. Comparison between honeycomb model and conventional model (a) honeycomb (b) conventional

At conventional armor, projectile penetrates first two layers completely and glass sub-layer of the third layer. Then it stuck at the epoxy-resin part of the third layer. However, at honeycomb model projectile goes through the first layer and stuck at the glass sub-layer of the second layer. With this comparison, effect of the shape of armor can be observed. Honeycomb model resists the projectile more than conventional model. While every other condition, beside the shape, is equal, honeycomb model acts like it is tougher than conventional model. Main reason of this action is the extra fibers at z direction. Comparison of these models is shown in Figure 5.5.

There are 100x100x6 mm glass plates and 100x100x4 mm epoxy plates in conventional model. In armor there is five of each plate. Conventional transparent armor consists of 300,000 cubic millimeter of glass and 200,000 cubic millimeters of epoxy. And that is approximately 0.768 kg of glass and 0.232 kg of epoxy. In total, a conventional transparent armor with decided properties has a weight of one kilogram. On the other hand, honeycomb model has a weight of 0.89 kg. In other words, with a different design, ten percent weight savings can be achieved. That is also means reduction in cost.

In a similar research [10], Kevlar-epoxy composite tested with similar methods with this research. 5.56 mm bullet is chosen, and the velocity of the bullet is 800 m/s. Geometry of this analysis is shown in Figure 5.6.

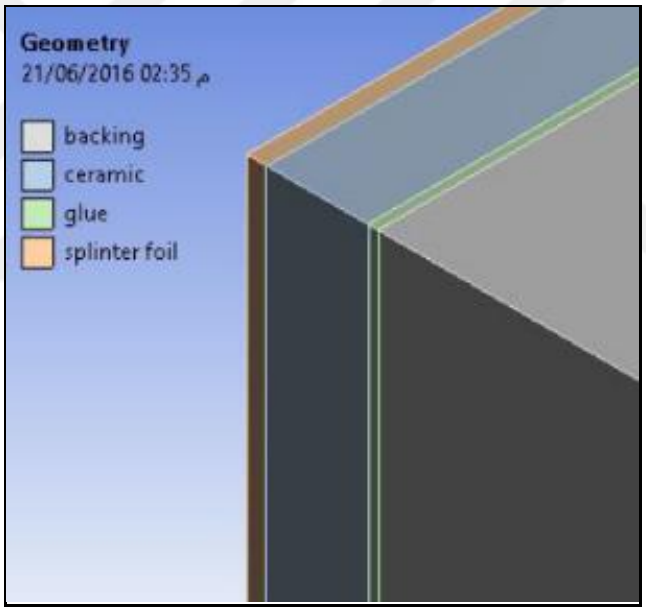

Figure 5.6. Geometry of 'Theoretical study of lightweight composite system for personal armor' research [10]

Thickness of the geometry is 10.45 mm and it is created from 300x300 mm plates. Conventional type geometry is preferred for the analysis. Results shows that the penetration distance of the bullet is greater than thickness of the armor. Even though the armor is not destroyed, it qualifies for failure because it may harm the individual behind it. Results of the finite element analysis of this test present in Figure 5.7.

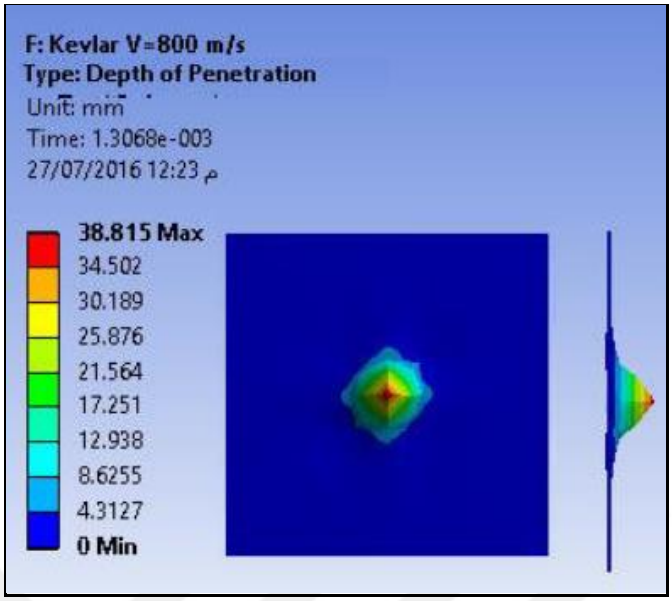

Figure 5.7. FEA analysis of research [10]

To compare and check the honeycomb model, same conditions are tested with CCA calculations in finite element analysis. At honeycomb model float glass is defined at little tubes and epoxy-resin is defined at main chassis for material information. After that finite element analysis automatically calculate the properties and simulate the behavior of the model. CCA model calculations must be similar with auto-calculated solutions, in order to have accurate results.

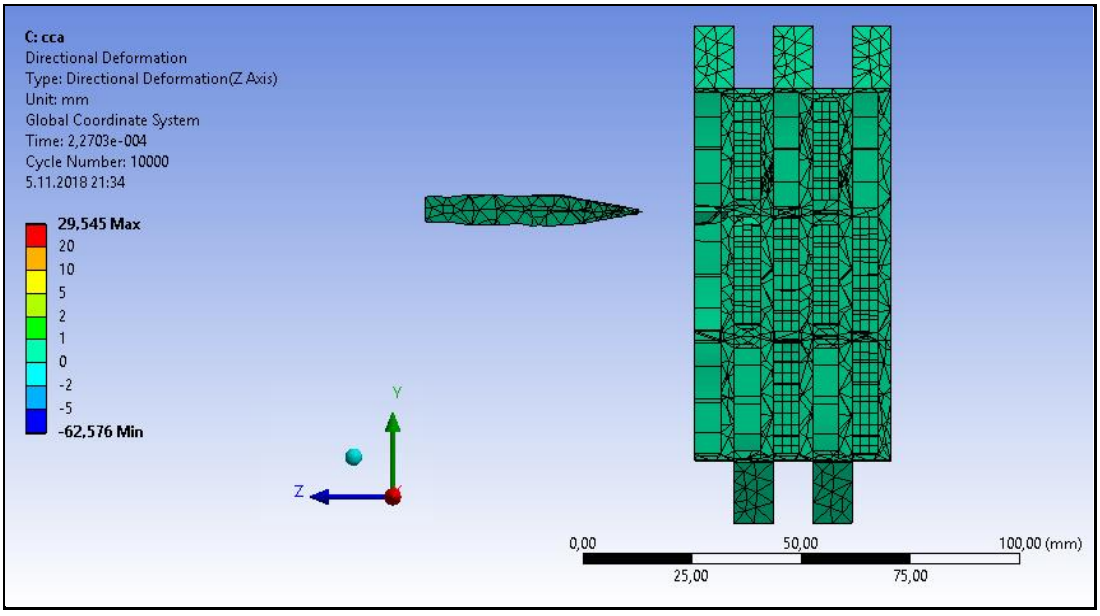

Figure 5.8. Beginning of CCA model

In Figure 5.8, setup of CCA model is shown. Everything is same with honeycomb model except the definition of material information. This time properties, which are calculated with CCA model, are put manually in finite element analysis. Little tubes and main chassis have same material information, but geometry is not drawn as one in order to see the reaction individually.

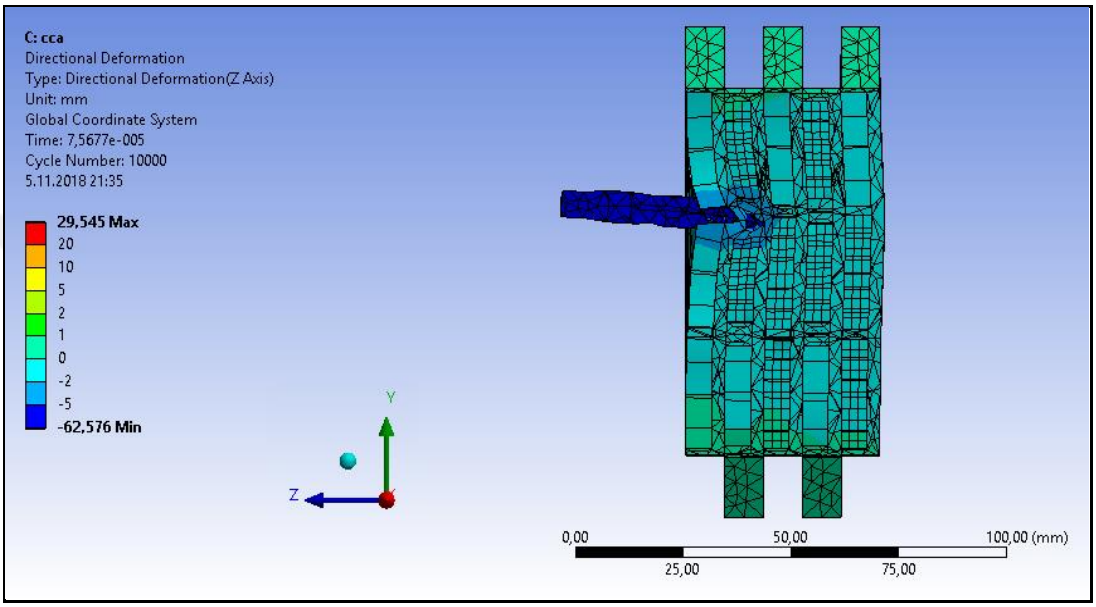

Figure 5.9. Step 1 of CCA model

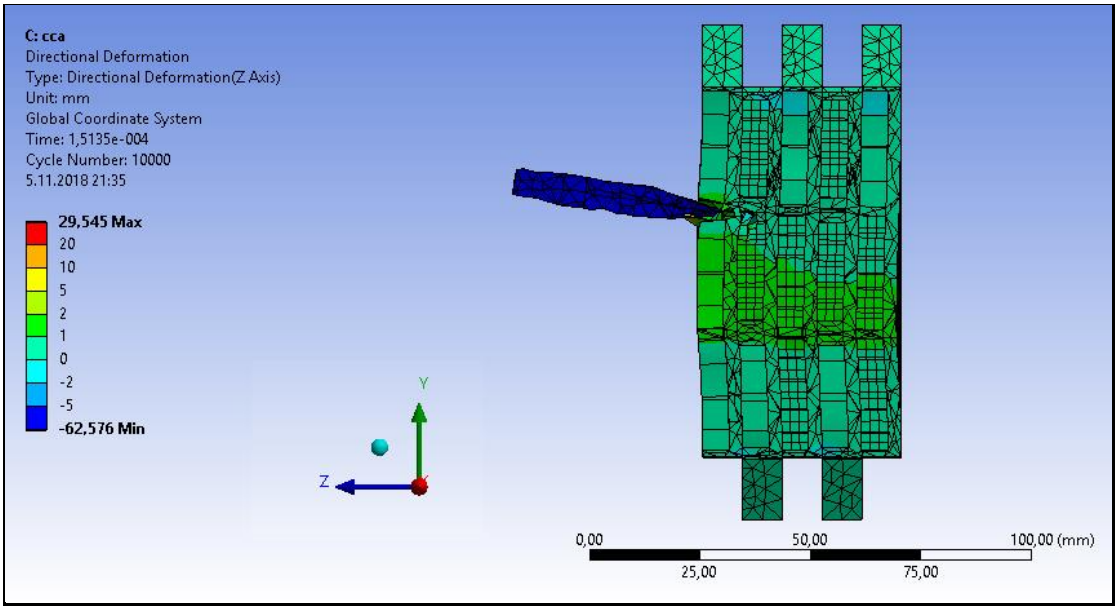

Figure 5.10. Step 2 of CCA model

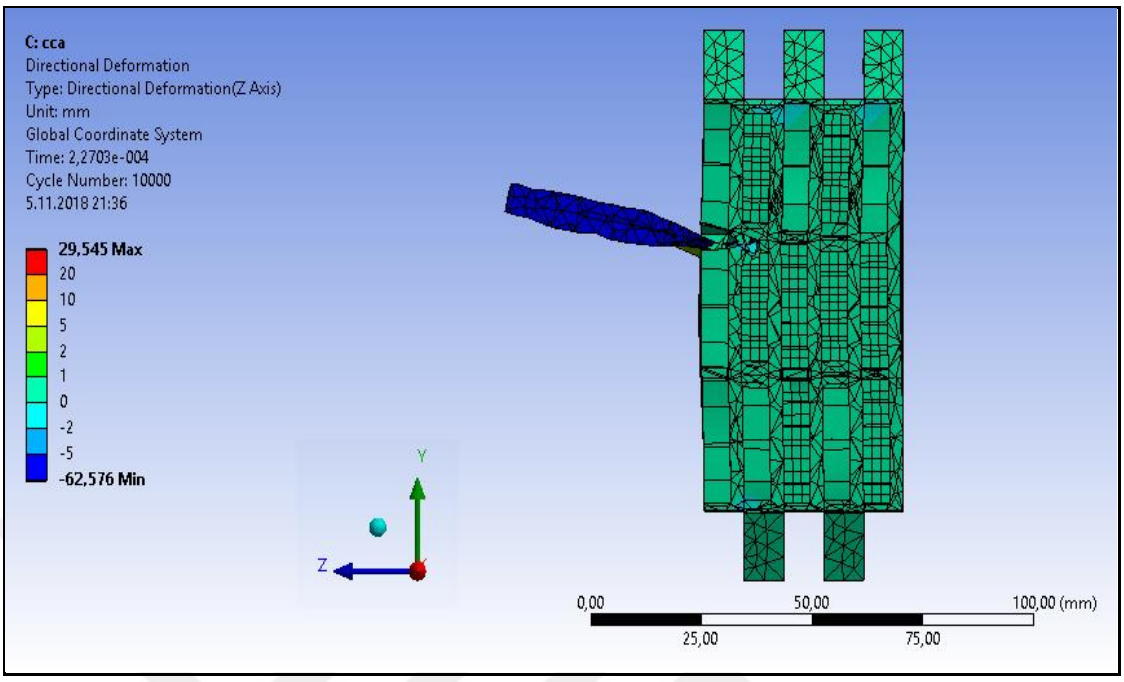

Figure 5.11. Ending of CCA model

At CCA [27] model, projectile velocity is 500 m/s. Thickness of layers is 10 mm and there are 5 layers. Properties are defined from the results of CCA calculations. Projectile goes through the first layer of the armor and failed at the middle of second layer. Then it bounces back from the middle of second layer and exits from armor completely.

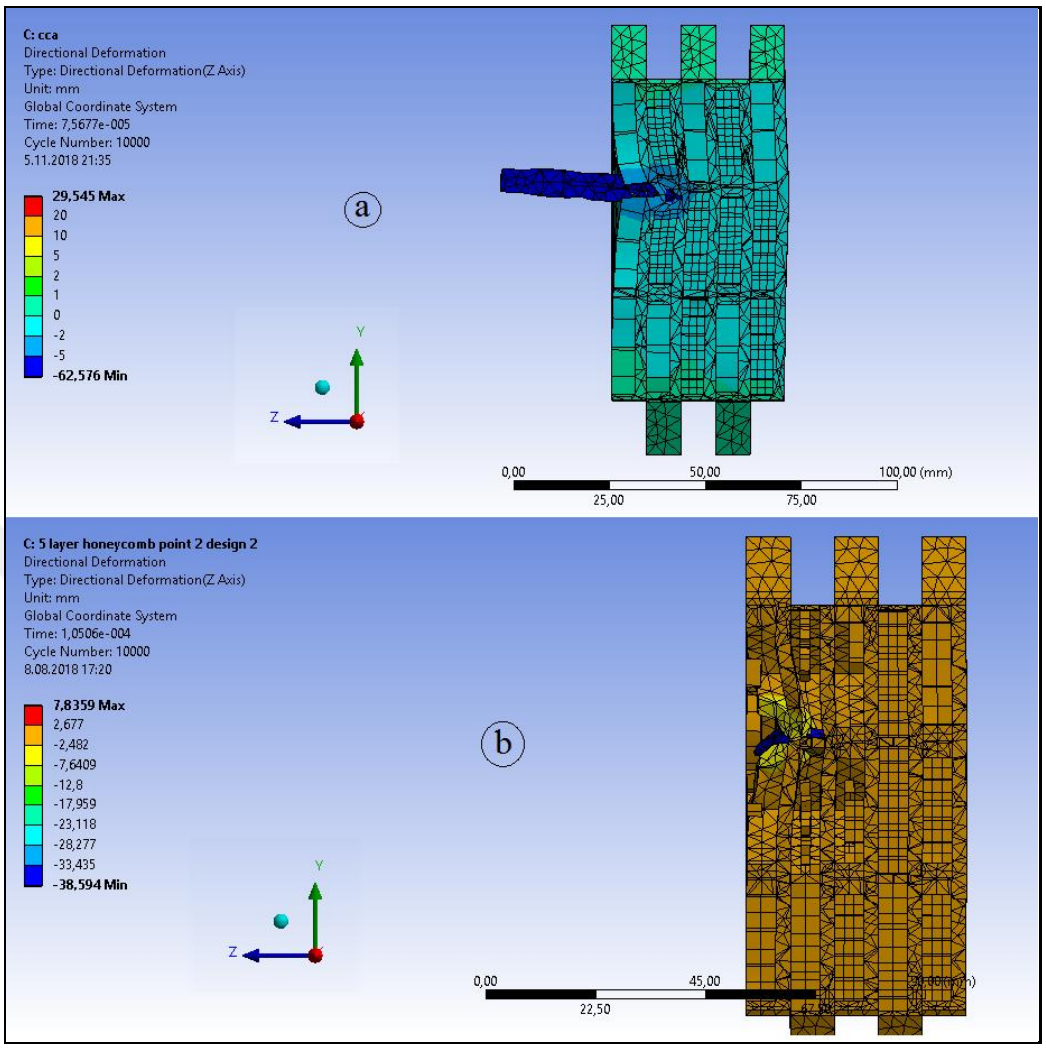

Figure 5.12. Comparison between (a) CCA, (b) honeycomb model

Figure 5.12 shows the maximum deformed point of the armor. Results are not identical, but they are similar. At Figure 5.12 a section in CCA model is presented and at b section, there is honeycomb model. Differences of these results can be occurred from brittleness and elasticity. When calculated with CCA, all geometry is defined same and acts like one. It is assumed that can affects brittleness and elasticity.

To sum up, calculated and simulated results are similar with each other. Even though, they have little differences, at the bigger picture they look same. From that, it can be said that, calculated results are accurate, according to simulations results.

6. CONCLUSION

Aim of this analysis is to create more efficient armor. More efficient armor means better properties which are cost, toughness, weight, effect of the projectile impact on the armor. At this research, these properties are improved to get better results. In order to improve the armor, a lot of different simulations are done in different conditions. These conditions must be adapted to environment, which is generally military and personal security, that armors are used.

First, shape of the projectile needs to be decided. Armor is trying to stop the projectile which means to beat the impact that projectile create on the armor. If the armor can overcome the greatest impact, then it can beat any projectile. Military base bullets are chosen for the experiment. Pointy tip projectile has 7.62 mm diameter and 51 mm length. It is made from steel.

On the other hand, thickness of the armor is another critical issue for this experiment. Even though the greater thickness means better results, it also means heavier and costs more. This transparent armor will be used at car, safe house windows etc. so it will also need to adapt to this situation. After several researches and discussions, our desired thickness is decided below 10 cm as much as possible.

Transparency is an obligation since the armor is transparent armor. This criterion must be considered, when materials of the armor are selected. Glass is the first material that is selected and used in this experiment. Although glass is a tough material, it is also very brittle. So, it needs to be reinforced with other materials which are also needs be transparent. After some trials in simulations, not a single material but a composite material is decided to use with glass. This composite is epoxy-resin. [20]

One of the most critical parts in this experiment is the design. Design of the armor is very important for a successful armor. Glass is tougher than epoxy-resin. But epoxy-resin has an important property which it holds the armor together. So even though glass is very brittle, it is the impact face of the layer. Behind the glass, there is epoxy-resin which is a holder for glass. This is the description of a layer. Amount of the layers needs to be decided. Some

trials and simulations are done, and it is observed that five layers of this combination, is more than enough for the objective. When the safety is considered, layer amount is decided to be five. Glass has six millimeters thickness and epoxy-resin has four millimeters thickness. Five layered transparent armor thickness is five centimeter which is satisfying for the thickness goal. [17]

To see the effect of the shape of the armor, different designs need to be implemented to the armor. Different ideas, shapes, sizes are implemented to the armor and in conclusion, honeycomb model is created. At this model, a lot of honeycombs are set side to side, in order to support each other. And it also has a critical advantage when compare to other models. It has extra fiber reinforcements, which is perpendicular to impact face, due to its shape. These fibers help the job of stopping the projectile.

REFERENCES

1. Patel PJ, Gilde GA, Dehmer PG, McCauley JW. Transparent armor. *Advanced Materials and Processing Technology.* 2000; 4(3):1–5.

2. Klement R. Transparent armour materials. *Journal of the European Ceramic Society*. 2008; 28(5):1091-1095.

3. Omnexus. [cited 6 November 2018] Available from: https://omnexus.specialchem .com/selection-guide/polymethyl-methacrylate-pmma-acrylic-plastic

4. Howell JA, Hellmann JR, Muhlstein CL. Nano mechanical properties of commercial float glass. *Journal of Non-Crystalline Solids*. 2008; 354(17): 1891-1899.

5. British plastic federation. [cited 10 May 2018] Available from: http://www.bpf.co .uk/plastipedia/polymers/Polycarbonate.aspx

6. Oertel G, Abele L. *Polyurethane handbook. 2nd ed*. Munich: Hanser-Gardner; 1985.

7. Zhang X, Hao H, Shi Y, Cui J. The mechanical properties of polyvinyl butyral (PVB) at high strain rates. *Construction and Building Materials*. 2015; 93: 404–415.

8. McCauley JW. Aluminum nitride and AlON ceramics, structure and properties. *Weapons and Materials Research Directorate, ARL*. 2002; 2740: 127-132.

9. Sickafus KE, Wills JM, Grimes NW. Structure of spinel. *Journal of the American Ceramic Society*, 1999; 82(12): 3279-3292.

10. Fadhil HA, Zuheir FE, Baqir HM. Theoretical study of light-weight composite system for personal armor. *International Journal of Engineering and Technology*. 2016; 6(9): 327–334.

11. Cunniff PM, Auerbach M, editors. High performance “M5” fiber forballistics/structural composites. *23rd Army Science Conference on*; 2002: Aberdeen Proving Ground.

12. Ünaler E. Development and characterization of light-weight armor materials. Izmir Institute of Technology. Master’s Thesis. 2005.

13. Open chemistry database. [cited 4 March 2018] Available from: https:// pubchem.ncbi.nlm.nih.gov/compound/aluminum_oxide#section=Top

14. Karthikeyan K, Russell BP, Deshpande VS. Multi-hit armour characterization of metal-composite bi-layers. *Journal of Mechanics of Materials and Structures*, 2013; 7(7): 721-734.

15. Cunat PJ. Stainless steel properties for structural automotive applications. *Metal Bulletin International Automotive Materials Conference on*; 2000: Euro Inox.

16. Meshram P, Sahu S, Ansari MZ, Mukherjee S. Study on mechanical properties of epoxy and nylon/epoxy composite. *Materials Today: Proceedings*. 2017; 5(2): 5925-5932.

17. Regassa Y. Modeling and simulation of bullet resistant composite body armor. *International Journal of Research Studies in Science, Engineering and Technology*. 2014; 1(3): 39-44.

18. Lanthier JM. The effects of soft textile body armor on the wound ballistics of high velocity military bullets. *21st. International Symposium on Ballistics*. Wayville, S. Aust: SAPMEA Conventions; 2004; 1084-1090.

19. Rajesh S, Ramnath BV, Elanchezhian C, Abhijith M, Riju RD, Kishan KK. Investigation of tensile behavior of kevlar composite. *Materials Today: Proceedings 5.1*, 2018; 1156-1161.

20. Grujicic M, Bell WC, Pandurangan B. Design and material selection guidelines and strategies for transparent armor systems. *Materials and Design*, 2012; 34: 808–819.

21. Fountzoulas CG, Cheeseman BA, Dehmer PG, Sands JM. A Computational study of laminate transparent armor impacted by FSP. *Proceedings of the 23rd International Symposium on Ballistic*; 2007: ISB.

22. Straßburger E. Ballistic testing of transparent armour ceramics. *Journal of the European Ceramic Society*, 2009; 29(2):267–273.

23. Patel P, Hsieh A, Gilde G. Improved low-cost multi-hit transparent armor. *Weapons and Materials Research Directorate, ARL*.2006:5069.

24. Hsieh JA, DeSchepper D, Moy P, Dehmer GP, Song WJ. The effects of pmma on ballistic impact performance of hybrid hard/ductile all-plastic- and glass-plastic-based composites. Army Research Laboratory. [cited 7 March 2018] Available from: http://stinet.dtic.mil/oai/oai?&verb=getRecord&metadataPrefix=html&identifier=ADA420878

25. Godzimirski J, Janiszewski J, Surma Z. Ballistic resistance tests of multi-layer protective panels. *Maintenance and Reability*, 2015; 17(3): 416–421.

26. Ling L, Zhengming HA. Note on mori-tanaka's method. *Acta Mechanica Solida Sinica*. 2014; 27(3): 234-244.

27. Böhm HJ. A short introduction to basic aspects of continuum micromechanics. Cdl-fmd Report 3. *Institute of Lightweight Design and Structural Biomechanics (ILSB).* 1998:207.

28. Sevostianov IA. Generalization of Maxwell homogenization scheme for elastic material containing inhomogeneities of diverse shape. *International Journal of Engineering Science*. 2013; 64: 23-26.

29. Weng GJ. A dynamical theory for the Mori–Tanaka and Ponte Castañeda–Willis estimates. *Mechanics of Materials*. 2010, 42(9): 886-893.

30. Peigney M. On Hashin–Shtrikman-type bounds for nonlinear conductors. *Comptes Rendus Mécanique, École des ponts ParisTech*. 2017; 345(5): 353-361.

31. Meng CW. Evaluation of the Eshelby solution for the ellipsoidal inclusion and heterogeneity. *Computers and Geosciences*. 2012; 40: 40-48.

APPENDIX A. SKETCH OF IDEAS

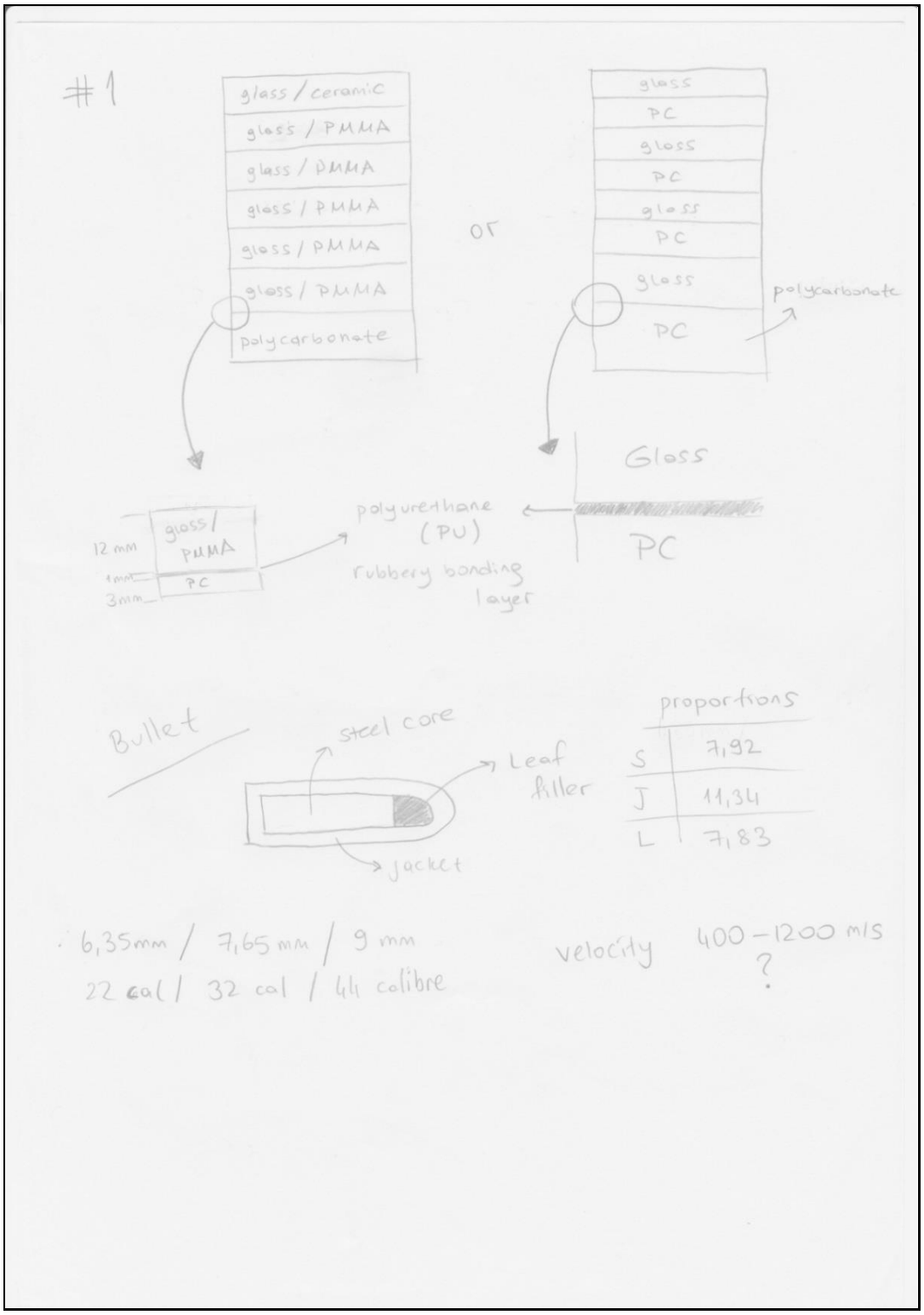

Figure A.1. Sketch of ideas #1

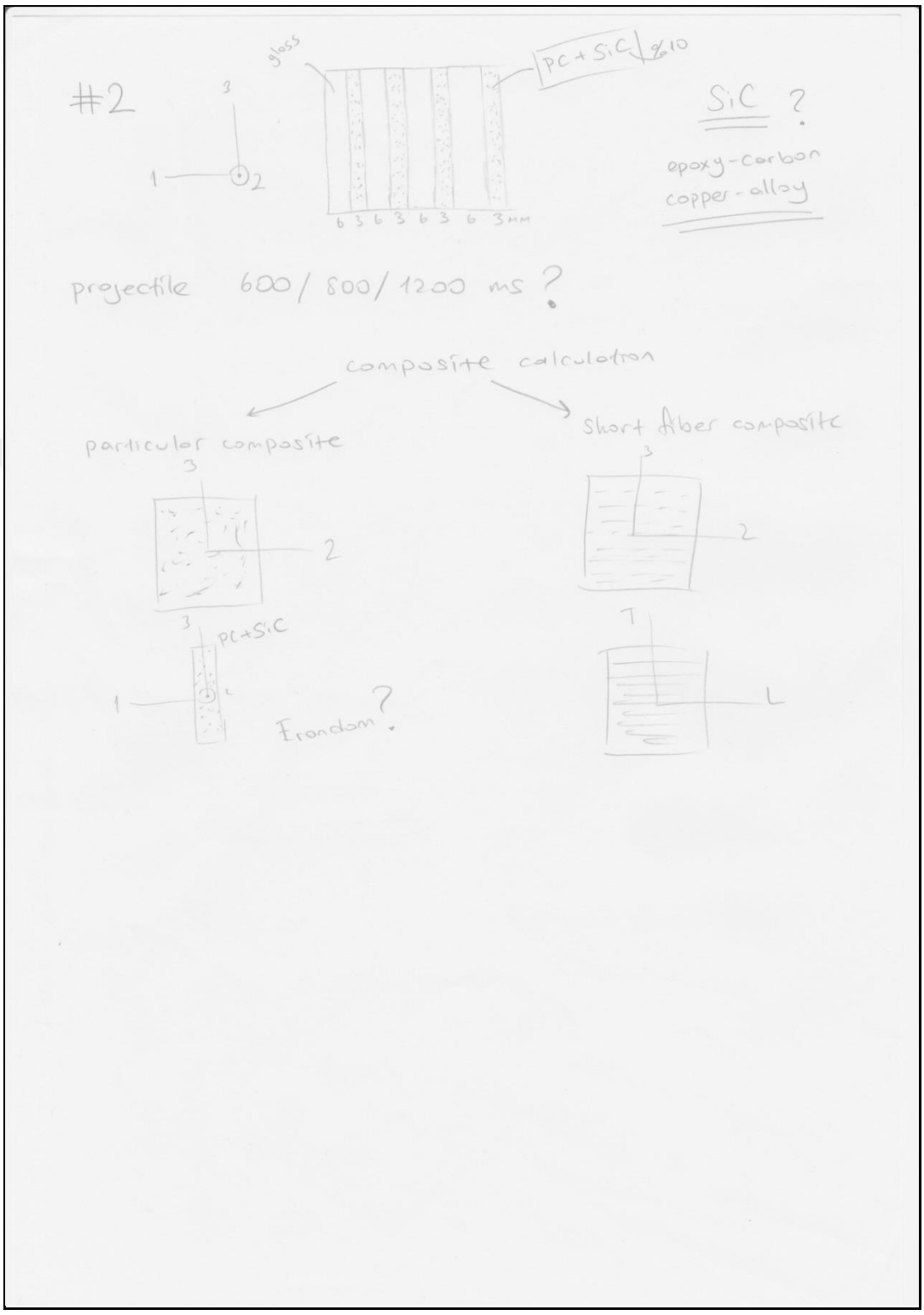

Figure A.2. Sketch of ideas #2

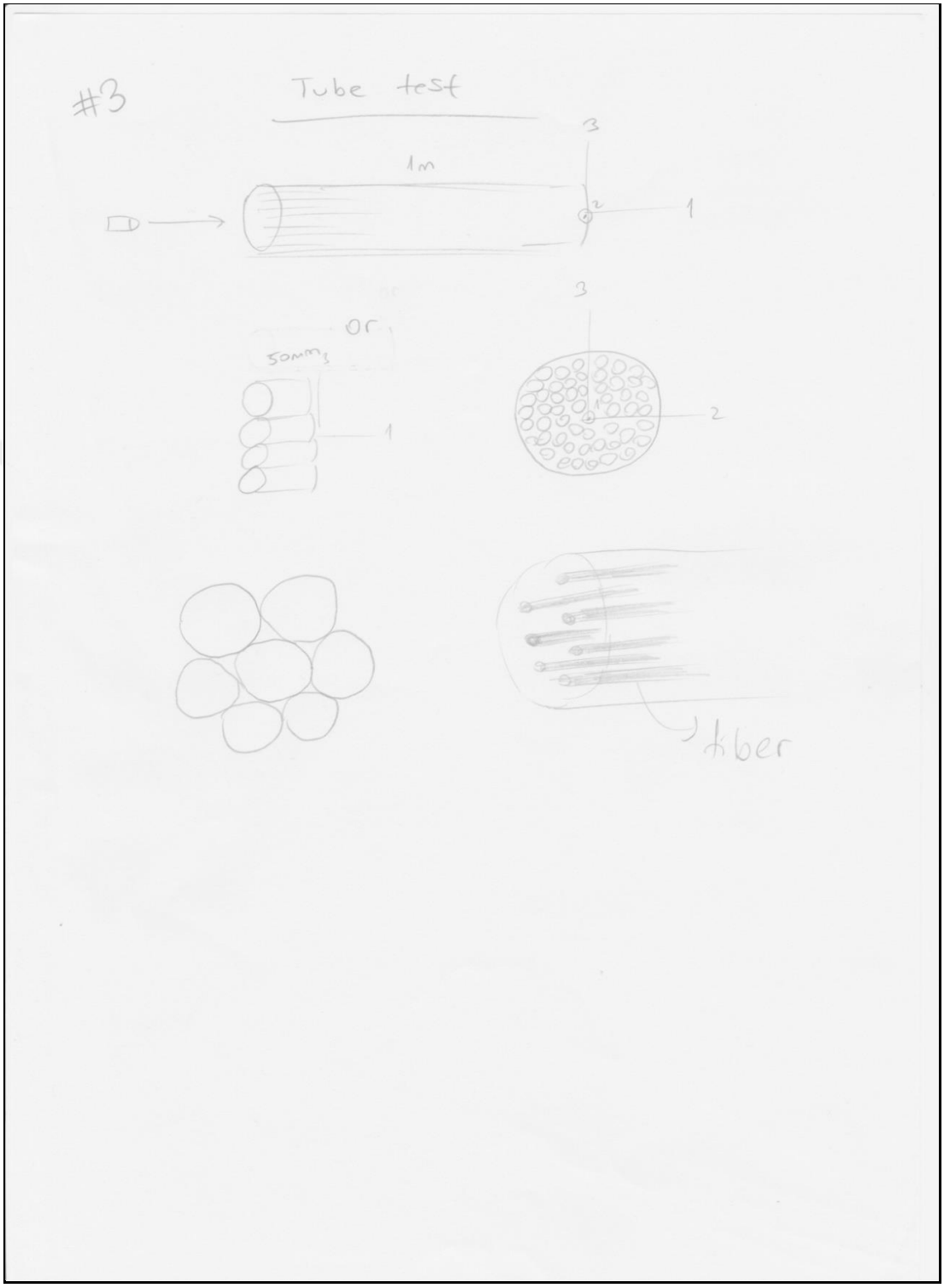

Figure A.3. Sketch of ideas #3

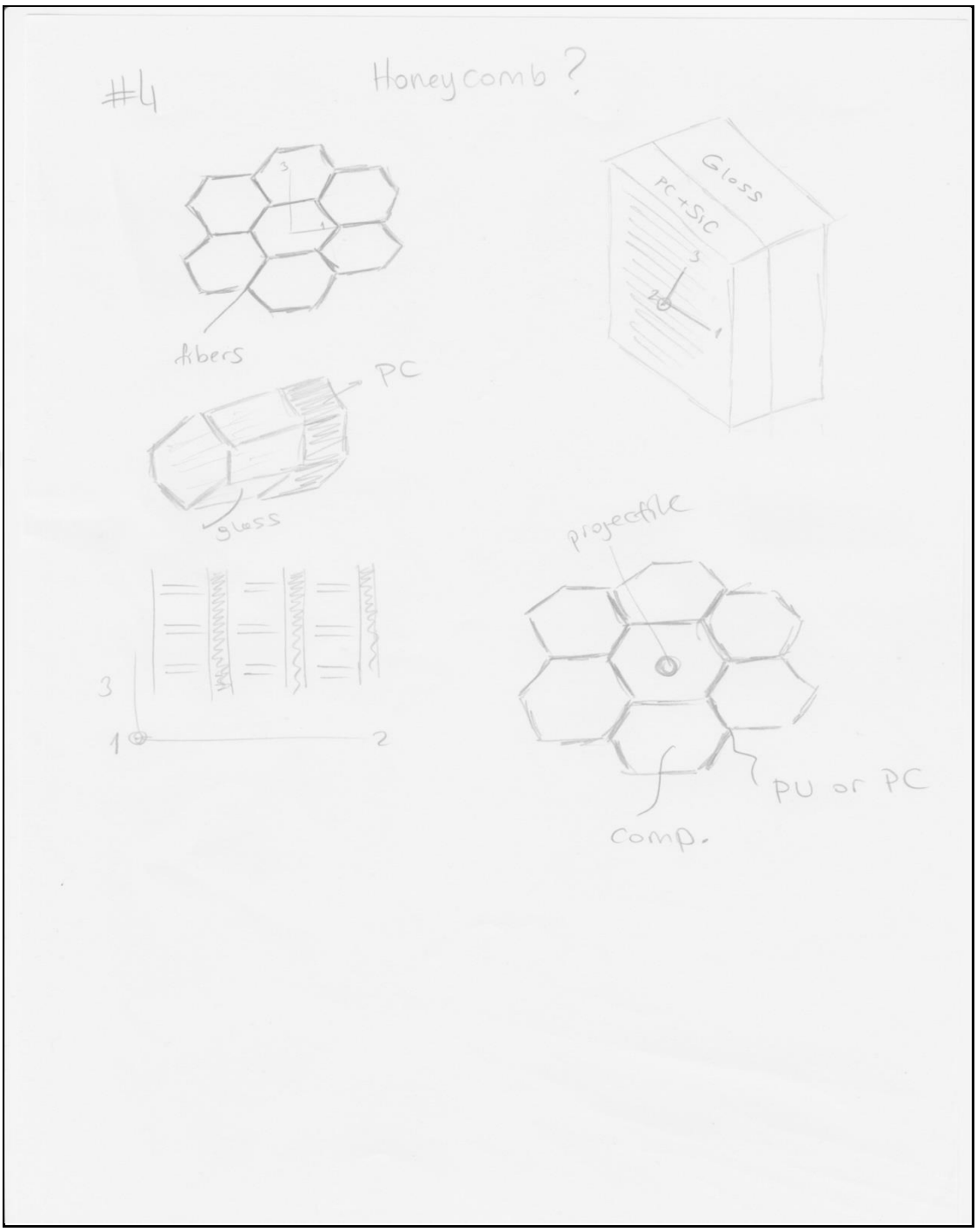

Figure A.4. Sketch of ideas #4

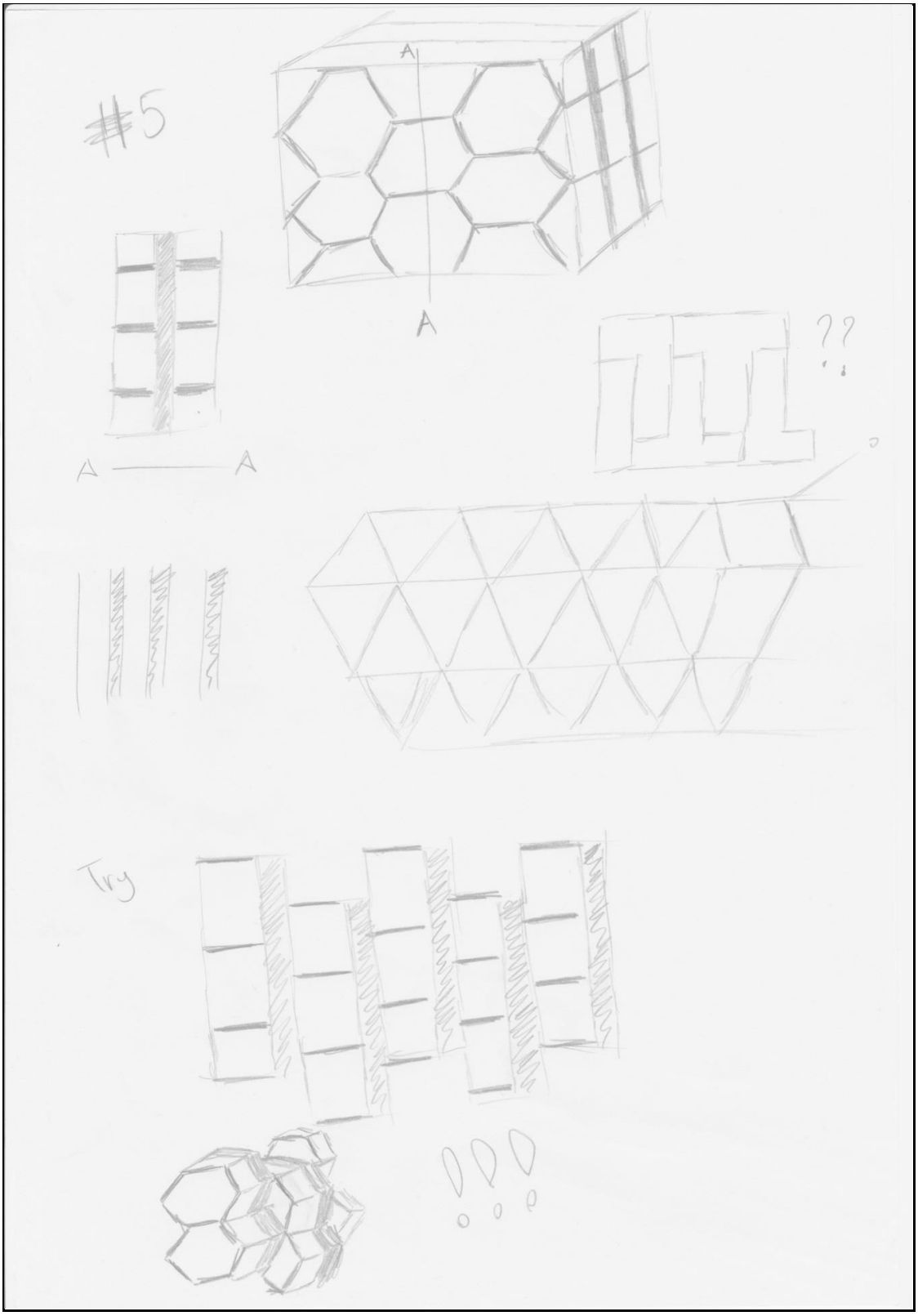

Figure A.5. Sketch of ideas #5

APPENDIX B. CODE

Acquiring the combined plots needs a lot of calculations. These calculations are done with the help of Matlab program. For the combined plot, necessary codes are;

```
Dm=1160;

Ym=3780000000;

Pm=0.35;

Bm=4250000000;

Sm=1400000000;

Vm=0.424;

Df=2530;

Yf=74500000000;

Pf=0.22629;

Bf=45400000000;

Sf=30400000000;

Vf=0.576;

Km=Sm/(3*(1-2*Pm));

Kf=Sf/(3*(1-2*Pf));

K=Km+Vf/((1/(Kf-Km))+(1-Vf)/(Km+Sm));

Y1=Vf*Yf+(1-Vf)*Ym;

Y2=Yf*Ym/(Yf+Vf*(Yf-Ym));

P12=Pf*Vf+(1-Vf)*Pm;
```

```
P23=1-P12*(Y2/Y1)-(Y2/(3*K));

S12=Sm+Vf/((1/(Sf-Sm))+(1-Vf)/2*Sm);

S23=Y2/(2*(1+P23));

c11=Y1+4*(P12)^2*K;

c12=2*K*P12;

c22=S23+K;

c23=-S23+K;

c66=S12;

q11=0:1000:105820000;

%% q11=c11*e11+c12*e22+c12*e33;

%% q22=c12*e11+c22*e22+c23*e33;

%% q33=c12*e11+c23*e22+c22*e33;

%% q13=2*c66*e13;

%% q12=2*c66*e12;

e11=((c22+c23)/(c11*c22-2*(c12^2)+c11*c23))*q11;

e22=((-c12)/(c11*c22-2*(c12^2)+c11*c23))*q11;

e33=((-c12)/(c11*c22-2*(c12^2)+c11*c23))*q11;

Eeq=(2/3)*sqrt(1/2*((e11-e22).^2+(e22-e33).^2+(e33-e11).^2));

 hold on

plot(Eeq,q11)

title('Combine Graphs')

E=3780000000;
```

```
e=q11/E;

plot(e,q11,'r');

Ef=73872000000;

ef=q11/Ef;

plot(ef,q11,'y')

xlabel('strain values') % x-axis label

ylabel('stress values') % y-axis label

legend('composite','fiber','matrix')

hold off
```

Comparing $\varepsilon_{22}, \sigma_{11}, \varepsilon_{11}, \varepsilon_{33}, \varepsilon_{eq}$ with each other to plot a graph needs another code to display. That is;

```
Dm=1160;

Ym=3780000000;

Pm=0.35;

Bm=4250000000;

Sm=1400000000;

Vm=0.424;

Df=2530;

Yf=74500000000;

Pf=0.22629;

Bf=45400000000;

Sf=30400000000;
```

```
Vf=0.576;

Km=Sm/(3*(1-2*Pm));

Kf=Sf/(3*(1-2*Pf));

K=Km+Vf/((1/(Kf-Km))+(1-Vf)/(Km+Sm));

Y1=Vf*Yf+(1-Vf)*Ym;

Y2=Yf*Ym/(Yf+Vf*(Yf-Ym));

P12=Pf*Vf+(1-Vf)*Pm;

P23=1-P12*(Y2/Y1)-(Y2/(3*K));

S12=Sm+Vf/((1/(Sf-Sm))+(1-Vf)/2*Sm);

S23=Y2/(2*(1+P23));

c11=Y1+4*(P12)^2*K;

c12=2*K*P12;

c22=S23+K;

c23=-S23+K;

c66=S12;

q11=0:1000:105820000;

%% q11=c11*e11+c12*e22+c12*e33;

%% q22=c12*e11+c22*e22+c23*e33;

%% q33=c12*e11+c23*e22+c22*e33;

%% q13=2*c66*e13;

%% q12=2*c66*e12;

e11=((c22+c23)/(c11*c22-2*(c12^2)+c11*c23))*q11;
```

```
e22=((-c12)/(c11*c22-2*(c12^2)+c11*c23))*q11;

e33=((-c12)/(c11*c22-2*(c12^2)+c11*c23))*q11;

Eeq=(2/3)*sqrt(1/2*((e11-e22).^2+(e22-e33).^2+(e33-e11).^2));;

plot(Eeq,q11)

xlabel('strain values') % x-axis label

ylabel('stress values') % y-axis label
```

At the plot line, which is denoted with exclamations, you can change the variables in order to plot the different comparisons.

```
Dm=1160;
Ym=3780000000;
Pm=0.35;
Bm=4250000000;
Sm=1400000000;
Vm=0.424;
Df=2530;
Yf=74500000000;
Pf=0.22629;
Bf=45400000000;
Sf=30400000000;
Vf=0.576;
K=4250000000;
df=30;
lf=6;
nL=((Yf/Ym)-1)/((Yf/Ym)+2*(lf/df));
nT=((Yf/Ym)-1)/((Yf/Ym)+2);
nG=((Sf/Sm)-1)/((Sf/Sm)+1);
E2=(1+2*(lf/df)*nL*Vf)*Ym/(1-nL*Vf);
E1=(1+2*nT*Vf)*Ym/(1-nT*Vf);
G12=(1+nG*Vf)*Sm/(1-nG*Vf);
P12=Vf*Pf+Vm*Pm;
G23=1400000000;
c11=E1+4*(P12)^2*K;
c12=2*K*P12;
c22=G23+K;
c23=-G23+K;
c66=G12;
P23=(c11*c23-(c12)^2)/(c11*c22-(c12)^2);
%Erandom=(3*E1/8)+(5*E2/8);
%Grandom=(E1/8)+(E2/4);
q11=0:10000:105820000;
e11=((c22+c23)/(c11*c22-2*(c12^2)+c11*c23))*q11;
e22=((-c12)/(c11*c22-2*(c12^2)+c11*c23))*q11;
e33=((-c12)/(c11*c22-2*(c12^2)+c11*c23))*q11;
Eeq=(2/3)*sqrt(1/2*((e11-e22).^2+(e22-e33).^2+(e33-e11).^2));
 hold on
plot(Eeq,q11)
title('Combine Graphs')
E=3780000000;
e=q11/E;
plot(e,q11,'r');
Ef=73872000000;
ef=q11/Ef;
plot(ef,q11,'y')
xlabel('strain values') % x-axis label
ylabel('stress values (Pa)') % y-axis label
legend('composite','matrix','fiber')
hold off
```

Figure B.1. Code of calculations